U.PORTO

MESTRADO EM ONCOLOGIA

ONCOLOGIA LABORATORIAL

Unveil the mechanisms of CCL18-mediated colorectal cancer cell invasion

Ana Catarina Ferreira Ribeiro

M

2024

Unveil the mechanisms of CCL18-mediated colorectal cancer cell invasion

Ana Catarina Ferreira Ribeiro

INSTITUTO DE CIÊNCIAS BIOMÉDICAS ABEL SALAZAR

Ana Catarina Ferreira Ribeiro

Unveil the mechanisms of CCL18-mediated colorectal cancer cell invasion

Dissertação de Candidatura ao grau de Mestre em Oncologia submetida ao Instituto de Ciências Biomédicas de Abel Salazar da Universidade do Porto.

Orientadora – Maria José Cardoso Oliveira

Categoria – Investigadora Principal

Afiliação – Grupo Tumour and Microenvironment Interactions do Instituto de Investigação e Inovação em Saúde da Universidade do Porto.

Co-Orientadora – Ana Patrícia Pereira Cardoso

Categoria – Investigadora Júnior

Afiliação - Grupo Tumour and Microenvironment Interactions do Instituto de Investigação e Inovação em Saúde da Universidade do Porto.

Tutora – Ângela Isabel Marques Magalhães

Categoria – Aluna de Doutoramento

Afiliação - Grupo Tumour and Microenvironment Interactions do Instituto de Investigação e Inovação em Saúde da Universidade do Porto.

This thesis work has been developed at the Tumour and Microenvironment Interactions Group of i3S in straight collaboration with IPO Porto under the scope of the P.CCC - Porto Comprehensive Cancer Center Raquel Seruca. This work counted with the straight collaboration with Doctor José Alexandre Ferreira and Andreia Miranda (IPO-Porto, Group of Pathology and Experimental Therapeutics) and with Prof. Doctor Raquel Almeida and Doctor Bruno Pereira (i3S, Group of Differentiation & Cancer). The contribution of i3S Scientific Platforms has also been fundamental: *in vivo* CAM assays (Doctor Marta Teixeira Pinto), Histology and Electron Microscopy (Doctor Nuno Mendes), and BioSciences Screening (Doctor André Maia). This work received the financial support of Ipatimup - Institute of Pathology and Molecular Immunology, University of Porto, through the project CANCER CHALLENGE.

“What we know is a drop. What we don’t know is an ocean.”

Isaac Newton

Acknowledgments | Agradecimentos

Este foi um caminho que não se fez sozinho e por isso quero agradecer a todas as pessoas que de alguma forma me ajudaram e contribuíram para que chegasse até aqui.

Primeiro que tudo quero agradecer às minhas orientadoras. À Maria por me ter aceite no seu grupo e ter mostrado uma simpatia e cuidado extremo desde o início. À Patricia, por todos os conhecimentos transmitidos e disponibilidade no início desta jornada.

À Ângela, que foi um barco salva-vidas este ano. Se não fosses tu, estaria à deriva nesta loucura. Um obrigada gigante por tudo o que me ensinaste, por toda a paciência nos meus desesperos, por todos os conselhos, toda a ajuda e, principalmente, por toda a disponibilidade para me ouvires e apoiares, até nos momentos mais críticos em que nada parecia estar a correr bem (e não estava!).

A todos os membros do grupo Tumor and Microenvironment Interactions, que me acolheram e integraram. Agradeço todo o tempo despendido para me ouvir e ajudar com o que fosse preciso, mesmo no meio de toda a azafama no laboratório.

À Marta Pinto, Bruno Pereira, Andreia Miranda e Diogo Estêvão, agradeço toda a paciência para me explicarem e esclarecerem todas as minhas dúvidas, e por toda a ajuda prestada que me garantiu conseguir fazer tudo o que pretendia.

Aos meus amigos i3s, a Bea, a Maria, a Mafalda e o Gonçalo, que partilharam bem de perto este percurso comigo. Fomos a rede uns dos outros dentro daquele edifício cinzento e inacabado e eu não escolheria outra coisa. Acompanharam o processo todo e deram todo um corpo amigo para me apoiar. Ficam as saudades de assaltar coffee-breaks convosco.

À Cat, Trish, Rosa, Pedro e Bea, os meus betos.com, que me acompanham de Aveiro para todo o lado, longe, mas sempre perto. Obrigada por estarem sempre lá, com palavras encorajadoras, e por podermos partilharmos todas estas experiências. São um apoio inestimável.

À Sara, a mãe adotiva que o Porto me deu. Foste das melhores coisas que este mestrado me trouxe. Obrigada pelos lanches, pelas sessões de muito estudo e trabalho, por todo o apoio e paciência quando eu duvidava do que andava a fazer, e pela constante companhia.

À Teresa, a Lisboeta que acompanhou quase a vida toda, mas acima de tudo neste ano, mesmo sem perceber nada do que eu andava a fazer. É bom ver que evoluímos de estar juntas a reclamar de colegas de turma para reclamar de colegas de trabalho. Estamos tão crescidas :')

À minha família, que são o pilar essencial da minha vida. Sem vocês não seria garantidamente a pessoa que sou hoje! Mãe, Pai, um grande obrigada por nunca me terem cortado as asas, por mais que isso vos custasse, e por estarem sempre lá para me apoiar e incentivar. Rafa, és um chato, mas obrigada por conseguires sempre distrair-me e relativizar os meus problemas. Ísis, obrigada por toda a companhia constante, mesmo nas noites de trabalho intensivo, e por todo o carinho quando eu mais precisava.

Abstract

The tumor microenvironment (TME) plays a significant role in colorectal cancer (CRC) development, the third most incident and the second more lethal cancer worldwide. Indeed, macrophages, the most frequent immune population in the stroma, influence cancer cells' behavior and may favor tumor progression through the production of signaling chemokines and growth factors. Particularly, our group demonstrated that CCL18, an immunosuppressive and pro-tumoral chemokine produced by anti-inflammatory macrophages, induces cancer cell invasion. Additionally, we described that CCL18 is highly expressed at the invasive front of more advanced human colorectal tumors at sites where anti-inflammatory macrophages and T regulatory cells are also preferentially located. Therefore, these findings render CCL18 as a potential marker of worse prognosis whose mechanism of action is still poorly understood in CRC.

This study aimed to further understand and identify the mechanisms by which CCL18 influences the behavior of tumor cells. Therefore, two colon cancer cell lines, RKO and HCT-15, were evaluated regarding their response to CCL18 in invasion and invasion-associated activities, such as migration, proliferation, and proteolysis. For that, invasion, wound-healing and single-cell migration assays, cell cycle analysis, and gelatin zymography were performed. To understand the impact of CCL18 on tumor growth and stimulation of angiogenesis *in vivo*, we used the chick chorioallantoic membrane (CAM) model. Finally, to unveil the mechanisms through which CCL18 induces cancer cell invasion, its putative receptor(s) and associated signaling pathways were explored through an educated-guess and a search approach. As a first strategy, the CRISPR-Cas9 technology was performed for the establishment of knockout (KO) models for two CCL18 canonical receptors (CCR8 and PITPNM3), previously described in other tumor types. Finally, a crosslinking mass spectrometry assay, using CCL18-coated magnetic beads as a decoy, was employed to identify possible interactors and receptors of this chemokine.

After optimizing the percentage of serum and the recombinant human (rh)CCL18 concentrations, we observed that this chemokine impacts both collective and individual cancer cell migration. In the single-cell assay, it promoted an overall decrease of the migrated distance, although the migratory activity was faster and more directed than that of unstimulated cells. In collective migration, we observed that colon cancer cells responded differently to stimulation with this immunosuppressive chemokine. Interestingly, rhCCL18 significantly increased RKO collective cell migration, without affecting HCT-15. Additionally, it was interesting to observe that cell morphology was also altered after stimulation with 10ng/mL of rhCCL18. RKO cells evidenced a more elongated and loose shape, with front cellular projections characteristic of migratory cells, as an attempt to interconnect other cells, while HCT-15 cells were more compact, remaining close to the neighboring cells.

Furthermore, our results evidenced that rhCCL18 does not influence the cell cycle of RKO nor of HCT-15 cells, as there were no statistically significant differences observed at any of the time points studied. Moreover, our results evidenced the presence of pro-active and active matrix metalloprotease (MMP)-9 forms, and the pro-form of MMP-2 in both conditions. However, no significant differences between the proteolytic activity of these MMPs were observed in the presence or absence of 10ng/mL rhCCL18, suggesting that this chemokine does not promote invasion through the degradation of the ECM, at least at this concentration. Additionally, our *in vivo* results with the CAM assay evidenced that 20ng/mL of rhCCL18 did not promote tumor growth or tumor neoangiogenesis, with no statistical differences observed regarding superficial tumor area or tumor new blood vessel formation. Regarding the CCL18 receptor, we were able to establish confirmed knockout (KO) CCR8 models, however, we were unable to achieve that for PITPNM3, with every clone displaying a heterozygous (polyclonal) phenotype. Western blots confirming receptor loss of expression and invasion assays with CCR8-KO cells will be important, in the future, to assess the role of CCR8 in inducing CRC cell invasion under CCL18 stimulation. Sequencing analyses are still required to understand the status of the deletion site in PITPNM3. Moreover, through the cross-linking approach followed by mass spectrometry analysis, we were confronted with 20 proteins enriched in RKO conjugates, that respond to CCL18-mediated invasion, in comparison to the unresponsive SW480 conjugates. Importantly, Annexin A2 (AXNA2), one of the differently expressed proteins, was described to interact directly with EGFR in the protein-protein interaction networks established by the STRING database, and with CCL18 by our PubMed research. Furthermore, these proteins are interconnected with several other proteins suggesting possible pathways of action that are now crucial to investigate.

Altogether, our results suggest that CCL18 may promote tumor cell invasion through cell migration, without enhancing ECM components proteolysis. Moreover, this chemokine does not seem to influence the cancer cell cycle *in vitro.* Although our educated-guess and search approaches did not led us to the identification of the CCL18 receptor, they permitted to establish CCR8 knockout clones and to appoint ANXA2 as a possible interactor between CCL18 and EGFR. Further experiments are now required to confirm that the obtained clones still respond to CCL18-mediated invasion, inducing EGFR and downstream partners phosphorylation. Functional assays using anti-EGFR and anti-ANXA2 antibodies are now crucial to establish the CCL18 interacting network.

Keywords: Colorectal cancer, Tumor microenvironment, Macrophages, CCL18, Cancer cell invasion, CCL18 Receptors.

Resumo

O microambiente tumoral (TME) desempenha um papel significativo no desenvolvimento do cancro colorretal (CRC), o terceiro mais incidente e o segundo tipo de cancro mais letal em todo o mundo. De facto, os macrófagos, a população imune mais frequente no estroma, influenciam o comportamento das células tumorais e podem favorecer a progressão do tumor através da produção de quimiocinas sinalizadoras e de fatores de crescimento. Em particular, o nosso grupo demonstrou que a CCL18, uma quimiocina imunossupressora e pró-tumoral produzida por macrófagos anti-inflamatórios, induz a invasão das células tumorais. Além disso, descrevemos que a CCL18 é altamente expressa na frente invasiva de tumores colorretais humanos mais avançados, em locais onde os macrófagos anti-inflamatórios e as células T reguladoras estão preferencialmente localizados. Por conseguinte, estes resultados fazem da CCL18 um potencial marcador de pior prognóstico cujo mecanismo de ação, ainda pouco conhecido no CRC, importa conhecer.

Este estudo teve como objetivo compreender e identificar os mecanismos pelos quais a CCL18 influencia o comportamento das células tumorais. Para tal, o impacto da CCL18 na invasão de duas linhas celulares de colon, as RKO e as HCT-15, e na modelação de atividades associadas à invasão, como a migração, o ciclo celular e perfil proteolítico, foi investigado. Para tal, foram efetuados ensaios de invasão, migração individual ou colectiva, análise do ciclo celular e zimografia em géis de gelatina. Para compreender o impacto da CCL18 no crescimento tumoral e na estimulação da angiogénese *in vivo*, utilizámos o modelo da membrana corioalantóica do ovo da galinha (CAM). Por último, para desvendar os mecanismos através dos quais a CCL18 induz a invasão das células tumorais, os seus recetores e as vias de sinalização associadas foram explorados através de duas estratégias. A primeira, baseada em dados da literatura, consistiu em realizar, através da tecnologia CRISPR-Cas9, o estabelecimento de modelos *knockout* (KO) dos recetores canónicos da CCL18 (CCR8 e PITPNM3), e previamente descritos noutros tecidos. Finalmente, a segunda estratégia, teve por base um ensaio de espetrometria de massa de ligação cruzada, utilizando como isco esferas magnéticas revestidas com CCL18, para identificar os possíveis recetores associados a esta quimiocina.

Após a otimização da percentagem de soro e da concentração de quimiocina humana recombinante (rhCCL18), verificámos que esta quimiocina modela a migração celular individual e coletiva. No ensaio de células individuais, a rhCCL18 promoveu uma diminuição da distância migrada, embora a atividade migratória tenha sido mais rápida e mais direcionada do que das células não estimuladas. Na migração coletiva, observámos que as células tumorais responderam de forma diferente à estimulação com esta quimiocina. Curiosamente, a rhCCL18 aumentou significativamente a migração coletiva das células

RKO, sem afetar a das células HCT-15. Além disso, foi interessante observar que a morfologia das células também se alterou após a estimulação com rhCCL18 (10ng/mL). As células RKO apresentaram uma forma mais alongada e individualizada, com projeções celulares frontais caraterísticas de células migratórias numa tentativa de estabelecerem interações celulares, enquanto as HCT-15 eram mais compactas, preferindo permanecer próximas às células vizinhas. Os nossos resultados sugerem ainda que a rhCCL18 não influencia o ciclo celular das RKO nem das HCT-15, uma vez que não foram observadas diferenças estatisticamente significativas em nenhuma das condições estudadas. Além disso, os nossos resultados evidenciaram a presença de formas pró-ativas e ativas de metaloprotease de matriz (MMP)-9 e a forma pró-ativa de MMP2 em ambas as condições. Não foram observadas diferenças significativas entre a atividade proteolítica destas MMPs, na presença ou ausência de rhCCL18 (10ng/mL), sugerindo que esta quimiocina não promove a invasão através da degradação da matriz extracelular, pelo menos com esta concentração. Além disso, o ensaio da CAM evidenciou que a rhCCL18 (20ng/mL) não promoveu o crescimento tumoral ou a neo-angiogénese *in vivo*, não tendo sido observadas diferenças estatísticas relativamente à área tumoral superficial ou à formação de novos vasos sanguíneos à volta do tumor. Relativamente ao recetor da CCL18, conseguimos estabelecer modelos KO para o recetor CCR8, no entanto, o mesmo não aconteceu para o PITPNM3, apresentando todos os clones um fenótipo heterozigótico (policlonal). Western blots a confirmar a ausência de expressão do recetor, e ensaios de invasão com linhas celulares KO para o CCR8 serão importantes, no futuro, para avaliar o papel deste recetor na indução da invasão mediada pela CCL18. Além disso, análises de sequenciação permitirão confirmar a deleção do PITPNM3. Em paralelo, numa análise de ligações cruzadas, identificámos 20 proteínas enriquecidas em conjugados RKO, que respondem à invasão mediada pela CCL18, mas não nos conjugados não responsivos das SW480. Notavelmente, a Annexin A2 (AXNA2), uma das proteínas diferencialmente expressas, foi descrita como interagindo diretamente com o EGFR, nas redes de interação proteína-proteína da base de dados STRING, e com a CCL18 na pesquisa avançada do PubMed. Além disso, estas proteínas estão interligadas com várias outras, sugerindo uma possível via de sinalização que importa agora investigar.

Em conclusão, os nossos resultados sugerem que a CCL18 pode promover a invasão das células tumorais através da migração celular, sem degradar os componentes da matriz extracelular. Além disso, esta quimiocina não parece influenciar o ciclo celular *in vitro*. Apesar das nossas estratégias não nos terem conduzido à identificação do recetor da CCL18, permitiram-nos estabelecer clones KO para o CCR8 e apontar a ANXA2 como um possível elemento de ligação entre a CCL18 e o EGFR. Serão agora necessárias experiências adicionais para confirmar se a CCL18 é capaz de induzir a invasão dos clones CCR8 KO gerados e a fosforilação do EGFR e dos seus parceiros de sinalização. Ensaios

funcionais, utilizando anticorpos anti-EGFR e anti-ANXA2 são agora cruciais para estabelecer a sinalização molecular subjacente.

Palavras-Chave: Cancro colorretal, Microambiente tumoral, Macrófagos, CCL18, Invasão das células tumorais, Recetores da CCL18.

Index

List of Figures and Tables

List of Abbreviations

18qLOH: Chromosome 18q loss of heterozygosity

ºC: grade Celsius

A

ACN: Acetonitrile

Akt: Protein kinase B

AMAC-1: Alternative macrophage activation-associated CC chemokine-1

AMP: Adenosine monophosphate

ANXA2: Annexin A2

APC: Adenomatous polyposis coli

APCs: Antigen-presenting cells

ATCC: American Type Culture Collection

ATP: Adenosine triphosphate

B

Bcl-2: Anti-apoptotic protein B cell lymphoma

BRAF: V-raf murine sarcoma viral oncogene homolog B1

BS3: Bis(sulfosuccinimidyl)suberate

BSA: Bovine serum albumin

C

CA 19-9: Cancer antigen 19-9

CAFs: Cancer-associated fibroblasts

CAM: Chorioallantoic membrane

CCIM: Colorectal cancer immune module

CCL: Chemokine C-C motif ligand

CCND1: Cyclin D1

CCR8: C-C motif chemokine receptor 8

CD: Cluster of differentiation

CDK1: Cyclin-dependent kinase 1

CEA: Carcinoembryonic antigen

CIMP: CpG Island methylator phenotype

CIN: Chromosomal instability

CKR-L1: Chemokine receptor-like 1

CRC: Colorectal cancer

CSK: Cytoskeletal

CT: Computed tomography

CXCL: Chemokine C-X-C motif ligand

CXCR: Chemokine C-X-C motif receptor

D

DAPI: 4′,6-diamidino-2-phenylindole

DC: Dendritic cells

DC-CK1: Dendritic cell chemokine 1

DFS: Disease-free survival

DNA: Deoxyribonucleic acid

DTT: Dithiothreitol

E

ECM: Extracellular matrix

EGF: Epidermal growth factor

EGFR: Epidermal growth factor receptor

EMT: Epithelial to mesenchymal transition

ER: Estrogen receptor

ERE: Estrogen response element

ERK1: Extracellular signal-regulated kinase 1

F

FACIT: Fibril-associated collagens with interrupted helices

FAK: Focal adhesion kinase

FAP: Familial adenomatous polyposis

FBS: Fetal bovine serum

FCN1: Ficolin-1

FGFR: Fibroblast growth factor receptor

FITC: Fluorescein-5-isothiocyanate

FOLR2: Folate Receptor Beta

G

GAG: Glycosaminoglycans

GFP: Green fluorescent protein

GM-CSF: Granulocyte-macrophage CSF

GO: Gene ontology

GPCR/GPR: G protein-coupled receptor

GPER1: G protein-coupled estrogen receptor 1

GTPases: hydrolases of nucleotide guanosine triphosphate

H

HEPES: 4-(2-hydroxyethyl)-1-piperazineethanesulfonic acid

HIV: Human immunodeficiency virus

HLA-DR: Human Leukocyte Antigen - DR

HNPCC: Hereditary non-polyposis

HSPA6: Heat Shock Protein Family A (Hsp70) Member 6

I

IAA: Iodoacetamide

IFN-y: Interferon-gamma

IGF1R: Insulin-like growth factor 1 receptor

IL: Interleukin

ILC2s: Group 2 innate lymphoid cells

IM: Invasive margin

INSR: Insulin receptor

IP3KB: Inositol 1,4,5-trisphosphate 3-kinase isoform B

IRF4: Interferon regulatory factor 4

J

JAK3: Janus Kinase 3

JMJD3: Jumonji domain-containing protein-3

JNK: Jun N-terminal kinase

K

KEGG: Kyoto Encyclopedia of Genes and Genomes

KO: Knockout

KRAS: Kirstein rat sarcoma

L

LB: Luria-Bertani medium

LOH: Loss-of-heterozygosity

LOX: Lysyl oxidase

LPS: Bacterial lipopolysaccharide

M

MAPK: Mitogen-activated protein kinase

MHC: Major histocompatibility complex

MIP-4: Macrophage inflammatory protein-4

MLH1: MutL homolog 1

MMP: Matrix metalloproteinases

MMR: Mismatch repair

MR: Magnetic resonance

MSH2: MutS homolog 2

MSI: Microsatellite instability

MSI-H: Microsatellite instability-high

MSI-L: Microsatellite instability-low

MSS: Microsatellite-stable

mTOR: Mammalian target of rapamycin

N

NADPH: Nicotinamide adenine dinucleotide phosphate

NF-κB: Nuclear factor kappa B

Nir1: PYK2 N-terminal domain-interacting receptor 1

NK: Natural killer

NOS: Nitrous oxide

O

OLR1: Oxidized low density lipoprotein receptor 1

OS: Overall survival

P

P/S: Penicillin-streptomycin

PARC: Pulmonary and activation-regulated chemokine

PBS: Phosphate-buffered saline

PCR: Polymerase chain reaction

PDGFR: Platelet-derived growth factor receptor

PFA: Paraformaldehyde

PI: Propidium iodide

PI3K: Phosphatidylinositol 3-kinase

PIP3: Phosphatidylinositol 3,4,5-trisphosphate

PIPES: Piperazine-N,N′-bis(2-ethanesulfonic) acid

PITP: Phosphatidylinositol transfer protein

PITPNM3: Membrane-associated phosphatidylinositol transfer protein 3

PKB: Protein kinase B

PKCζ: Protein kinase C-ζ

PKC-α: Protein kinase C alpha

PLCy1: Phospholipase Cy1

PMS1: PMS1 Homolog 1

PMS2: PMS1 Homolog 2

PN: Pioneer

PTK: Protein tyrosine kinase

PTK2B: Protein tyrosine kinase 2 beta

PYK2: Proline-rich tyrosine kinase 2

R

rhCCL18: Recombinant human CCL18

RNS: Reactive nitrogen species

ROS: Reactive oxygen species

RT: Room-temperature

S

sgRNAs: Single-guide RNAs

SMAD: Suppressor of Mothers against Decapentaplegic

SOC: Super optimal broth with catabolite repression

STAT1: Signal Transducer and Activator Of Transcription

STRING: Search tool for the retrieval of interacting genes/proteins

T

TAMs: Tumor-associated macrophages

TC: Tumor center

TFs: Transcription factors

TGF-β: Transforming growth factor β

Th1: T helper cell type 1

Th2: T helper cell type 2

TI: Tumor islets

TLR-2: Toll-like receptor 2

TME: Tumor microenvironment

TNF-α: Tumor necrosis factor α

TP53: Tumor protein-53

Tregs: T regulatory cells

TS: Tumor stroma

V

VEGF: Vascular endothelial growth factor

W

WT: Wild-type

Chapter 1: Introduction

Cancer

Cancer is defined as aberrant cell growth that results from gene mutations that either accelerate the rate of cell division or inhibit the organism from executing its normal controls, such as cell cycle arrest or programmed cell death. Additionally, mutations may provide these cells the ability to degrade the underlying extracellular matrix components, to migrate through the basement membrane and the stroma, overcome tissue boundaries and invade nearby tissues and occasionally even form metastases (1,2).

This disease represents a major social, public health, and economic problem of the 21st century, being the leading cause of mortality and an important obstacle in increasing life expectancy worldwide. Globally, the burden of cancer incidence and mortality is growing at a rapid rate. This can be attributed to several factors, including population growth and aging, and shifts in the distribution and prevalence of the primary risk factors for cancer, many of which are linked to socioeconomic development. Apart from its significant impact on life expectancy, cancer entails substantial social and macroeconomic expenses that differ according to gender, geographic location, and cancer type. Decreasing the global cancer burden requires a combination of primary prevention, early intervention, improvements to health systems, and treatment alternatives (3).

Colorectal Cancer

Epidemiology and Etiology

Colorectal cancer (CRC) was estimated to be responsible for about 10% of the worldwide cancer burden, being ranked in third place in incidence and second in mortality, in 2022 (Figure 1). In Portugal, it surpasses both breast and prostate cancer, occupying the place of the most common cancer, while being the second most deadly, after lung cancer (3).

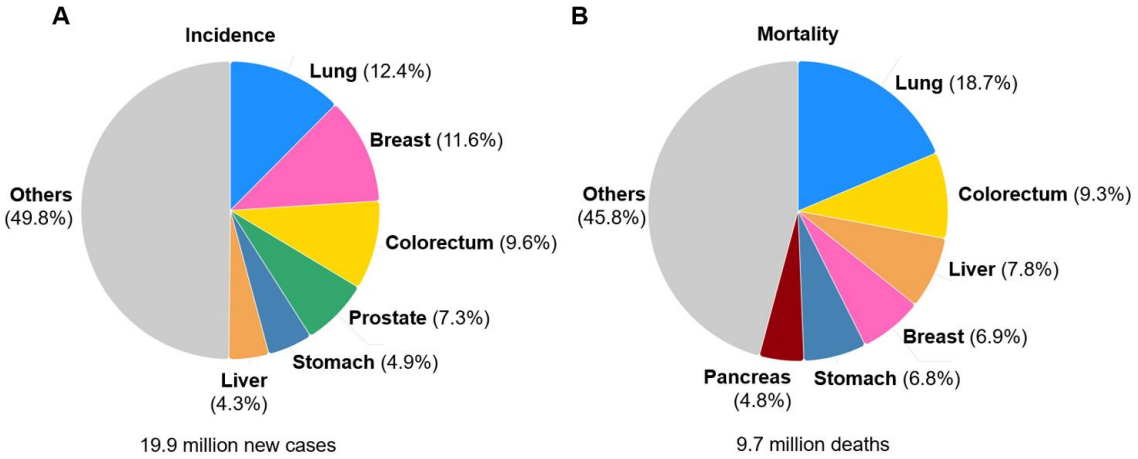

Figure 1. Estimated 2022 worldwide cancer incidence and mortality rates for both genders. Adapted from Globocan (3).

The most significant risk factor for CRC is aging, with the chance of developing disease increasing after 50 years. Other risk factors include the personal history of CRC or of inflammatory bowel disease, and a familial history of CRC in proximal relatives, especially in those under fifty years of age at diagnosis (4). Furthermore, specific lifestyle habits also constitute a risk for CRC development. A more sedentary lifestyle, with a high intake of animal-source aliments, usually correlates with a lack of physical activity and obesity, which are all modifiable risk factors. Additionally, heavy alcohol intake, smoking, and consumption of red or processed meats also contribute to this disease risk. However, physical activity, consumption of wholegrains, foods containing dietary fiber, dairy products, calcium supplements, regular use of aspirin, and hormone replacement therapy appear to have a protective effect (5,6).

Pathogenesis and Classification

The formation of CRC implicates the transformation of normal glandular epithelial cells into benign adenomas or polyps, progressing to advanced forms and, finally, to invasive carcinoma. The accumulation of genetic and epigenetic alterations are responsible for the neoplastic changes (7).

CRC can be classified as sporadic, inherited, or familial depending on the origin of the mutations (8).

Sporadic cancers represent 70% of CRC and result from a specific succession of mutations that are translated into the adenoma-carcinoma sequence. This sequence states that non-malignant adenomas, or polyps, originate from a mutation in the tumor suppressor gene *adenomatous polyposis coli* (APC), that acts as an initiating event. This is followed by the accumulation of additional mutations in genes like *Kirstein rat sarcoma* (KRAS),

suppressor of mothers against decapentaplegic 4 (SMAD4), and tumor protein-53 (TP53). It is estimated that approximately 15% of those adenomas will progress to the carcinoma stage in 10-15 years (8,9).

Inherited cancers represent only 5% of the CRC cases. These cancers are caused by inherited mutations that affect one of the mutated gene's alleles; consequently, a point mutation in the other allele will cause the formation of a mutated cell and eventually lead to the development of carcinoma. Two groups of inherited cancers have been established: polyposis and non-polyposis. Familial adenomatous polyposis (FAP), typified by the development of multiple potentially malignant polyps in the colon, is the primary cause of the polyposis variant. By contrast, germline mutations in DNA mismatch repair (MMR) genes are linked to hereditary non-polyposis colorectal cancer (HNPCC), also called as Lynch syndrome (7,8).

Familial CRC represents about 25% of cases and is also caused by inherited mutations. However, it does not integrate any inherited cancer variant, and as such it is not considered inherited cancer *per se* (8).

One important factor underlying CRC is genomic instability. Three distinct pathways can be identified as the pathogenic mechanisms causing this malignancy, namely chromosomal instability (CIN), microsatellite instability (MSI), and CpG island methylator phenotype (CIMP) (10).

The CIN pathway, also referred to as the classical pathway, is responsible for 80% to 85% of the CRC cases. These cancers are characterized by a cascade of events that accumulate numerical or structural chromosomal abnormalities, resulting in aneuploid karyotype, frequent loss-of-heterozygosity (LOH) at tumor suppressor gene loci, and chromosomal rearrangements (11). Moreover, these mechanisms include alterations in chromosome segregation, telomere dysfunction, and DNA damage response, which impact key oncogenes and tumor suppressor genes that are vital for the preservation of cell function, including APC, KRAS, phosphatidylinositol 3-kinase (PI3K), *V-raf murine sarcoma viral oncogene homolog B1* (BRAF), SMAD4, and TP53 (8,11). APC mutations trigger the translocation of β-catenin to the nucleus and drive the transcription of genes implicated in tumorigenesis and invasion. Mutations in KRAS and PI3K have downstream effects on cell growth, survival, motility, and differentiation, while loss-of-function mutations in TP53 cause an uncontrolled entry into the cell cycle (8,12). All of these alterations culminate in carcinogenesis.

MSI is found in approximately 15% of sporadic CRCs (13). The inactivation of MMR genes, which are essential for maintaining genetic stability through repairing errors in DNA replication, preventing the recombination of non-identical DNA sequences, and interfering

with DNA damage responses, is the primary cause of MSI tumorigenesis. Loss of expression can result from spontaneous events, like promoter hypermethylation, or germinal mutations such as those in Lynch syndrome. These mutations can impact non-coding regions and codifying microsatellites, and tumors develop when reading frames of oncogenes or tumor suppressor genes encoded in microsatellites are changed. Genes mutated in these tumors include those involved in MMR as *MutL homolog 1* (*MLH1*), *MutS homolog 2* (*MSH2*), *MutS homolog 6* (*MSH6*), *PMS1 Homolog 1* (*PMS1*), and *PMS1 Homolog 2* (*PMS2*) (8). Depending on the proportion of loci that correlate to MSI features, it can be further divided into microsatellite instability-high (MSI-H) and microsatellite instability-low (MSI-L) categories. Microsatellite-stable (MSS) tumors are those that do not exhibit MSI characteristics (13).

Finally, the CIMP pathway is caused by epigenetic instability. The main feature of CIMP tumors is the hypermethylation of oncogene promoters, which results in the loss of protein expression and genetic silencing (8).

Screening and Treatment

For resectable CRC the primary therapy is surgical removal of the tumor, while in non-resectable CRC, standard therapies include chemotherapy, radiotherapy, and immunotherapy. These treatments can be combined, depending on the extent of the CRC confinement and progression (14). However, at advanced stages, the currently available therapies have limited curative impact, leading to poor prognosis and high mortality rates (15).

The main goal of screening is to identify early-stage CRC, that are mainly asymptomatic (15). Currently, colonoscopy is the standard method, however, although it allows for the easy identification of advanced lesions, early lesions are sometimes missed. Furthermore, since early lesions may appear as subtle mucosal lesions, an incomplete or inadequate colonoscopy may enhance the risk of cancer developing. For this reason, computed tomography (CT) and magnetic resonance (MR) are used as a complement to colonoscopy. Other methods include sigmoidoscopy and, to a lesser extent, stool-based testing (4,16).

Nevertheless, despite advances in the development of less invasive screening and diagnostic approaches, about 25% of patients present distant metastatic disease at diagnosis (4). This lack of early detection impacts the survival of CRC patients, with 5-year relative survival ranging from more than 90% in stage I CRC patients to about 10% in stage IV CRC patients (15). Therefore, reliable biomarkers that can detect CRC at early stages could improve the prognosis, treatment response prediction, and risk of recurrence.

Biomarkers

A biomarker is a biological entity that aids the measurement of normal biological processes, the presence and progression of pathological diseases, and responses to an intervention or treatment (17). A good biomarker must have high sensitivity, specificity, and positive predictive value. Additionally, it should be safe, easy to measure, helpful for establishing an accurate diagnosis, and aid in selecting the type of treatment (18).

Carcinoembryonic antigen (CEA) is the biomarker of excellence used in CRC. It is used to monitor therapy response and recurrence, with constant increased levels associated with disease progression. CEA was initially considered specific for CRC, but elevated levels of this marker were later found in other diseases, such as gastric and pancreatic cancer, and inflammatory conditions. Furthermore, CEA is not recommended for screening, considering that high concentrations are rarely found in stage I CRC. Another limitation of its use in screening is the difficulty and inability of differentiating between benign and malignant polyps (18).

Cancer antigen 19-9 (CA 19-9) is a glycoprotein whose application in CRC diagnosis remains a discussion. Elevated levels of this biomarker are associated with poor prognosis (18). However, CA 19-9 sensitivity and specificity for CRC are inferior when compared to CEA and therefore, this remains as the preferred antigen to use as a prognostic marker after diagnosis and to monitor disease progression (19).

Chromosome 18q loss of heterozygosity (18qLOH) in the coding place of SMAD4 proteins is another prognostic marker, specific to CRC, particularly in patients with stages II and III. Deletion of this chromosome is associated with poorer overall survival compared to patients without it (18).

Other molecules and characteristics are emerging as biomarkers for CRC, including MSI, and microRNA, however all failed at early diagnosis. Moreover, current non-invasive screening stools are not sensitive enough to detect pre-cancerous lesions and miss significant early CRC (14,15).

In order to improve CRC diagnosis and treatment, we must gain a deeper understanding of the biological mechanisms of cancer cells and of their microenvironment that underly the initiation, progression, and dissemination of the disease.

Tumor Microenvironment

Cancer is also associated with complex tissues and organs damaged by malignant and transformed cells within the tumor microenvironment (TME). The TME is formed by dynamic and intricate interactions of communication between various molecules and cells, which has a crucial impact on tumor initiation, development, and progression (20). This TME comprises all cellular, non-cellular, and soluble components that surround the malignant cells and that modulate and are modulated by cancer cell activities (Figure 2). This might include fibroblasts, adipocytes, immune cells, stromal cells, endothelial cells, and surrounding extracellular components, such as the extracellular matrix, and signaling molecules (20).

Infiltrating immune cells, cancer-associated fibroblasts (CAFs), and angiogenic endothelial cells perform critical functions in sustaining cell proliferation, evading growth suppressors, promoting survival, invasion, and metastasis, and reprogramming energy metabolism. They are embedded in a modified extracellular matrix (ECM), which offers support and regulates bidirectional communication between cells and ECM macromolecules to determine tumor progression and metastatic dissemination (20–22). Finally, the vasculature carries oxygen and nutrients from the tumor-associated stroma, along with soluble and matrix-bound growth factors, cytokines, chemokines, angiogenic factors, and enzymes that aid disease development (23). Researchers acknowledge that different cancer types and patients have different TME compositions and structures. Therefore, studying the immune TME is essential and can be used in addition to histopathological and molecular biomarkers (20).

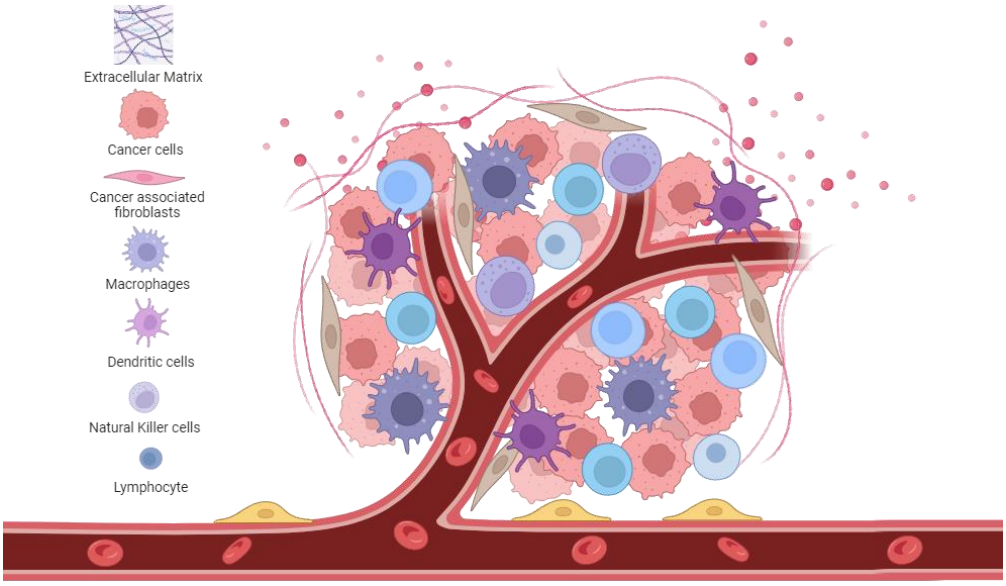

Figure 2. The tumor microenvironment. Cancer cells are surrounded by distinct immune cell populations (such as macrophages, dendritic cells, natural killer cells, lymphocytes, and endothelial cells), cancer-associated fibroblasts, normal epithelial cells, stromal cells, adipocytes, extracellular matrix components, and soluble factors. Created with Biorender.com.

Macrophages

Macrophages, the most predominant immune population at the TME, are myeloid-derived cells that may result from peripheral blood monocytes differentiation (20,24). They are found in nearly every tissue, being crucial for its maintenance and homeostasis. However, the ontogeny and the surrounding microenvironments result in resident macrophages varying between tissues. Therefore, these resident populations are frequently heterogeneous (24). Among their many roles are the phagocytosis of pathogens, dead cells, and cellular debris, antigen presentation through the presentation of processed antigens linked to major histocompatibility complex (MHC) molecules, and the synthesis of various cytokines (25).

Macrophages are essential for regulating innate immune and inflammatory responses, and crucial to preserve tissue homeostasis (26). Furthermore, they exhibit several functions associated with cancer development and progression, angiogenesis, tumor cell escape into the circulatory system, and inhibition of antitumor immune mechanisms and responses. They can also assist circulating cancer cells extravasation, by enhancing transendothelial migration at distant sites which may result in the persistent dissemination of metastatic colonies (20).

Macrophages are highly plastic cells that exhibit distinct functional phenotypes according to specific signals and stimuli received from the microenvironment. Although macrophage polarization is a spectrum of differentiation with several intermediate stages, there are two extreme macrophage populations: the classically activated (M1-like), generally pro-inflammatory, and the alternatively activated (M2-like) macrophages, which generally display anti-inflammatory features (Figure 3). These M2 macrophages are further divided into distinct subpopulations as M2a, M2b, M2c, and M2d. These macrophages differ in their cell surface markers, secreted cytokines, and biological functions (25,27).

The pro-inflammatory M1-like macrophages are typically induced by T helper cell type 1 (Th1) cytokines, including interferon-γ (IFN-γ) and tumor necrosis factor α (TNF-α), bacterial lipopolysaccharide (LPS), and granulocyte-macrophage CSF (GM-CSF), chemokine (C-X-C motif) ligand 9 (CXCL9), CXCL10, CXCL11, and C-X-C chemokine receptor type 3 (CXCR3). They are characterized by expressing toll-like receptor 2 (TLR-2), TLR-4, the co-stimulatory clusters of differentiation 80 (CD80) and CD86, and the major histocompatibility class II (MHC-II) molecules. Furthermore, the activation of transcription factors (TFs) like the Signal transducer and activator of transcription 1 (STAT1), the Nuclear factor κB (NF-κB), the Janus kinase 3 (JAK3), and the c-Jun N-terminal kinase (JNK) can promote the expression of pro-inflammatory cytokines, including interleukin 1 (IL-1), IL-6, IL-12, IL-23, and TNF-α by these macrophages (25,27,28). Functionally, the M1-like

macrophages remove pathogens by activating the nicotinamide adenine dinucleotide phosphate (NADPH) oxidase system with subsequent generation of reactive oxygen species (ROS). Consequently, ROS-induced tissue damage, mediated by pro-inflammatory macrophages, may also hinder wound healing and tissue regeneration (25). Additionally, these macrophages activate CD8+ T cells and attract natural killer (NK) cells to inhibit tumor growth. Clinical trials have demonstrated a positive correlation between increased infiltration of these pro-inflammatory macrophages and prolonged patient survival, as well as better clinical outcomes in multiple cancers, including colorectal, lung, ovarian, and triple-negative breast cancer (25,27,28).

On their turn, the anti-inflammatory M2-like macrophages are described to drive regulatory mechanisms that inhibit the chronic inflammatory response to prevent tissue damage and the induction of autoimmune diseases (27).

Cytokines like transforming growth factor β (TGF-β), IL-4, IL-13, IL-10, and IL-33 cause monocyte polarization into this anti-inflammatory phenotype. Interestingly, only IL-4 and IL-13 directly induce M2 macrophage activation, while T helper cell type 2 (Th2) produced cytokines as IL-33 and IL-25, seem to amplify M2 macrophage activation. Many of these exogenous stimuli may promote the expression of several transcription factors (TFs), as the Jumonji domain-containing protein-3 (JMJD3), the signal transducer and activation of transcription 6 (STAT6), and the interferon regulatory factor 4 (IRF4) that, on their turn, regulate the transcriptions of other genes. Currently, the STAT6 pathway is considered to be the major pathway responsible for the activation of genes related to the acquisition of an M2-like phenotype (25,27,28).

The anti-inflammatory macrophages are characterized by the expression of surface markers like the mannose receptor CD206, the scavenger receptor CD163, the C-type lectin CD209, the Resistin-like molecule alpha 1 (FIZZ1), and the Ym1/2 lectin (27,29,30).

They also produce high levels of anti-inflammatory cytokines as IL-10, TGF-β, chemokine (C-C motif) ligand 1 (CCL1), CCL17, CCL18, CCL22, and CCL24, which contribute to sustain their anti-inflammatory profile. These macrophages are highly capable of phagocytosing debris and apoptotic cells, promoting tissue repair and wound healing, and exhibiting pro-fibrotic and pro-angiogenic properties. Consequently, anti-inflammatory M2-like macrophages generally participate in Th2 responses and parasite clearance, reducing inflammation, inhibiting T cell-mediated anti-tumor immune response, and promoting tissue remodeling, angiogenesis, immunoregulation, tumor initiation, progression, and metastasis (25,28).

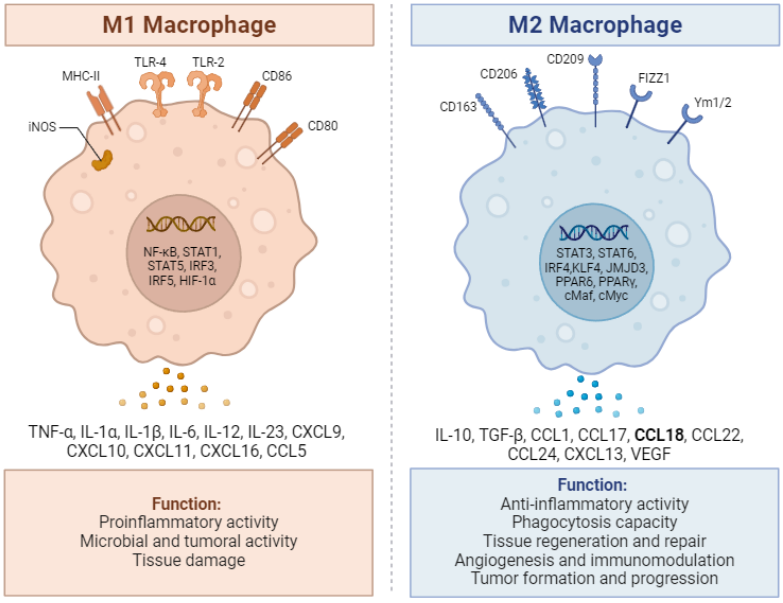

Figure 3. M1/M2 macrophages profile. The polarization of macrophages is driven by the surrounding microenvironment that induces them to adopt different properties. These distinct differentiated profiles represent extremes of a continuum of polarization. The pro-inflammatory M1-like macrophages usually express CD86, CD80, iNOS, and MHC class II receptors, and produce pro-inflammatory cytokines, such as IL-6, IL-1β, IL-12, and TNF-α, inducing a Th1 response. Their functions are proinflammatory, microbial and tumoral activity, and promotion of tissue damage. The anti-inflammatory M2-like macrophages frequently express CD206, CD163, CD209, FIZZ1, and Ym1/2, and are characterized by the production of anti-inflammatory cytokines, such as IL-10, TGF-β, and CCL18, generally inducing a Th2 response. Their functions are anti-inflammatory, phagocytosis, tissue regeneration and repair, angiogenesis and immunomodulation, and tumor formation and progression. Adapted from (27).

Macrophages in Cancer

The role of macrophages in cancer has been extensively studied, with new information emerging periodically. In many human cancers, the extent of macrophage infiltration functions as a valuable diagnostic and prognostic biomarker. Numerous techniques, including morphological discrimination, gene expression analysis, and cell-surface marker profiling, can be used to identify and quantify tumor-associated macrophages (TAMs). The most common way to identify them is by the expression of the macrophage lineage receptor CD68. However, anti-inflammatory M2-like macrophages can also be distinguished by their expression of CD163, of CD206, and of CD204. Oppositely, CD40 and HLA-DR expression can be used to identify human macrophages that exhibit a pro-inflammatory M1-like phenotype (31).

At first, the high density of macrophages in tumors was correlated with patients' prognosis. As such, infiltration of TAMs in the TME was associated with poor prognosis in breast, prostate, ovarian, cervical, gastric, bladder, thyroid, urogenital cancer, and oral squamous cell carcinoma (32,33). Contrarily, in patients with colorectal cancer, the abundance of macrophages was initially correlated with a better prognosis (33). In prostate, stomach, lung, and brain cancer there was conflicting evidence (32,33). Overall, increased

TAMs presence was associated with cancer progression, metastasis, poor treatment efficacy, and limited survival (32,34).

Later, two meta-analyses assessed the relationship between macrophages and CRC patients' prognosis, considering different factors, such as heterogeneity of TAMs subsets, the location of macrophage infiltration, tumor type, and MMR status. This integrative analysis may contribute to the debate regarding the relationship between TAMs and CRC outcomes (35,36).

In one of these studies, a high density of CD68+ TAMs in CRC tissue was correlated with a favorable prognosis, according to stratification by TAMs subsets. Additionally, it was found that 40% of the CD68+ macrophages were CD163 positive, whereas 60% were nitric oxide synthase (NOS2 or iNOS) positive. The presence of NOS2+ macrophages was suggested to be the primary factor influencing the positive correlation between CD68+ infiltrates and CRC survival, rather than the presence of CD163+ macrophages (36). This meta-analysis analyzed TAMs infiltration in tumor islets (TI) and tumor stroma (TS) (36), while other evaluated TAMs in the tumor center (TC), which includes stromal and intraepithelial compartments, and the invasive margin (IM) (35). The presence of TAMs in tumor islets was correlated with better CRC survival, while TAMs in tumor stroma predicted worse survival (36). Poor tumor differentiation and a worse prognosis were linked to high densities of anti-inflammatory M2-like macrophages at the tumor center. Notably, the presence of these macrophages at the tumor invasive margin was also correlated with a poor prognosis, particularly regarding disease-free survival (DFS) (35).

Importantly, many of these studies instructed that the effect of TAMs infiltration on prognosis may differ according to the TAMs subsets. Particularly, higher CD68+ TAMs density was positively associated with better CRC prognosis, but neither $CD68^{+}NOS2^{+}$ pro-inflammatory nor $CD68^{+}CD163^{+}$ anti-inflammatory TAMs density was correlated with CRC survival. In particular, the high density of $CD68^{+}$ TAMs at the tumor stroma or at the tumor islets and tumor stroma predicted better overall survival (OS). However, the infiltration of $CD68^{+}$ TAMs at tumor islets was not a statistically significant prognostic marker for OS (36). Instead, a high density of $CD68^{+}$ TAMs at the tumor center was associated with improved DFS, but no correlation with OS was found. In addition, the high density of $CD68^{+}$ TAMs at the tumor margin was associated with high infiltration of $CD3^{+}$ and $CD8^{+}$ T cells, which correlated with better prognosis (35).

Our group has also contributed to this knowledge by profiling, through immunohistochemistry, the macrophages present in a series of 150 CRC cases. For this characterization, we have used CD68, CD80 and CD163 as lineage, pro-inflammatory and anti-inflammatory macrophage markers, respectively. Quantifications performed by computer-assisted analysis revealed that $CD163^{+}$ macrophages were predominantly

distributed at the tumor invasive front, while $CD80^+$ macrophages were preferentially located at the adjacent normal mucosa. Tumor stage stratification revealed that $CD163^+$ macrophages are more abundant in stage II tumors, while $CD80^+$ macrophages were predominant in T1 tumors. Notably, in stage III tumors, higher CD68 and lower CD80/CD163 ratio correlated with reduced overall survival and a multivariate regression analysis appointed the protective role of $CD80^+$ macrophages against tumor relapse risk. This work emphasizes that in addition of studying the number it is also relevant to map the distribution of the distinct macrophage populations to uncover their prognostic value.

$CD68^+$ TAMs infiltration was also found to have opposite survival effects on colon and rectal cancer. An abundance of TAMs was shown to be a favorable prognostic factor for colon cancer but a negative indicator for rectal cancer. Considering that preoperative radiation therapy, which modulates macrophage recruitment and function in the TME, is administered to most patients with rectal cancer, this could be a possible explanation for the difference between these types of cancer (36).

Moreover, differences regarding macrophage infiltration between MMR-proficient and MMR-deficient CRC cases were found. It was demonstrated that only MMR-proficient cancers with increased TAM density had a favorable prognosis; MMR-deficient cancers did not exhibit any correlation with TAM infiltration. This suggests that the MMR status and the prognostic value of TAMs might be associated (36).

Altogether, this data supports that quantifying and profiling the $CD68^+$ macrophages and their subpopulations may provide potential prognostic information to complement tumor staging and guide decisions for therapeutic targets in CRC (35,36).

Another relevant aspect is the macrophage profile. As previously mentioned, macrophages polarize in a continuum spectrum, with two extremes of polarization, the M1 and M2 macrophages. The M1-like macrophages present pro-inflammatory characteristics, which confer them an anti-tumoral phenotype. Contrarily, the M2-like phenotype presents anti-inflammatory traits which correlate to pro-tumoral abilities (37). TAMs also exhibit distinct polarization and regulate the progression of tumors. They are primarily polarized to the M1 type in the early stages of tumor progression, gradually evolving into M2-like TAMs during tumor development (28). In the TME, macrophage polarization can also be induced by hypoxia, pH imbalances, and ECM alterations. Since they deal with a wide range of signals and origins, TAMs are highly heterogeneous. TAMs are a major source of reactive mediators including cytokines, chemokines, growth factors, ROS and reactive nitrogen species (RNS), and proteolytic enzymes, and have been shown to impact fundamental aspects of tumor biology and progression (20,38).

Anti-inflammatory TAMs are described to lack cytotoxic activity, to release cytokines and growth factors that favor cancer cell aggressiveness, and that promote and sustain an immune-suppressive environment. They have the ability to increase, mediate, or antagonize the antitumor activity of irradiation, cytotoxic agents, and checkpoint inhibitors. These macrophages may also produce multiple enzymes and proteases such as matrix metalloproteinases (MMPs), cathepsins, plasmin, and osteonectin that regulate the degradation of the ECM, consequently promoting tumor motility, invasion, and metastasis (20,25). Additionally, while suppressing the anti-tumor Th1-mediated adaptive immunity (38), they may also produce pro-angiogenic factors essential for tumor proliferation and for the neo-angiogenesis switch. These include the epidermal growth factor (EGF), TGF-β, the and vascular endothelial growth factor (VEGF) (38).

Recently advances in omics technologies have significantly expanded our understanding of the biological processes that promote CRC progression (39). Comprehensive genomic and transcriptomic research has played a pivotal role in linking immune-related genomic abnormalities, such as microsatellite instability, neoantigen load, and other immune-related genomic distortions, to immune-cell infiltration and prognosis in CRC. Several approaches have been used to identify transcriptomic and epigenetic changes that correlate with cancer development. These approaches include microdissection of CRC lesions and tissue comparisons between normal, adenoma, and carcinoma tissues. Lately, single-cell transcriptomics has yielded more detailed insights into the tumor immune microenvironment by identifying discrete subsets of immune, stromal, and malignant cells and by establishing the molecular interactive networks in CRC. Also, premalignant gene expression programs have been found through single-cell sequencing of precancerous polyps. Furthermore, during malignant transformation, significant alterations at the tumor microenvironment were described, particularly regarding fibroblast subpopulations, enrichment of regulatory T cells, and reduced B cells in polyps (39,40). Moreover, macrophage profiles and locations have also been studied with this extensive analysis, since it has been considered that the initial M1 and M2 classifications were not suitable in CRC, considering the heterogeneity of CRC immune populations. One example of a recent study explored the monocyte/macrophage populations in CRC and identified ficolin-1 (FCN1)+ monocyte, heat shock protein family A (Hsp70) member 6 (HSPA6)+ monocyte, OAS+ macrophage, oxidized low-density lipoprotein receptor 1 (OLR1)+ macrophage, and folate receptor β (FOLR2)+ macrophage populations with distinct gene expression signatures. Furthermore, they detected abundant $FOLR2^{+}$ macrophages, T regulatory (Treg) cells, exhausted $CD4^{+}$Tcells, exhausted $CD8^{+}$Tcells, and tolerant $CD8^{+}$Tcells in cancer tissues, constituting what they defined as the CRC immune module (CCIM). Colocalization of these cells was observed in tumor tissues, indicating the potential roles of CCIM topology in reprogramming the suppressive TME in CRC (40).

The Extracellular Matrix

Another important feature of the TME is the composition and organization of the ECM, whose biochemical and biomechanical properties affect the behavior of the cells. The main role of the ECM is to provide support and anchoring for the cellular components of the TME, through an intricate and dynamic network of ECM proteins but also to act as a signaling reservoir of multiple growth factors, hormones, and cytokines. It is composed of various macromolecules, including proteoglycans, glycoproteins, adhesive (laminin and fibronectin) and structural (collagen and elastin) proteins, polysaccharides, various metabolites, growth factors, enzymes, and cytokines (20,22). Subtypes of these ECM components also exist, which further define their roles within the ECM's general structure and characteristics. Since structure determines function, various ECM molecule subtypes and combinations confer distinct functions that are necessary for the body as a whole to function (41).

Collagen constitutes the major component of the ECM, around 90% in humans, and comprises 3 polypeptide α chains arranged in a triple helical configuration. Numerous cellular functions, such as adhesion, migration, and proliferation, are influenced by collagen. The collagen family, thought to consist of about 28 proteins, is further subdivided into fibril-forming collagens, fibril-associated collagens with interrupted helices (FACIT), and network-forming collagens. Fibrillar collagens are fibrous proteins that are frequently present in the skin, cartilage, tendons, and cornea. Depending on tissue location, a collagen fiber can contain multiple subtypes of collagen. Type I collagen, the most abundant type of fibrillar collagen, is found in connective tissues such as skin, bones, tendons, and cornea, being highly implicated in processes like wound repair and organ development. FACITs are associated to the surface of collagen microfibrils and bind with other ECM proteins to mediate the formation of a higher-order structure. Network-forming collagens are abundant at the basement membranes. Collagen IV is one example; via its N-terminal domain, it forms a tetramer, which subsequently binds to another similar molecule to form a hexamer. As a result, it can create a stable collagen network that divides the interstitial stroma from the basal lamina. In healthy tissues, the orientation of collagens can be very consistent; in pathological conditions, however, this orientation can vary. Overall, the amount of the different collagens in the ECM determines a variety of its properties, including elasticity and the availability of biomolecules like chemokines and growth factors. Collagens play additional vital roles. For instance, they are crucial in basement membranes, contributing to separating the various tissue layers. The normal exchange of biomolecules and cell movement within basement membranes can be disrupted by increased collagen deposition that causes membrane hardening. Since less collagen is deposited, basement membranes in many pathological conditions, including cancer, are thinner than those in normal tissues (22,41).

Proteoglycans consist of a core protein to which glycosaminoglycans (GAG) are covalently bound. GAGs contain repeating disaccharide units resulting in long, linear, anionic polysaccharides. Hyaluronic acid, keratan sulfate, chondroitin/dermatan sulfate, and heparan sulfate, which includes heparin, are the four categories of GAGs. Proteoglycans are able to sequester water and divalent cations, which confers them space-filling and lubricating properties, due to the highly negatively charged GAG chains. Large proteoglycans, as versican and aggrecan, small leucine-rich proteoglycans, as decorin and lumican, and basement membrane proteoglycans, as perlecan, are examples of secreted proteoglycans. Proteoglycans can be cell-surface-associated, like syndecans, and intracellular, as serglycin. Numerous biological functions are supported structurally by the molecular diversity of proteoglycans. Aggrecan, for example, produces elasticity and a high biomechanical resistance to pressure in cartilage. Decorin and lumican play a role in regulating collagen fibril assembly. Proteoglycans are also implicated in cell signaling and biological processes, including angiogenesis. Furthermore, they also interact with growth factors and their receptors (22,41,42).

Laminins are trimeric glycoproteins composed of α, β, and γ chains that are frequently observed in the basal lamina and certain mesenchymal compartments. Laminins perform a variety of cell type-specific functions, including adhesion, migration, differentiation, phenotypic maintenance, and resistance to apoptosis. When combined with the type IV collagen network, which is associated with basement membrane maturation, they form a cross-linked web, essential for structural stability. Laminins can establish a dynamic connection between cells and ECM by binding integrins, which facilitates the induction of signaling pathways and the organization of the intracellular cytoskeleton (41,42).

Fibronectin, a multi-domain protein, connects the cell to the ECM by interacting with its constituents. Although it is encoded by a single gene, alternative splicing of the mRNA results in 20 different isoforms in humans. Similar to collagen, fibronectin creates an ECM fibrillar network. The two cysteine disulfide bonds in fibronectin allow it to exist as a dimer outside of cells naturally, which is essential for its fibrillar assembly. Selective binding to integrins facilitates the assembly of the fibronectin matrix. It is via these integrins that the compact and soluble fibronectin that is secreted is unfolded, exposing hidden binding sites that allow additional fibronectin molecules to form the fibrillar network of fibronectin. High concentrations of fibronectin are locally produced at the cell surface through integrin clustering induced by fibronectin binding. Once fibronectin is bound to the cell surface by integrins, the actin cytoskeleton can pull onto fibronectin molecules to alter its conformation. As a result, cryptic binding sites for fibronectin, heparan sulfates, heparin, collagen, and other ECM proteins will become visible in the C-terminal regions of fibronectin. The fibronectin network matures and becomes insoluble through strong non-covalent protein-protein

interactions; however, mature lateral interactions between fibrils may be mediated by other ECM proteins. At individual sites, these interactions stabilize the relatively weak binding sites. Fibronectin is known to play various roles, including the assembly of collagen type I, since it has multiple binding sites for other ECM proteins. In the absence of fibronectin, collagen fibrils do not accumulate (22,41,42).

The ECM components confer unique physical, biochemical, and biomechanical properties, when orderly arranged, that aid in the regulation of cell behavior. The physical properties are associated with ECM's role in scaffolding to support tissue architecture and integrity. Features such as rigidity, porosity, insolubility, spatial arrangement, and orientation comprise the physical properties of ECM. Cell migration is influenced by these characteristics since they function as a barrier, anchorage site, or movement track (22,42,43). The EMC's biochemical characteristics are related to its direct and indirect signaling abilities, which enable cells to sense and interact with their surroundings through a variety of signal transduction cascades that alter gene expression or other aspects of cell behavior (42,43). EMC's biomechanical properties, which include ECM's elasticity that allows a shift from soft to stiff, also determines cell behavior, including cell differentiation and tissue functions, by providing environmental cues that aid cells in sensing and perceiving external forces (43).

One of the most prominent features of cell-ECM interactions is that they are reciprocal. Cells are constantly creating, decomposing, reorganizing, and realigning the components of the ECM, altering its properties. In turn, any changes in the ECM resulting from cellular activities will influence adjacent cells and modify their behavior, since the ECM regulates various cellular behaviors. This regulatory feedback mechanism between cells and the ECM allows cells and tissues to adapt quickly to their environment. Another relevant feature of ECM properties is that they are intertwined and not independent, conferring ECM the ability to be highly dynamic, and not just an inert scaffold that solely provides structure for the cells (41,43,44).

The ECM can act as binding sites, regulating cell adhesion and migration. The intricate composition and structure of the basement membrane, which acts as a partition between epithelial cells and the interstitial stroma, highlights this. The ECM is a key signaling mediator and a reservoir of multiple cytokines, chemokines, and growth factors, regulating their release and presentation to target cells, in addition to their structural integrity and anchorage. Ultimately, the cytoskeletal apparatus and multiple intracellular signaling pathways are triggered by the mechanical signals that the ECM delivers to the cells (43). ECM also regulates cell growth and communication, as well as maintaining cell polarity and division. Moreover, it also regulates several biological processes related to disease progression, including increased cell proliferation, apoptosis and hypoxia resistance, invasion, metastasis, angiogenesis, immune evasion of cancer cells, and stemness (22,45).

Normally, the ECM is highly organized into sheets that provide resistance and strength to tissues and organs. However, in pathological conditions, such as cancer, the type and composition of ECM may differ. This difference depends on the resident cells and the needs of the specific tissue (20,22,45).

ECM proteins are generally present in both malignant and normal tissues. In normal tissues, these proteins exhibit a homogenous distribution, in contrast to their highly irregular and heterogeneous distribution in tumors. Laminin, type I collagen, fibronectin, and hyaluronic acid are richly present in tumors. In addition to its protein composition, the ECM also undergoes structural changes in cancer. Tumors are stiffer than adjacent normal tissues. Cancer cells, together with CAFs and TAMs, modulate the ECM through excessive deposition of structural components such as collagens, as well as cross-linking enzymes from the lysyl oxidase (LOX) and transglutaminase families. Collagen and elastin fibers are reoriented and cross-linked by these enzymes, resulting in larger, more rigid fibrils that facilitate cell migration, as well as causing a loss of structural organization of the ECM (22,45).

Mechanical stimuli, including compression, matrix stiffness, and fluid mechanics, are constantly affecting solid tumors (22). Since the gastrointestinal tract is naturally exposed to increased endogenous mechanical stress from intestinal transit, this results in a complex mechanical microenvironment in the case of CRC (45). A dense ECM may also act as a signaling reservoir for several multiple growth factors and cytokines, activating molecular pathways that modulate cell behavior (22)

Considering the available research performed regarding cell-ECM interactions, it has been demonstrated that cells present a different behavior in 2D and 3D cultures. As such, new models have been developed in an effort to better mimic the native TME. Decellularized ECMs from native tissues have been widely used (45). Previous research performed by the group demonstrated that normal and tumor-decellularized matrices, obtained from CRC patients' surgical resections, distinctly promoted macrophage polarization. Indeed, macrophages in tumor-derived matrices differentiated towards an anti-inflammatory M2-like phenotype and exhibited higher levels of CCL18 compared to their normal counterpart. Matrigel invasion assays revealed that tumor ECM-educated macrophages efficiently stimulated cancer cell invasion through a CCL18-dependent mechanism. Importantly, we have also demonstrated that this chemokine is preferentially expressed at the invasive front of more advanced tumors, at areas where anti-inflammatory macrophages and Tregs are abundantly located (46).

CCL18

Immune cells communicate. Chemokines are a large family of low-molecular-weight chemotactic cytokines, known for mediating immune cell recruitment and lymphoid tissue development. Chemokines can also, directly and indirectly, impact cancer and endothelial cells in the TME to regulate tumor cell growth and proliferation, angiogenesis, cancer stem-like cell properties, invasiveness, and metastasis, and to influence tumor immunity and cancer progression (47). One of these is CCL18.

CCL18 was first discovered in the late 1990s and was named considering organ-specific expression and synthesis by specific cell types. It was found to be a highly expressed gene in the lungs and to be produced by the anti-inflammatory alternatively activated macrophages. As a result, four distinct names coexisted at the same time: pulmonary and activation-regulated chemokine (PARC), macrophage inflammatory protein-4 (MIP-4), dendritic cell chemokine 1 (DC-CK1), and alternative macrophage activation-associated CC chemokine-1 (AMAC-1). Currently, it is commonly known as CCL18 (48,49).

The human chromosome 17q11.2 contains the gene encoding this chemokine *(CCL18)*, which is constituted of 7.2kb divided into three exons and two introns. The synthesized mature protein has a weight of 78kDa and a length of 69 amino acids, with a typical structure of a CC chemokine, containing two-disulfide bonds (Cys10-Cys34 and Cys11-Cys50) required for its activity (49,50). The active biological form can be truncated to 68 amino acids without a terminal alanine at the C-terminus. It is believed that after rodents and primates diverged, duplicated CCL3-like genes fused to form the *CCL18* gene strictly present in primates. To date, no *CCL18* ortholog has been discovered in rodents (48,49). The absence of a proper animal model has diminished immunologists' interest in this chemokine signaling and function.

Under normal conditions, CCL18 is expressed in high levels in the lungs, and lower in lymph nodes, thymus, bone marrow, and placenta. It is present in blood and serum at approximately 30ng/mL, a significantly higher concentration than most chemokines, and it is upregulated in pathological conditions, such as inflammatory diseases and cancer (48).

Myeloid antigen-presenting cells (APCs) are the primary source of CCL18. These include alveolar macrophages, follicular dendritic cells *in vivo*, monocyte-derived dendritic cells (DCs), mast cells, eosinophils, and alternatively activated macrophages *in vitro*. However, it must be emphasized that CCL18 secretion frequently requires triggering through specific stimuli. In fact, human-isolated monocytes and DCs do not naturally produce CCL18 *ex vivo*; however, IL-4, IL-13, IL-33, IL-10, or TGF-β can induce the secretion of CCL18 (51). Additionally, CCL18 production is also regulated by environmental factors, such as microbial

infections that cause fibrotic and inflammatory diseases, and allergen exposure (48). Moreover, macrophage irradiation is described to up-regulate CCL18, while hypoxia and IFN-γ are reported to down-regulate CCL18 expression in DCs and macrophages (51,52).

Chemotaxis, inflammation, and fibrosis are three well-described functions of CCL18 (Figure 4). Human naive T cells, Th2 cells, memory T cells, B cells, immature DCs, NK cells, basophils, bone marrow progenitor cells, and fibroblasts are all attracted to CCL18 due to its chemotactic activity. Importantly, CCL18 was the first chemokine to demonstrate a predominant capacity to attract human Tregs, which suggests CCL18 is a potent regulatory chemokine. CCL18 acts in order to maintain tolerance and to suppress deleterious inflammation, under normal and pathological conditions (48,53).

CCL18 also directly affects immunity, fibrosis, cancer cell invasion, and immune escape. It influences immunity by directly modulating immune cells, as CCL18 promotes monocytes to dendritic cell differentiation, or by presenting tolerogenic characteristics, including increasing IL-10 production and the ability to suppress effector $CD4^+CD25^-$ cell proliferation. Additionally, CCL18 polarizes memory $CD4^+$ T cells into $Foxp3^+$ Tregs, which produce high levels of IL-10 and TGF-β, sustaining CCL18 expression and an immunosuppressive environment. However, in allergic patients, the immunosuppressive effect of CCL18 on DCs and on memory T cells is eliminated, possibly as a result of the reduced tolerance to environmental stimuli observed in these conditions (48,53).

Interestingly, CCL18 appears to have a moderate pro-inflammatory potential in addition to its anti-inflammatory properties. In particular, although CCL18 drives monocytes to differentiate into M2-like anti-inflammatory macrophages, they exhibit a mixed pattern of inflammatory and regulatory characteristics, respectively a high capacity for phagocytosis and the expression of pro-inflammatory cytokines CXCL8, CCL2, CCL3, and CCL22; and high IL-10 production. CCL18's dual role is a current matter of debate and investigation, being also noted in inflammatory diseases. In order to prevent inflammation, CCL18 inhibits inflammatory responses. However, CCL18 is highly expressed in several inflammatory disorders, including allergies, asthma, giant cell arthritis, rheumatoid arthritis, or scleroderma (33,38).

Finally, CCL18 may promote the synthesis of collagen by lung macrophages, skin and lung fibroblasts, contributing to tissue repair in healthy, or to fibrosis in pathological conditions. Higher levels of CCL18 were associated with an increased risk of death, lung function deficit, collagen accumulation, and T lymphocyte infiltration, especially in interstitial lung diseases like idiopathic pulmonary fibrosis. Due to its relevance, CCL18-related fibrosis signaling pathways have been described and include protein kinase C α (PKC-α) and extracellular signal-regulated kinase 1 (ERK1) pathways, or Smad3 and TGF-β activity.

Accordingly, CCL18 is currently a good prognosis marker in fibrosis-related interstitial lung diseases. However, more research is needed to determine CCL18's role and function in other diseases, such as inflammatory and malignant pathologies (48,53).

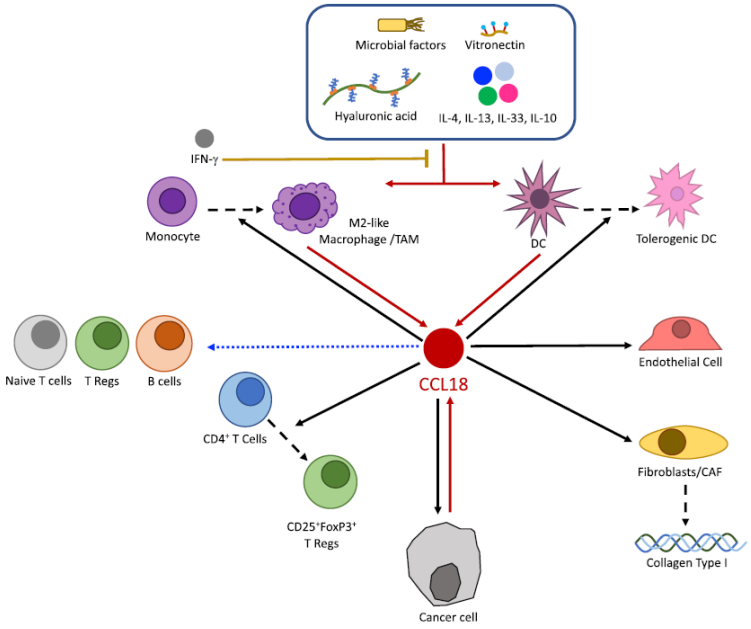

Figure 4. CCL18 expression and roles under physiological and pathological conditions. CCL18 is mainly produced by anti-inflammatory macrophages and immature DCs, upon activation by microbial products, specific interleukins, and ECM components, such as vitronectin and hyaluronic acid. Cancer cells also produce CCL18 (straight, red arrows). The pro-inflammatory cytokine IFN-γ is reported to inhibit CCL18 production. CCL18 is described to promote differentiation of M2-like macrophages, tolerogenic DC and CD25+FoxP3+Treg cells (dashed black arrows) and, to stimulate fibroblast proliferation and collagen production, promote endothelial cell migration and angiogenesis, stimulate cancer cell invasion (straight, black arrows), and act as a chemoattractant to naïve T cells, Tregs and B cells (dashed blue arrow) (53).

CCL18 Receptors

The CCL18 receptor remained unknown for many years following its discovery. Recently, three different CCL18 receptors were described: C-C motif chemokine receptor 8 (CCR8) (54), membrane-associated phosphatidylinositol transfer protein 3 (PITPNM3) (55), and G protein-coupled receptor 30 (GPR30) (56) (Figure 5).

CCR8

CCR8, formally referred, by the lack of known ligand, as the orphan receptor TER1, ChemR1, or CKR-L1, is classified as a class A G protein-coupled receptor (GPCR). It was recognized for its capacity to bind to the CC chemokine I-309, also known as CCL1. It is encoded by a gene located in chromosome 3p21, containing 2 exons, that predicts a polypeptide of 355 amino acids (57–59).

Many chemokines, including CCL1, CCL8, CCL16, and CCL18, can bind to CCR8, with CCL1 being the only chemokine that exclusively interacts with CCR8. It is highly

expressed in the thymus, and the spleen, and at residual levels in peripheral blood lymphocytes (57,58). Numerous cell types, such as Th2 cells, eosinophils, monocytes, phagocytes, and endothelial cells, express this receptor (57).

It was suggested that CCR8 may exacerbate allergic inflammation and asthma (60–62), although opposing information has been reported as well (63–65). Additionally, CCR8 may also function as a human immunodeficiency virus (HIV) co-receptor, promoting HIV-1 and HIV-2 infections, at least *in vitro* (66,67). CCR8 is also expressed on mouse and human group 2 innate lymphoid cells (ILC2s) and on a subgroup of IFN-γ producing intestinal ILCs (68–70). The CCL1-CCR8 axis protects from acute intestinal damage in a mouse model of experimental inflammation and plays an important role in the homing of lymphocytes to the healthy skin which is the reason to be crucial in the physiology of this tissue (70,71).

CCR8 is also associated with cancer. When activated by CCL1, it promotes angiogenesis, resistance to apoptosis, and cancer cell proliferation and migration, in several cancer types, including T-cell leukemia, bladder, colorectal, and breast cancer (71). Through CCL18, CCR8 stimulates cancer cell migration and epithelial-to-mesenchymal transition (EMT) in breast, lung, and bladder cancer. This chemokine attaches itself to glycosaminoglycans on extracellular vesicles, enabling cells that express CCR8 to retain them (71). A highly enriched and specific pattern of CCR8 expression was also observed in tumor-resident Tregs, which suppress anti-tumor effector T cell responses (72–74). This observation was supported by the correlation of reduced xx cancer patients survival with the presence of $CCR8^+$ Tregs in the TME (72,73). Another critical function is the ability of the involvement of the CCL18/CCR8 axis in the recruitment of Treg cells into the tumor niche and the subsequent conversion of $CD4^+$ T cells into Tregs, unveiling the immunosuppressive functions of this chemokine (71).

Increased expression of CCR8 influences the prognosis of several cancers. In glioma, renal, and testicular cancer, it is associated with a worse prognosis. In contrast, in melanoma, colorectal, head and neck, stomach, pancreatic, cervical, and ovarian cancer, its higher expression is associated with a better prognosis. No correlation was, however, found in thyroid, lung, liver, urothelial, prostate, breast, and endometrial tumors (71).

Targeting CCR8 has shown promising therapeutic effects in the treatment of autoimmune diseases and cancer. The progression of the disease was inhibited in an experimental multiple sclerosis model when CCR8 in Treg cells was activated via a CCL1-Ig fusion protein (75). Interestingly, blocking the CCL1-CCR8 axis with an anti-CCL1 or with an anti-CCR8 antibody enhanced anti-tumor immune responses and reduced tumor burden (76,77). CCR8-targeted therapy led to Treg depletion and also prevented tumor growth, when used in parallel with anti-PD-1 therapy, or even in situations where tumors are resistant to

PD-1 antibody treatment (78). A few small molecules that target CCR8 have been developed recently. The nonpeptide agonist LMD-009 has a strong affinity for CCR8 in the nanomolar range and functions similarly to CCL1 in terms of efficacy and potency (57).

Numerous chemical classes of small molecules with agonistic or antagonistic activity profiles have been discovered as a result of the search for possible therapeutic candidates and pharmacological tools that target CCR8. These include analogues of phenoxybenzyl, oxazolidinone, and diazaspiroundecane, as well as naphthalene-sulfonamide based scaffolds (79).

PITPNM3

PITPNM3, a six-transmembrane receptor, also known as PYK2 N-terminal domain-interacting receptor 1 (Nir1), encodes a protein belonging to the phosphatidylinositol transfer protein (PITP) family. It is encoded by a gene located on chromosome 17p13.1, containing 22 exons and, depending on the isoform, the protein encoded by this gene presents approximately around 930 amino acids (80). This consists of a membrane-bound receptor, in contrast to PITPNM1 and PITPNM2, other family members that are highly enriched in the Endoplasmic reticulum and in the Golgi complex. The phosphatidylinositol transfer protein domain (PITP), the acid region/Ca2+ binding domain, the six transmembrane domains, the DDHD, and the C-terminal domain that interacts with proline-rich tyrosine kinase 2 (PYK2) are all present in members of the PITP family (81).

Notably, the human PITPNM3 is frequently expressed in distinct tissues, including the brain, retina, and other neural tissues, but also in spleen, breast, and ovary (82). This transmembrane receptor transfers phosphatidylinositol and phosphatidylcholine between membranes, which helps to regulate lipid signaling pathways and the lipid metabolism. It also interacts with the protein tyrosine kinase PYK2, and takes part in adenosine triphosphate (ATP)-dependent $Ca2^{+}$-activated secretion. Furthermore, it interacts with phosphoinositides to influence important signaling pathways related to modulation of cell survival and growth and, through its C-terminal region, migration (80,82).

PITPNM3 has been implicated in several cancers, and described to promote cell migration, invasion, tumor growth, EMT, and metastasis, exhibiting high expression in breast, pancreatic, ovarian, prostate, and non-small lung cancer, hepatocellular carcinoma, oral squamous cell carcinoma, and squamous cell carcinoma of the head and neck (55,83).

It frequently facilitates the growth of tumors by acting as a co-receptor for ligands such as chemokines like CCL18, known to promote tumor progression in lung and ovary cancer. Upon binding to this chemokine, PITPNM3 may phosphorylate its downstream factor protein tyrosine kinase 2 beta (PTK2B) via the PTK2B binding domain, which leads to

metastasis-related signaling pathways activation, such as NF-κB, also associated to EMT (80,81,84). Moreover, PITPNM3 activation may also cause phosphorylation of the phospholipase Cγ1 (PLCγ1) and the activation of the protein kinase C-ζ (PKCζ) pathway. The expression of the inositol 1,4,5-trisphosphate 3-kinase isoform B (IP3KB) may also increase, activating intracellular calcium signaling. It also causes signal transduction within the JAK2/STAT3 pathway, leading to cancer cell proliferation, migration, and EMT (49). In parallel, the PI3K-Akt/protein kinase B (PKB) pathway may also activated, playing a role in cancer cell migration, proliferation, and survival (85).

Given its ability to modulate crucial pathways associated to cell migration, invasion, and metastasis, PITPNM3 is regarded as a possible target for anti-metastatic treatments. Strategies to block the interaction between PITPNM3 and CCL18 are being investigated in order to inhibit cancer cell migration. There have been reports of therapeutic agents that target PTK2B and CCL18, as the NVP-TAE 226, a small molecular inhibitor. However, although this compound can inhibit the PTK2B, it appears to be a non-selective tyrosine kinase inhibitor since it also inhibits the insulin-like growth factor 1 receptor (IGF1R), the platelet-derived growth factor receptor (PDGFR), the fibroblast growth factor receptor (FGFR), and the cyclin-dependent kinase 1 (CDK1) (81). Several attempts are currently being considered towards the development of more specific inhibitors targeting the PITPNM3 receptor and its downstream associated signaling pathways.

GPR30

GPR30, also referred to as G protein-coupled estrogen receptor 1 (GPER1), is a receptor that exerts rapid signaling activities. It is categorized as a membrane-bound protein, member of the GPCR family, localized at the plasma membrane and in membranous organelles, such as the endoplasmic reticulum and Golgi apparatus. The gene coding for GPR30 is located on the chromosome 7p22.3, contains 3 exons, and encodes a 375 amino acid protein (86,87). As a GPCR, GPR30 presents seven transmembrane domains with an extracellular N-terminal region. The C-terminal region is cytoplasmic and interacts with hydrolases of nucleotide guanosine triphosphate (GTPases) or trimeric G-protein. Estrogen response elements (EREs) in the promoter region enable the binding of estrogen, which then modulate gene transcription (86,87).

Adaptive and innate immune response cells including circulating B and T lymphocytes, monocytes, macrophages, neutrophils, eosinophils, and DCs are reported to express GPR30. The binding of estrogens to this receptor leads to conformational changes that lead to the phosphorylation of the C-terminal region, which acts as docking sites for additional proteins binding. Generally, trimeric G-proteins are then recruited, become on their turn also phosphorylated and activate several downstream signaling pathways, stimulating

adenylate cyclase and increasing cyclic adenosine monophosphate (AMP) levels. It also facilitates intracellular calcium mobilization and synthesis of phosphatidylinositol 3,4,5-trisphosphate (PIP_3). Furthermore, it stimulates Src proteins and promotes MMP-2/9 activation, which may cleave surface bound Heparin-bound Epidermal growth factor (HB-EGF) and lead to epidermal growth factor receptor (EGFR) transactivation. In order to increase the expression of multiple genes connected to cell survival, proliferation, differentiation, migration, and invasion, GPR30 can also activate mitogen-activated protein kinase (MAPK) and PI3K/Akt in succession. Several tissues, such as the heart, kidneys, liver, brain, vascular system, and reproductive organs, express GPR30. It is essential for numerous biological processes, including bone and nervous system development, metabolism, cognition, reproductive health, cardiovascular, and uterine functions (86,87).

GPR30 can bind to any of the three physiological forms of estrogen: estriol, estradiol, and estrone. Estriol appears to act as an antagonist for this receptor, while estrone and estradiol act as agonists (87). Estradiol and estrogen receptor α (ERα) inhibitors, including tamoxifen, fulvestrant, raloxifene, aldosterone, and natural substances like kaempferol, can activate GPR30, triggering tissue-specific signaling. There have also been descriptions of synthetic ligands, such as G-1, which is a selective agonist that works to activate GPR30 without interfering with the function of the classical nuclear estrogen receptors (ERα and ERβ). Thus, given its specificity, G-1 become a crucial tool in the investigation of GPR30 function and possible therapeutic applications, particularly in the treatment of cancer and cardiovascular illnesses. Additionally, G36 is described as a selective antagonist of GPR30. This synthetic ligand blocks the receptor and prevents it from being activated by other ligands, endogenous or synthetic, becoming useful to differentiate GPR30-specific signaling effects (86,87).

As GPR30 responds to estrogen, it may contribute to the protective effects associated with estrogen in cardiovascular diseases. Additionally, this receptor can be connected to diseases such as diabetes and obesity, since it also affects insulin secretion and glucose metabolism (87).

Tumor progression has also been associated with GPR30 expression, especially in hormone-sensitive cancers. Depending on the type of tumor, it may show tissue-specific activity that is either pro- or anti-tumoral. The level of the receptor varies according to its function; in gastric, ovarian, and hepatic cancer, for example, when it exhibits anti-tumoral activity, its expression is lower than in normal tissues. Activation or overexpression correlates to decreased tumorigenic properties, which supports the anti-tumoral role of GPR30 in these cancer types. An example is that its activation inhibits the growth of malignant cells through GPER/ERK signaling in hepatocarcinoma and xenograft models. Additionally, histone H3 deacetylation and promoter methylation have also been linked to the low expression of this

receptor in the hepatocarcinoma model. Moreover, tamoxifen-induced GPR30 activation reduces the anti-inflammatory macrophage phenotype and suppresses pancreatic cancer proliferation, migration, and invasion while controlling the tumorigenic milieu (86).

GPR30 is also described to contribute to carcinogenesis. Despite intracellular GPR30 is primarily found on the endoplasmic reticulum, receptor cytoplasmic location has been linked to an advanced stage of cancer. Increased expression of GPR30 in cancer cells and tissues promotes cancer development, serving as an indicator of predictive poor prognosis. This occurs in lung, prostate, cervical, glioblastoma, and breast cancer models. The expression of cell adhesion molecules, MMPs, focal adhesion (FA) pathway genes, cyclin D1 (CCND1), anti-apoptotic protein B cell lymphoma (Bcl-2), and TFs have been linked to GPR30 activation in tumorigenic cells (86).

In CRC, GPR30 presents dual activity, associated to gender, depending on estrogen levels. Men with higher levels of GPR30 had a better prognostic outcome, while women showed the opposite effect. In contrast, *in vitro* studies have shown that GPR30 activation, which promotes cell migration and proliferation, is connected to CRC. Conversely, the receptor and GPR30-induced gene expression are subject to epigenetically controlled processes that require further investigation (86) .

This receptor is also associated to CCL18 in acute lymphocytic leukemia B. However, this binding does not result in direct signal transduction. Instead, it only disturbs the signal transmission from the receptor for the CXCL12. This reduces the chemotaxis and proliferation of tumor cells with a high expression of the CXCL12 chemokine (56).

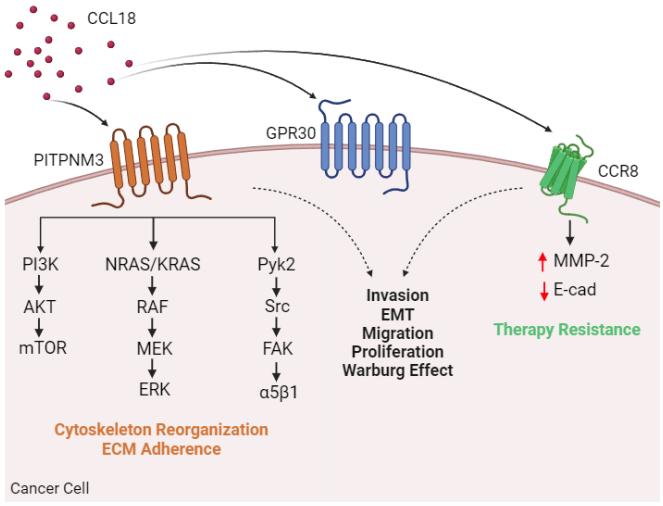

Figure 5. CCL18 receptors and signaling pathways in cancer cells at the tumor microenvironment. Until now, the known receptors of CCL18 are PITPNM3 (orange), GPR30 (blue), and CCR8 (green) and upon binding with CCL18 signaling pathways such as PI3K/AKT/mTOR, Ras, Pyk2/Src/FAK are activated. Consequently, cellular responses related with cancer progression are triggered, namely, cell growth, survival and proliferation, EMT, migration, invasion, stemness, cytoskeleton reorganization, ECM adherence, and therapy resistance. Created with Biorender.com.

CCL18 in Cancer

The invasion of neighboring tissues is the initial stage of metastization and a required step for latter vessels intravasation, extravasation, and metastasis. This entails significant cellular alterations, many of which are aided by EMT reprogramming. These changes include cytoskeleton reorganization and alteration in the cell-matrix adherence, culminating in increased migration, increased proteolytic activity of ECM components, and inhibition of cancer cell apoptosis (88). It is reported that CCL18 influences all these processes (Figure 5), culminating with an association with increased metastasis and subsequently lower survival (83,84,89–93).

At the TME, CCL18 is produced in large amounts by TAMs, however, CAFs and cancer cells can also produce this chemokine, even if in smaller amounts, creating an anti-inflammatory microenvironment rich in CCL18, where it may act in an autocrine manner, sustaining immunosuppression (94,95).

CCL18 is described to influence cancer cell proliferation but this effect is dependent on the type of tumor. In non-small cell lung cancer cells and pre-B acute lymphocytic leukemia cells, CCL18 reduces cancer cell proliferation (56,96). In contrast, in breast cancer, diffuse large B cell lymphoma, ovarian cancer, osteosarcoma, urothelial carcinoma, and glioma, this chemokine increases the proliferation of cancer cells (90,91,97–100). Moreover, CCL18 does not seem to affect the proliferation of gastric cancer, pancreatic ductal adenocarcinoma, multiple myeloma, and glioblastoma multiforme cells (92,93,101,102).

CCL18 is described to induce EMT in tumor cells (46). During this transition, epithelial cells lose their polarity and adhesion and gain migratory and invasive properties (103). CCL18 has been demonstrated to induce EMT in many cancers, including hepatocellular, pancreatic, lung, breast, and bladder cancers, by activating the TFs Slug and Snail 1 (84,93,104–108), which in turn regulate promoter activation and gene transcription. The up-regulation of Slug depends on the mammalian target of the rapamycin mTOR signaling pathway (107).

Other effects that CCL18 are stimulation of cancer cell adherence, migration, and invasion, as seen in breast, pancreatic, ovarian, gastric, prostate, and bladder cancer, hepatocellular carcinoma, osteosarcoma, oral squamous cell carcinoma, multiple myeloma, glioblastoma multiforme, and glioma (84,93,100–102,108–110). PITPNM3 appears to be the major receptor involved in these CCL18-induced activities. In fact, PITPNM3 activation by CCL18 was associated with NF-κB signaling, and the activation of focal adhesion kinase (FAK), Pyk2, and Src. Other pathways are also involved such as protein kinase B (Akt), and PI3K (49).

PITPNM3 activation by CCL18 also results in the induction of angiogenesis, which is closely related to the migration and metastasis of cancer cells. In this case, CCL18 and VEGF synergistically promote endothelial cell migration and angiogenesis in breast cancer (111). Moreover, in bladder cancer, CCL18 causes an increase in the production of VEGF-C and MMP-2, which are factors involved in lymphangiogenesis, being this process dependent of CCR8 (104).

CCL18 as a Tumor Marker

Given its enhanced expression and importance in the cancer context, CCL18 is considered a marker of malignant diseases. Research has shown that tumor tissues have higher expression of CCL18 compared to normal ones in tumors such as cutaneous basal cell carcinoma, glioma, breast cancer, and glioblastoma multiforme (102,112–114). Additionally, cancer patients have higher CCL18 serum concentration, especially in cases of T-cell acute lymphoblastic leukemia, breast cancer, cutaneous T-cell lymphoma, laryngeal squamous cell carcinoma, non-small cell lung cancer, ovarian cancer, pancreatic ductal adenocarcinoma, prostate cancer, and multiple myeloma. Higher urinary CCL18 concentration were also found in bladder cancer patients, than in healthy individuals (93,101,114–123). Notably, CCL18 levels were described to be proportional to the degree of disease development, including tumor stage, Ki67 proliferation marker expression, and presence of lymph node metastasis (101,114,118,124,125). Regarding association with patients' prognosis, in cancers like breast cancer, cutaneous T-cell lymphoma, laryngeal squamous cell carcinoma, lung cancer, oral squamous cell carcinoma, ovarian cancer, osteosarcoma, pancreatic ductal adenocarcinoma, esophageal squamous cell carcinoma, uveal melanoma, and multiple myeloma, increased levels of CCL18, in the tumor or the serum, reflected worse prognosis (89–91,93,101,117–120,126–129). In contrast, gastric adenocarcinoma is associated with a better prognosis (130). An exception is non-small cell lung cancer, in which a greater infiltration of CCL18-producing cells is associated with a better prognosis, although the level of this chemokine in the plasma has been, paradoxically, associated with a worse prognosis (118,131).

In CRC the minimum available information is contradictory. Higher levels of CCL18 have been associated with a better prognosis, however, our group found that macrophage-produced CCL18 stimulates CRC cell invasion *in vitro* (46,132). In this work, normal and tumor-decellularized matrices, obtained from CRC patients' surgical resections, distinctly promoted macrophage polarization. While over normal matrices, monocytes differentiated into pro-inflammatory macrophages, in tumor-derived matrices monocytes differentiated towards an anti-inflammatory phenotype, characterized by high expression of the immunosuppressive molecules IL-10, TGF-β, and CCL18, and lower expression of CCR7 and TNF, both characteristic markers of pro-inflammatory macrophages (46). Matrigel

invasion assays revealed that tumor ECM-educated macrophages efficiently stimulated cancer cell invasion through a mechanism involving CCL18. Importantly, we also found that this chemokine is preferentially expressed at the invasive front of more advanced colorectal tumors (stage III and stage IV) (46).

In summary, the potential of CCL18 as a diagnostic and prognostic biomarker in various cancers is evident. Nevertheless, the possibility of CCL18 premature detection in patients' blood or serum, specifically in pre-malignant lesions, requires further investigation as it could be helpful in early diagnosis.

Chapter 2: Aim

The sequence of events leading to the development of tumor cell invasion and metastasis is of primary importance in the prognosis of cancer patients, considering that secondary tumors in distant organs are largely responsible for cancer mortality and morbidity. It is well described that CCL18 influences several of these events, in various cancer types, being considered an important factor in cancer progression and prognosis, and suggested as a potential therapeutic target (49). However, in CRC, little is known about the effect of this immunosuppressive chemokine on tumor cells. Our group has previously demonstrated that when monocytes were seeded over tumor-decellularized matrices, derived from CRC patients' surgical resections, they differentiated as anti-inflammatory macrophages, expressing high levels of CCL18 (46). Interestingly, we reported that this immunosuppressive chemokine was secreted and able to stimulate colon cancer cell invasion and that was expressed at the invasive front of more advanced colorectal tumors. However, the inherent mechanism of action was not explored and remains to be understood. Furthermore, we also described that CCL18 stimulates the phosphorylation of EGFR and of its associated downstream partners, FAK, Src, Akt, and ERK. However, EGFR has never been described as a putative CCL18 receptor and other three canonical cell membrane receptors as GPR30, PITNM3 and CCR8 were appointed as CCL18 receptors in other conditions (53).

Therefore, this project aims to understand and identify the exact mechanisms by which CCL18 influences cancer cell behavior and to identify its putative receptor. To accomplish that, three major tasks were established:

Task 1 – Disclose the impact of CCL18 on invasion-associated activities *in vitro*.

Invasion can result from enhanced cell migration and/or proteolysis of underlying ECM components. After invading, tumor cells aim to metastasize, and, to do so, they need to proliferate and to escape immune recognition to form a sustainable secondary tumor. With this in mind, we decided to explore, in this first task, the influence that CCL18 may have on cancer cell invasion, migration, and cell cycle, as well as its ability to induce matrix metalloproteases activity.

Task 2 – Dissect the impact of CCL18 on tumor growth and angiogenesis *in vivo*.

Exacerbated tumor growth leads to deficient nutrient availability, exposure to toxic metabolites, and low oxygen levels, which overall stimulates the formation of new blood vessels (neoangiogenesis), facilitating nutrient and oxygen acquisition for the cells within the tumor. Therefore, in this second task, we aimed to assess the *in vivo* effect of CCL18,

studying the impact of this chemokine on tumor growth, neoangiogenesis and invasion through the chorioallantoic membrane of fertilized chicken eggs.

Task 3 – Identify the CCL18 receptor(s) and signaling pathways in CRC cell lines.

Lastly, although we know that CCL18 influences tumor cells to invade, we are still unsure of the exact mechanism. As such, in this third task, we seek to identify the CCL18 receptor in our CRC cell lines and the associated signaling pathways of action. In order to achieve this, we decided to follow an educated-guess and a search approach. Through the first strategy, we aim to inhibit the previously described canonic CCL18 receptors (CCR8 and PITPNM3) and to understand the functional implications of their absence. Through the second strategy, we aim to carry out a pull-down assay using CCL18 as a decoy, following through a detailed proteomic analysis to understand which proteins are expressed upon the interaction between CCL18 and our cancer cells.

Chapter 3: Materials and Methods

3.1. Cell Culture

RKO and HCT-15 cell lines, derived from human colon adenocarcinomas, were purchased from the American Type Culture Collection (ATCC, USA). CRC cells were cultured at 37ºC, under a 5% CO_2 humidified atmosphere, in RPMI 1640 GlutaMAX™ Medium (Gibco, USA), supplemented with 10% fetal bovine serum (FBS) (Labclinics, Spain) and 1% penicillin-streptomycin (P/S) (Biowest, USA) (referred as complete RPMI 1640 medium).

3.2. Invasion Assay

The impact of CCL18 on RKO or HCT-15 (wild type or CRISPR-Cas9 $CCR8^{KO}$) cell invasion was evaluated using Matrigel invasion assays. Therefore, $5x10^4$ cells were seeded into the upper compartment of BD BioCoat™ BD MatrigelTM Invasion Chamber, of 8.0 µm pore-size PET Membrane filters, preinserted into 24-well cell culture plates (Ref: 354480, BD Biosciences, USA). These cells were treated or not with 10ng/mL of rhCCL18 in complete RPMI 1640 medium, at the moment of the seeding. At the lower compartment, only complete RPMI 1640 medium was added. A positive control of conditioned media from anti-inflammatory human macrophages (treated with 10ng/mL of IL10 for 72h) was also integrated into the experiments, in the lower compartment, in a proportion of 1/3 of the final volume. After 24h of incubation at 37ºC and 5% CO_2, filters were washed in phosphate-buffered saline (PBS) 1x, and fixed in 4% paraformaldehyde (PFA) (Sigma-Aldrich, USA). Non-invasive cells, present in the filter upper compartment, were scrabbed while, after washing in PBS 1x, invasive cells adhered at the filter lower compartment were counterstained with DAPI (Vector Laboratories, USA). Invasive cells were then scored, in at least 12 microscopic fields (20x objective) using a Zeiss Axiovert 200M microscope (Carl Zeiss, Germany). The invasive ratio was calculated relatively to unstimulated cells.

3.3. Cell Migration

In this work, two types of cell migration were evaluated: a collective wound-healing and single-cell assays, where cells move collectively as an assembly of multiple cells or individually, respectively.

Wound-Healing

This assay was performed on 24-well plates (SPL, Korea). While RKO cells were seeded at a density of $4x10^4$ cells/well, HCT-15 cells were seeded at a density of $7x10^5$ cells/well, to reach confluency at 72 hours (h) and 16h, respectively. Then, a gap was manually created using a 10µL pipette tip. The media was removed, and new media with 1% FBS and 1ng/mL or 10ng/mL of recombinant human CCL18 (rhCCL18) (Ref: 256089, Abcam, UK) was added. For the experiments with 1ng/mL of CCL18, the gap was monitored for 18h, and images were recorded every 10 minutes (min), in areas selected in the middle of the well, using Operetta CSL (Revvity, USA). For the experiments with 10ng/mL, the gap was monitored manually, with images recorded every 3h through an inverted microscope (Olympus), in areas also selected in the middle of the well. This sequential imaging allowed to register the progress of collective cell migration over time, until gap closure through cell-cell contact inhibition. The percentage (%) of gap closure was evaluated using the *Wound_healing_size_tool* plugin in ImageJ.

Single-Cell

RKO and HCT-15 cell lines were seeded into 24 Well Black ID 14mm ibiTreat plates (Ibidi, Germany) at a $5x10^4$ cells/well density, in RPMI 1640 supplemented with 1% FBS and 1% P/S and incubated at 37ºC, under a 5% CO_2 humidified atmosphere. After 6h, 1ng/mL or 10ng/mL of rhCCL18 was added to each well. Individual cells trajectories were then tracked for 15h (for 1ng/mL) and 20h (for 10ng/mL) and images were acquired every 10min using Operetta CSL (Revvity, USA). Accumulated migratory distance (µm), cell displacement (µm), cell speed (µm/sec), and straightness of movement were evaluated using Harmony 5.2 software (Revvity, USA).

3.4. Cell Cycle

Cell proliferation was evaluated through the assessment of cell cycle phases (G1, S, G2, M). For that, RKO and HCT-15 cells were seeded into 24-well plates (SPL, Korea), with a $2x10^4$ cells/well density. After 48h, 10ng/mL of rhCCL18 or equivalent volume of complete RPMI 1640 medium were added to the wells. Upon 72h, cells were detached and separated as a single cell suspension in FACS buffer (PBS, 2% FBS, and 0.01% sodium azide). After fixation with 70% ethanol, cells were washed twice in FACS buffer, treated with RNase (50µL of 100µg/mL stock, Thermo Fisher Scientific, USA) for 15min, to ensure that only DNA would be stained, and washed again twice. All these steps were performed at 4ºC. Before analyzing, propidium iodide (PI) (1µL of 100µg/mL stock, BD Pharmingen™, USA) was added to samples, as a viability dye. Then, around $2x10^5$ cells were acquired on FACS Canto

II Flow cytometer (BD Biosciences, USA), using FACS Diva Software. Cell cycle phases were evaluated with FlowJo software.

3.5. Gelatin Zymography

Invasion assay-derived conditioned media was analyzed by gelatin zymography to evaluate MMP-9 and MMP-2 activity. Protein content was determined by Dc Protein kit (Bio-Rad, Portugal). 10µg to 20µg of protein were mixed with sample buffer (10% sodium dodecyl sulfate (SDS), 4% sucrose, and 0.03% bromophenol blue in 0.25 M Tris–HCl, pH 6.8), loaded and separated on 10% polyacrylamide gels containing 1% of bovine gelatin (Sigma-Aldrich, USA) as substrate. Proteins were separated by electrophoresis at 100V. Following, gels were washed twice, to remove the SDS remnants, with a washing solution of 2% Triton X-100 (Fisher Bioreagents, USA), and once with deionized water. Gels were then incubated for 16h at 37ºC in MMP substrate buffer (50 mM Tris–HCl, pH 7.5, 10 mM $CaCl_2$, and 0.5% NaN_2). After this, gels were rewashed with deionized water and stained with Coomassie Brilliant Blue R-250 (Sigma-Aldrich, USA) solution (0.1% Coomassie blue; 10% acetic acid; 40% methanol) for 20min with agitation. After staining, the Coomassie solution was removed, and de-staining solution (10% acetic acid and 20% methanol) was added to the gels under agitation, to increase contrast. Gels were scanned (Bio-Rad) and stored in deionized water. MMPs molecular weight and activity were estimated by densitometric band analysis using the ImageJ software.

3.6. CAM Assay

Tumor growth and stimulation of angiogenesis were evaluated using the chorioallantoic membrane (CAM) model. This assay is performed in association with chick embryo development. Upon arrival, the eggs were cleaned with 70% ethanol, to eliminate dirt and residues in the eggshell. Then, they were placed laterally in autoclaved paper racks and incubated at 37ºC and 5% CO_2. At day 3 the eggs were removed from the incubator and a window was made. With a closed scissor, the wide base of the egg was punctured diagonally and 2.5 to 3mL of albumin was removed, to detach the CAM from the eggshell. A piece of transparent scotch tape was placed on top of the egg to form a window, and a small rectangle was made (1x2cm). Unfertilized eggs were discarded, and the window and the cut in the lateral of the egg were sealed in the viable ones. The eggs were returned to the incubator. At day 10, the CAM covers all the area beneath the window, thus a highly vascularized site was chosen, and a silicone ring was placed on top of it. RKO and HCT15 at a density of $1x10^6$ cells/egg and resuspended in 5µL of Matrigel (Ref: 356231, Corning, USA) were seeded into the ring. Cells were inoculated with 20ng/mL of rhCCL18 or with equivalent volume of complete RPMI 1640 medium. At day 13, the embryos were euthanized,

the rings were removed and the CAM surrounding the inoculation site was dissected. The images were acquired from the perspective of the embryo, with the CAM on top of the tumor. The tumor growth and the number of new vessels formed and intersecting the are of the silicone ring were evaluated using ImageJ.

3.7. Immunohistochemistry Analysis

For histological analysis, CAMs were fixed in 10% neutral-buffered formalin, embedded in paraffin slide sections, and stained with hematoxylin-eosin. In order to characterize the phenotype of the CAM tumors, slides that displayed the tumors were also processed for cytokeratin immunohistochemical detection. Briefly, the sections were dewaxed, rehydrated, and then endogenous peroxidase activity was blocked with 3% H2O2 in methanol for 30 minutes. After, sections were incubated for 30 minutes with normal rabbit or swine serum diluted 1:5 in PBS containing 10% BSA, followed by incubation with the monoclonal antibodies overnight at 4°C. Then, incubation with biotinylated rabbit anti-mouse and swine anti-rabbit secondary antibodies (DAKO, Denmark) was done for 30 minutes at RT. After, avidin/biotin complex detection (Vectastain, USA) was performed. Staining was performed with 3,3′-diaminobenzidine tetrahydrochloride (Sigma-Aldrich, USA) containing 0.02% hydrogen peroxide and Mayer's hematoxylin was used for counter-staining of the nucleus. Cytokeratins AE1/AE3 1:300 monoclonal antibodies were employed, and antigen retrieval was achieved with citrate buffer pH 6.0. A blind evaluation of tumor invasion was conducted by two independent observers. The semi-quantitative evaluation considered the quantity of human AE1/AE3 labeled cells in the CAM mesenchyme.

3.8. CRISPR-Cas9

To knockout (KO) the putative CCL18 receptors, we employed the Clustered Regularly Interspaced Short Palindromic Repeats (CRISPR)-Cas9 system following a protocol adapted from Ran *et al*. 2013 (133), as described below.

Guide Selection and Reconstruction

Appropriate single-guide RNAs (sgRNAs) for deletion were designed (Table 1). For that, the gene coding sequences of interest were checked in the UCSC Human Genome Browser tool. All guides were selected considering the following parameters: MIT Specificity Score, which gives information regarding possible off-targets; and Doench/Fusi 2016 score, which shows how efficient the gene editing might be. The Expasy Translate tool was used to verify the functional effect of the predicted deletions in terms of protein expression. Commercially acquired sgRNAs were eluted with autoclaved dH_2O for a final concentration of 100µM according to the manufacturer’s instructions (Invitrogen, USA).

To generate the sgRNAs expression constructs, a plasmid-based procedure was chosen. First, for each pair of sgRNAs, a polymerase chain reaction (PCR) reaction was performed, with the program: 37ºC for 30min, followed by 95ºC for 5min, and to finalize, the temperature decreased for 5ºC/min until 25ºC. The phosphorylated and annealed oligos were then diluted 1:200 in dH_2O. Afterwards, the sgRNAs were cloned into the pSpCas9(BB)-2A-GFP vector (Ref: PX458, Addgene, USA). For that, a mixture of the following components was prepared for each pair of guides: PX458 (100ng), annealed sgRNAs, Tango buffer 10X (Thermo Fisher Scientific, USA), DTT (10mM) (Invitrogen, USA), ATP (10mM) (Thermo Fisher Scientific, USA), FastDigest *Bbsl* (Thermo Fisher Scientific, USA), T4 DNA ligase (Thermo Fisher Scientific, USA), and dH_2O. The cloning was performed through PCR in 6 cycles of the following program: 37ºC for 5min and 21ºC for 5min.

Table 1. Guide and Primer Sequences to target CCR8 and PITPNM3.

Gene	Primer Category [a]	Primer Sub-Category [b]	Guide/Primer Sequence 5'- 3' [c]
CCR8	sgRNA – Upper	Top	CACCGAGATGTATACCTCTTGAACC
		Bottom	AAACGGTTCAAGAGGTATACATCTC
	sgRNA – Lower	Top	CACCGTTTCTGGGTCCCATTCAACG
		Bottom	AAACCGTTGAATGGGACCCAGAAAC
	Wild-Type (WT)	Forward	TGGTCATCCTGGTCCTTGTGG
		Reverse	GCTGTTGGCTTATGCTACATCC
	Pioneer (PN)	Forward	CAGTGGGTGTTTGGGACTGT
		Reverse	CCTGATGGCCTTGGTCTTGT
PITPNM3	sgRNA – Upper	Top	CACCGCGGACACATCGAAGTCAAAG
		Bottom	AAACCTTTGACTTCGATGTGTCCGC
	sgRNA – Lower	Top	CACCGTCGGACAGCATGGCACCCGT
		Bottom	AAACACGGGTGCCATGCTGTCCGAC
	Wild-Type (WT)	Forward	CCACTCCAGCGTGCTAAAGGAT
		Reverse	GATCCTCTTGCTTCCCCACCA
	Pioneer (PN)	Forward	ACAGCTTCTTCCATTGCGCAG
		Reverse	CAGGGGCATCCAGAAGTGGC

(a) Depletion requires two cut regions with two pairs of sgRNAs: "upper" (double-strand 5'-3') and "lower" (double strand 3'-5').

(b) DNA double strands named as "top" (single-strand 5'-3') and bottom (single-strand 3'-5').

(c) In orange, the complementary sequence of the sgRNA scaffold with Bbsl restriction enzyme; in blue, an extra "G" and the complementary "C"; in black, the oligos' (sgRNAs and primers) sequences.

Vector Production by Transformation of Competent Bacteria

Sterile petri dishes were coated with 15mL of Luria-Bertani (LB) agar (Invitrogen, USA) supplemented with 100µg/mL Ampicillin (selection antibiotic; Invitrogen, USA) for bacterial culture, and left at room-temperature (RT) to polymerize. After, 2µL of the cloning reaction was added to 25µL of ice-cold chemically competent *E. coli* strain *Stbl3* (Invitrogen, USA) and incubated on ice for 30min. In order to create pores in the membrane to allow DNA entrance, cells underwent heat shock at 42ºC for 45 seconds and then immediately placed on ice for 2min. Super Optimal broth with Catabolite repression (SOC) medium (Invitrogen, USA) was added to cells that were subsequently left to recover at 37ºC for 1h, for bacterial stabilization to allow vector expression that confers antibiotic resistance. Cells were added to the LB agar-coated plates previously prepared and spread homogeneously. Plates were incubated for 16h at 37ºC to allow colony formation. Afterward, two isolated colonies were picked from each condition to expand into a falcon tube with LB medium with ampicillin overnight at 37ºC under agitation (~180rpm). Bacterial DNA was extracted using the NZYMiniprep kit (NZYTech, Portugal) and quantified using Nanodrop 1000 (Thermo Fisher Scientific, USA). DNA was prepared for Sanger sequencing, to check for the correct insertion of sgRNA by PCR reaction (Table 2). Afterward, the PCR product was purified using Sephadex columns, and the plasmid sequence was confirmed by Sanger sequencing.

Table 2. Conditions of Sequencing PCR reaction.

PCR cycling step	Temperature (ºC)	Protocol run time	Cycle Repeat
Denaturation	96	1 minute	1x
Denaturation	96	10 seconds	25x
Annealing	50	5 seconds	
Extension	60	4 minutes	
Hold	4	∞	1x

Transfection

RKO and HCT-15 cell lines were seeded in 6-well plates at a concentration of $4x10^5$ cells/well, and allowed to adhere for 24h. After that, cells reached a confluency of around 70%, which was suitable for a transient transfection with 4µg of plasmid DNA. Transfection was performed using Lipofectamine 2000 (Invitrogen, USA) as the transfection agent combined with serum-free Opti-MEM medium (Gibco, USA) in a proportion of 1,5µL Lipofectamine per 1µg plasmid DNA. After 16h, the transfection medium was replaced with fresh-supplemented complete RPMI 1640. After 48h, transfection was confirmed by identifying green fluorescent protein (GFP)-positive cells using ZOE Fluorescent Cell Imager (Bio-Rad, USA). DNA was extracted using the ExtractMe DNA Tissue Kit (Blirt S.A, Poland)

and quantified using Nanodrop 1000 (Thermo Fisher Scientific, USA). To confirm the plasmid DNA internalization by the cells a PCR reaction was performed (Table 3).

Table 3. PCR extension times for CCR8 and PITPNM3.

PCR cycling step	Temperature (ºC)	Protocol run time	Cycle repeat
Denaturation	95	5 minutes	1x
Denaturation	95	30 seconds	35x
Annealing	60	30 seconds	
Extension	72	CCR8 – 1 second PITPNM3 – 7 seconds	
Extension	72	5 minutes	1x
Hold	12	∞	∞

Sorting

Upon transfection with the plasmid DNA for 48h, RKO and HCT-15 cells were detached using accutase (GRISP, Portugal) and washed with PBS 1X. Live-dead (1:10000 in cold PBS; eBiosciences, Germany) was added to the cells, as a viability dye. After a 30min incubation in ice, under agitation, cells were washed with cold FACS Buffer. The pellet was resuspended in cold FACS Buffer, filtered, and placed in the sorting tube (10 million cells per 1mL). Cells were sorted using FACS Aria II (BD Biosciences, USA) into 96-well plates with 50µL of supplemented RPMI 1640. In each well was placed 1 cell, except for a well control that was sorted with 100 cells. After 7 days, wells with dead cells and more than one clone were excluded. Without removing the old medium to avoid detaching the clones, 100µL of new medium was added to wells until the formation of a concise clone. Autoclaved water with P/S was added to interstices to delay the evaporation of the medium. Every two days, the clones were monitored until they reached 95%-100% confluency when they underwent trypsinization and plated first into 24-well plates and then into 6-well plates. At this point, part of the cells from each well were collected for DNA extraction for KO confirmation, while the other part was maintained in culture. Those clones of KO confirmation were further expanded to frozen stocks in liquid nitrogen, to lysates to confirm reduction of protein expression by western blots, or to functional invasion assays.

3.9. Proteomic crosslinking assay

Coating of the magnetic beads

For the preparation of the beads, $20x10^6$ Dynabeads™ M-450 Tosyl-activated (Thermo Fisher Scientific, USA) were washed twice with Washing Buffer 1 (0.1M phosphate

buffer, pH 7.4-8). Then, the beads were incubated with 10µg of rhCCL18 for 1h30min at RT with agitation (1000rpm). Following incubation, Buffer 1 containing 1% bovine serum albumin (BSA) (final concentration of 0.167% BSA) was added to the beads and incubated overnight at 37°C with agitation (1000rpm) to ensure thorough protein binding. The beads were subsequently washed twice with 20mM 4-(2-hydroxyethyl)-1-piperazineethanesulfonic acid (HEPES) and incubated for 2h at RT in 25mM bis(sulfosuccinimidyl)suberate (BS3) crosslinker (Thermo Fisher Scientific, USA) diluted in 20mM HEPES. After this period, the beads were washed with Buffer 3 (0.2 M Tris, 0.1% BSA, pH 8.5) and subjected to further incubation overnight at RT (1000rpm) to deactivate any remaining free tosyl groups on the beads. Afterwards, the beads were washed with Buffer 2 (PBS with 0.1% BSA and 2mM EDTA, pH 7.4), and the correct binding of proteins to the beads was verified by flow cytometry using anti-human CCL18 (Ref: 300057, Abcam, UK]). Coated beads were stored in the same buffer at 4°C until further use (normally for up to 1 week).

Conjugate formation and Synapse isolation

For tumor cell line-coated bead conjugation, the SW480 and RKO colon cancer cells were resuspended in Imaging Medium (RPMI Medium 1640, glutamine and no phenol red, Gibco, USA) and added in a 1:1 ratio with CCL18-coated beads for 60min at 37°C with agitation (1000rpm). Following confirmation of successful conjugation via microscopy, by visualizing the beads in the cells' surroundings, the tumor cell-bead conjugates were transferred to ice and subjected to several washes with cold cytoskeletal buffer (CSK buffer; 300mM sucrose, 100mM sodium chloride, 10mM piperazine-N,N′-bis(2-ethanesulfonic) acid (PIPES), pH 6.8, 3 mM magnesium chloride) to remove unbound cells. The conjugates were resuspended in a fresh buffer containing CSK buffer supplemented with 0.5% Triton X-100 and protease inhibitors, followed by sonication in optimized cycles (15sec on, 15sec off for 3 cycles). Consecutively, the conjugates underwent a repetitive washing process with CSK buffer containing 0.5% Triton X-100 to eliminate any residual cellular debris. Afterwards, the proteins bound to the beads were eluted with 20µL of Loading buffer for 30min at 70°C with agitation (1000rpm). The beads were discarded, and the eluates were stored at -20°C for up to one week.

In-gel digestion

The eluates were loaded into electrophoresis gel wells, and after electrophoresis, the gel was stained with a Zinc Reversible Stain Kit for protein quantification. Gel bands, excised into 1 to 2mm pieces, were dissolved in Tris-glycine buffer (25mM Tris, 192mM glycine, pH 8.0) and washed three times with Milli-Q water for 10min each. Thenceforth, the gel pieces underwent dehydration with acetonitrile (ACN) (LC-MS Grade) for 5-10min. In turn, disulfide bonds were reduced by rehydrating the gel pieces in 20mM dithiothreitol (DTT) (Sigma-

Aldrich, USA) at 56°C for 30min, followed by another dehydration step with 100% ACN. To prevent reoxidation of disulfide bonds, the gel pieces were rehydrated with 55mM iodoacetamide (IAA) (Sigma-Aldrich, USA) for 20min in the dark at RT, then washed with 100mM ammonium bicarbonate and dehydrated once more. When the conditions were met, enzymatic digestion was carried out by adding 75µL of 0.02µg/µL trypsin (Promega, USA) to the gel pieces and left to absorb on ice for 20min. When all the trypsin solution had been absorbed, 40mM ammonium bicarbonate/10% ACN was added to cover the gel pieces and incubated for 18h at 37ºC in a humid chamber. Following this, 100% ACN was added and another incubation for 15min at 37°C was performed. The supernatant was then collected into a clean tube, and the extraction process was repeated twice with 50% ACN/5% formic acid (LC-MS Grade). Finally, the samples were dried using a SpeedVac concentrator for 5-8h.

Mass spectrometry analysis

The nanoLC system employed in this experiment consisted of a Vanquish Neo UHPLC system coupled in line with a QExactive Plus Hybrid Quadrupole-Orbitrap mass spectrometer (Thermo Fisher Scientific, USA), which was fitted with a nano-electrospray ion source (EASY-Spray source; Thermo Fisher Scientific, USA). The mobile phases used were aqueous formic acid (0.1%) for eluent A and formic acid (0.1%) in acetonitrile (80%) for eluent B. A sample volume of 10µL was directly injected into a trapping column (C18 PepMap Neo, 5µm particle size), which then directed the sample to the analytical column (EASY-Spray C18 PepMap, 100 Å, 75µm x 150mm ID, and 3µm particle size) at a flow rate of 0.25µL/min. The temperature of the column was maintained at 35°C. Furthermore, peptide separation was achieved using the following gradient: 7min from 2.5% B to 12% B, 50min from 12% B to 46% B, 5min from 46% B to 99% B, and 10min at 99% B. For mass spectrometry, the instrument was operated in positive ion mode across the *m/z* range of 300-2000, with a spray voltage set at 1.9kV and a transfer capillary temperature of 275°C. Full MS parameters included a resolution of 140,000, an AGC target of $3x10^6$, and a maximum injection time of 200ms. The top 15 most intense ions were selected for high-energy collision dissociation (HCD). Data were collected and analyzed using Xcalibur software version 4.5 (Thermo Fisher Scientific, USA).

Data was analyzed automatically using the SequestHT search engine with the Percolator algorithm for validation of protein identifications (Proteome Discoverer 3.1, Thermo Scientific, USA). Data were searched against the human proteome obtained from the SwissProt database selecting trypsin as the enzyme and allowing for up to 2 missed cleavage sites and a precursor ion mass tolerance of 10ppm and 0.6Da for product ions. Carbamidomethylcysteine was selected as a fixed modification, while oxidation of methionine (+15.9) was defined as a variable modification.

Bioinformatics

To generate the final curated protein list, the proteins with less than 2 unique peptides and the proteins with low or medium protein FDR confidence were removed. Proteins named contaminants based on their abundance in control conditions (tumor cell interaction with non-coated beads) were manually removed using Proteome Discoverer 3.1.

For the curation of plasma membrane proteins, protein annotation tables for each cell line were generated using gene ontology (GO) terms for cellular location through Proteome Discoverer 3.1. Molecular and biological functions were also explored.

The selection of the proteins enriched in the RKO and in the SW480 samples resulted from the interactions with CCL18-coated beads was based on exploring Volcano Plots (VolcaNoseR; https://huygens.science.uva.nl/VolcaNoseR2/) selecting proteins with Log2 of fold change (RKO/SW480) higher than 1.5 and with adjusted p-value lower than 0.05 ($-Log_{10}$p-value higher than 1.3). Three different cell line passages of RKO and SW480 were used as biological replicates of the experiment. The subset of proteins enriched on the samples from RKO-(CCL18) Bead interactions were further analyzed regarding their protein-protein interactions, molecular and biological functions and involved Kyoto Encyclopedia of Genes and Genomes (KEGG) pathways using the Search Tool for the Retrieval of Interacting Genes/Proteins (STRING) version 12.0 (http://string-db.org/). A network with biological processes considering only significant pathways ($p \leq 0.05$) was constructed for these common proteins using the following parameters: a GO tree interval of min. 4 and max.10, and a kappa score of 0.64 in ClueGO plugin for Cytoscape Software 3.10.2.

3.10. Statistical Analysis

Data was first analyzed for Normal (Gaussian) distribution, considering the Shapiro-Wilk normality test. For two groups (either paired or non-paired), data was analyzed with a two-tailed Student t-test for parametric samples and Mann-Whitney test for non-parametric samples. For more than two groups, a One-Way ANOVA and Kruskal-Wallis tests were performed for parametric and non-parametric samples, respectively. Additionally, multiple comparisons were performed when necessary. All statistical analysis and the respective representative graphs were performed using GraphPad Prism Software v8.4.2 (GraphPad-trial version) and expressed as mean values of at least three independent experiments ± standard deviation (SD). Data was considered significant at a P-value of <0.05.

Chapter 4: Results

4.1. rhCCL18 stimulates colon cancer cell invasion

4.1.1. rhCCL18 (1ng/mL) stimulates RKO and HCT-15 colon cancer cell invasion

Our group has previously demonstrated that when monocytes were seeded over tumor decellularized matrices, derived from colorectal cancer patients' surgical resections, they differentiated as anti-inflammatory macrophages, expressing high levels of CCL18. Interestingly, we reported that this immunosuppressive chemokine was secreted and able to stimulate colon cancer cell invasion. Four distinct cell lines (RKO, HCT-15, SW480, and SW620) were tested, but only RKO and HCT-15 cells seemed to respond and to invade upon incubation with rhCCL18 (Figure 6). In addition, we demonstrated that this pro-invasive effect was impaired through a neutralizing monoclonal antibody targeting CCL18 (Figure 6) (46). Additionally, we demonstrated that CCL18 was preferentially expressed at the invasive front of more advanced CRC cases, at areas where macrophages and Tregs were also more abundant (46).

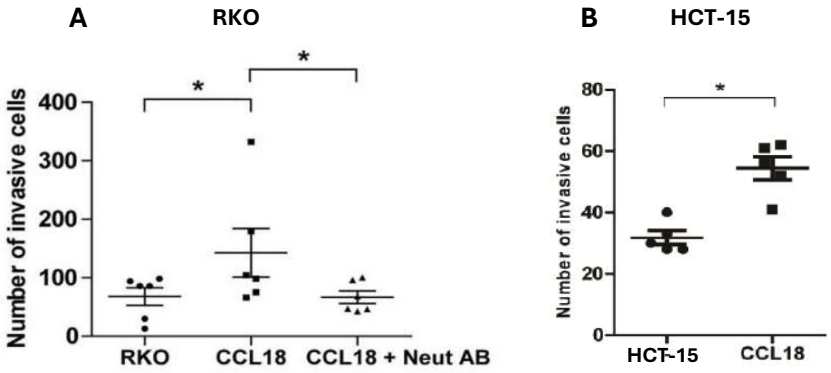

Figure 6. rhCCL18 (1ng/mL) stimulates RKO and HCT-15 colon cancer cell invasion. (A) RKO colon cancer cells were maintained untreated or treated with 1ng/mL of rhCCL18, in the presence or not of 1ng/mL of a neutralizing monoclonal anti-CCL18 antibody, on Matrigel invasion assays. **(B)** HCT-15 colon cancer cells were maintained untreated or treated with 1ng/mL of rhCCL18 on Matrigel invasion assays. After 24h of incubation, the invasive cells were counterstained with DAPI and counted under the microscope. Graphic data are representative of 6 independent experiments (panel A, adapted from *Pinto ML et al, Biomaterials, 2017*, panel B, new data). *p<0.05.

4.1.2. rhCCL18 (10ng/mL) stimulates RKO but not HCT-15 colon cancer cell invasion

During this MSc thesis, we decided to further exploit the impact of other concentrations and other biological effects of rhCCL18 on the responsive cell lines. Thus, Matrigel invasion assays were performed with both RKO and HCT-15 cells exposed at

10ng/mL of rhCCL18. We found that although there was still stimulation of invasion of the RKO cells, the HCT-15 cells decreased their invasive capacity, when stimulated with this cytokine concentration (Figure 7). However, the latter results were not statistically significant, probably due to the reduced number of biological replicates.

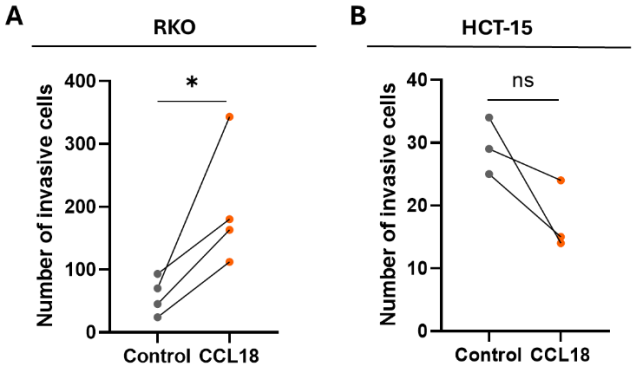

Figure 7. rhCCL18 (10ng/mL) stimulates RKO cell invasion. (A) RKO and **(B)** HCT-15 cells were stimulated with 10ng/mL of CCL18 on Matrigel invasion assays. After 24h of incubation, the invasive cells were counterstained with DAPI and counted under the microscope. Graphic data are representative of 3-4 independent experiments. *p<0.05; ns: not significant.

4.2. rhCCL18 modulates colon cancer cell migration

4.2.1. rhCCL18 (1ng/mL) in serum-containing conditions has limited effect on RKO cell migration

Considering preliminary data from the group and that invasion may result from enhanced migration and proteolysis of ECM components, we decided to exploit the effect of rhCCL18 (1ng/mL) on RKO cancer cell migration. Distinct migration assays were then established, specifically for the analysis of single-cell and collective Wound-healing migration.

Single-cell migration

For single-cell migration, $5x10^4$ cells of a single-cell suspension were seeded per well of a 24-well plate and after 6h, 1ng/mL of rhCCL18 was added to each well, in the presence of complete RPMI 1640 medium (with 1% P/S and 10% of FBS). Individual cell trajectories were then tracked for 15h, and images were acquired every 10min. Time-lapse microscopy analysis was performed and four parameters were evaluated: accumulated distance (total distance that the cells migrated); displacement (distance between the cell first and the last position observed); speed (ratio between the accumulated distance and the track duration in seconds); and straightness (a measurement that indicates how straight the migration was). Our results evidenced that RKO cells stimulated with 1ng/mL of rhCCL18 had the tendency

to migrate faster (speed), with a significant straight direction and a significant reduction of the accumulated distance than those cells without stimuli (Figure 8).

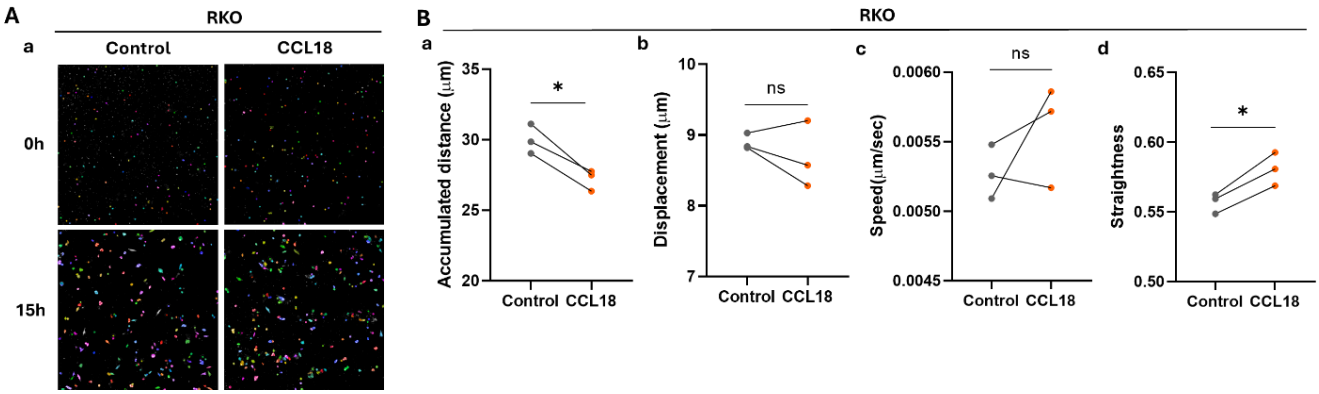

Figure 8. rhCCL18 (1ng/mL) has limited effect on RKO single-cell migration. (A) Representative images of the trajectory of individual cells from one of the fields analyzed per condition. Single-cell analysis of RKO cells stimulated or not with 1ng/mL of rhCCL18 and followed every 10min until 15h. **(B)** Four migration-associated parameters were assessed per cell: (a) Accumulated distance (µm), (b) displacement (µm), (c) speed (µm/sec), and (d) straightness. Each dot represents the average of all the areas evaluated in each independent experiment. Images and graphic data are representative of 3 independent experiments. *p<0.05; ns: not significant.

Collective cell migration

For collective wound-healing migration, RKO cells were seeded at an initial density of $4x10^4$ cells/well in a 24-well plate and, when reached confluency, the monolayer was scratched and the ability of cells to migrate collectively and to repair the wound was evaluated along 18h. The results obtained suggested that rhCCL18, at the concentration of 1ng/mL, did not affect collective RKO cell migration, and no significant differences were visible between conditions (Figure 9).

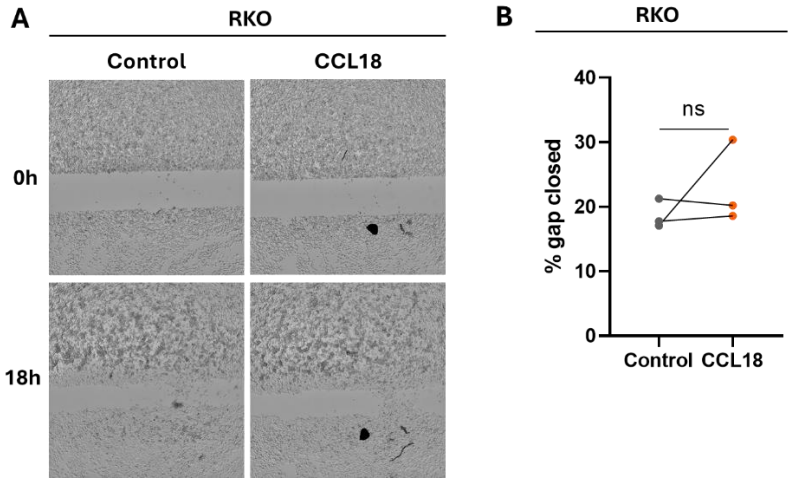

Figure 9. rhCCL18 (1ng/mL) has no effect on collective RKO cell migration. (A) Representative images of collective cell migration. Wound-healing assay where RKO cells were stimulated with 1ng/mL of rhCCL18, and the gap was monitored every hour until the final timepoint of 18h. **(B)** The % of gap closure was evaluated. Each dot represents the average of all gap closures evaluated in each independent experiment. Images and graphic data are representative of 3 independent experiments. ns: not significant.

4.2.2 The percentage of FBS influences colon cancer cell migration

Considering that the literature suggests that one should inhibit proliferation to ensure that only cell migration is being evaluated during migration assays, specifically Wound-healing, we decided to explore this possibility. Since the most common method applied for suppressing proliferation is using low serum concentrations (serum starvation) (134), we decided to evaluate the impact of media supplementation with 1%, 5%, or 10% of FBS on RKO and on HCT-15 Wound-healing migration, in the absence of external stimuli.

The results suggested that, in both cell lines, media supplementation with a lower percentage of FBS generates a favorable environment for migration. Although not statistically significant, RKO cells showed a higher % of gap closure upon culture in media with 1% of FBS (Figure 10A-B), while HCT-15 preferred being cultured with 5% (Figure 10C-D). Aiming at standardizing all experimental conditions, we decided to repeat the previous migration assays using media supplemented with 1% of FBS for both cell lines.

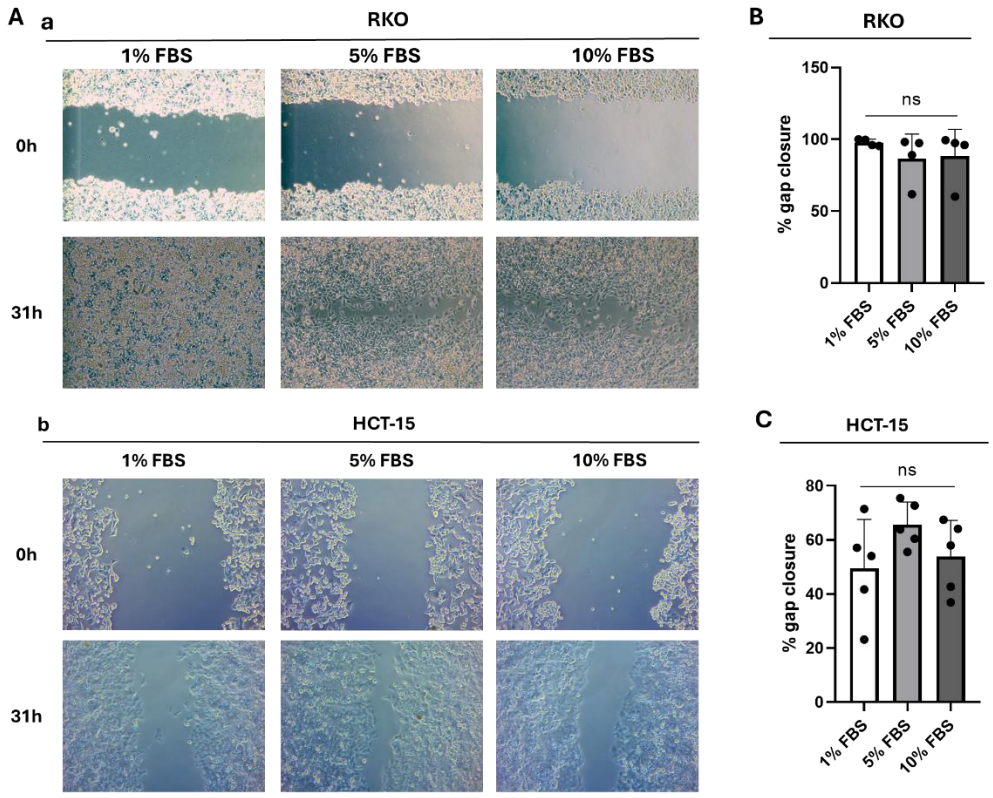

Figure 10. The percentage of FBS influences colon cancer cell migration. (A) Representative images of collective cell migration. Wound-Healing assays were performed on (a) RKO or (b) HCT-15 cells cultured with RPMI 1640 supplemented with 1%, 5%, or 10% of FBS, and the gap was monitored every 3h until the final timepoint of 31h. **(B, C)** The % of gap closure was evaluated, comparing the initial and final gap measure. Each dot represents the average of all gap closures evaluated in each independent experiment. Images and graphic data are representative of 4-5 independent experiments. *p<0.05; ns: not significant.

4.2.3. rhCCL18 (10ng/mL) affects colon cancer cell individual and collective migration

Similar to previous migration experiments, the impact of rhCCL18 on both RKO and HCT-15 individual and collective migration assays were evaluated but, this time using 10ng/mL of rhCCL18 in media supplemented with 1% of FBS.

Single-cell migration

For single-cell migration, cells were seeded, stimulated with the desired concentration of rhCCL18, and followed for 20h. Under these restricted serum conditions, rhCCL18 impacted the individual cell migration of both RKO and HCT-15 cells (Figure 11). In contrast to what was expected, rhCCL18 (10ng/mL) decreased the migration of RKO-stimulated cells for all parameters assessed (Figure 11A-B), with significant differences in cell displacement and speed of migration. Interestingly, upon treatment with rhCCL18 (10ng/mL), HCT-15 stimulated cells exhibited lower accumulated distance and displacement, correlating with a decreased migration. However, moving cells migrated faster, presenting higher speed, and performing a straighter trajectory, than non-stimulated cells (Figure 11C-D).

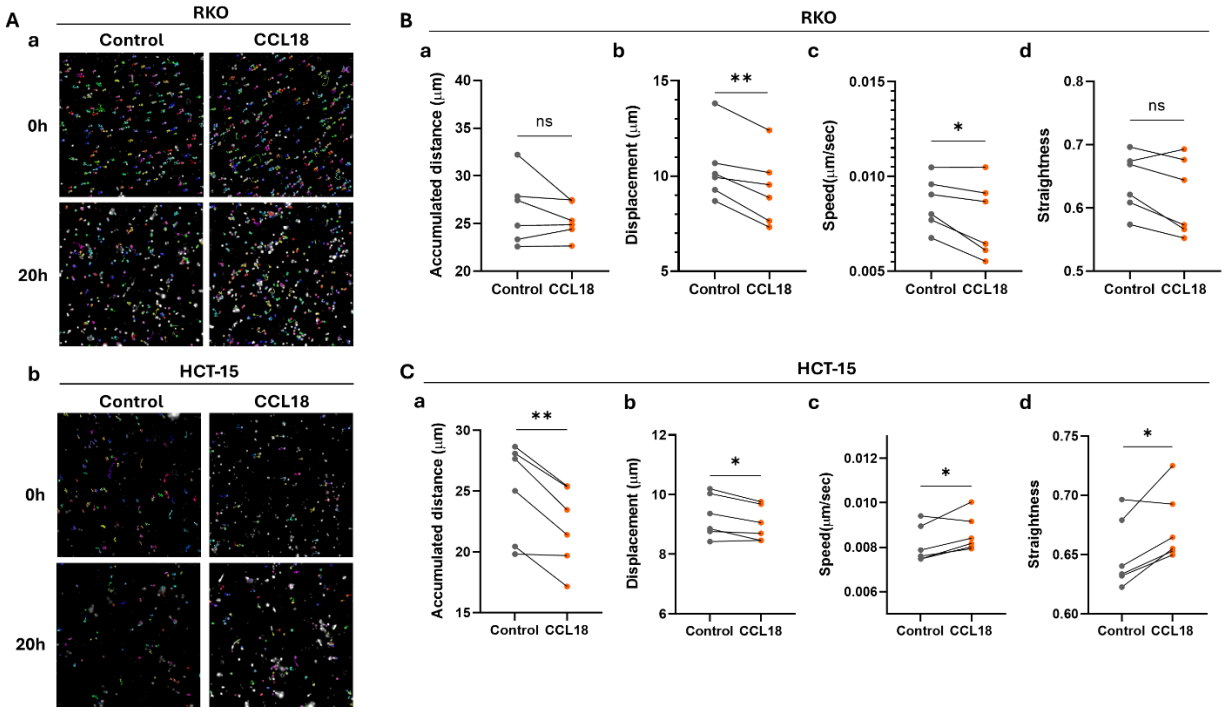

Figure 11. rhCCL18 (10ng/mL) affects colon cancer cells individual migration. (A) Representative images of the trajectory of individual cells from one of the fields analyzed per condition. Single-cell analysis where (a) RKO and (b) HCT-15 cells were stimulated or not with 10ng/mL CCL18 and followed every 10min until 20h. **(B, C)** Four migration-associated parameters were assessed per cell: (a) Accumulated distance (µm), (b) displacement (µm), (c) speed (µm/sec), and (d) straightness. Each dot represents the average of all the areas evaluated in each independent experiment. Images and graphic data are representative of 6 independent experiments. *p<0.05; **p<0.01; ns: not significant.

Collective cell migration

Furthermore, collective cell migration was also evaluated. For Wound-healing, cells were seeded and, upon reaching confluency, a gap was manually created and cells were then treated with rhCCL18 (10ng/mL) and their trajectories followed for 31h. Our results demonstrated that colon cancer cells responded differently to stimulation with this immunosuppressive chemokine (Figure 12). Interestingly, rhCCL18 significantly increased RKO collective cell migration, as evidenced by the enhanced percentage of gap closure, (Figure 12B), without affecting HCT-15 colon cancer cells collective migration (Figure 12C).

Interestingly, we observed that cell morphology also altered after stimulation with rhCCL18 (10ng/mL). RKO cells evidenced a more elongated and loose shape, with front cellular projections characteristic of migratory cells, as if they were trying to reach and interconnect other cells (Figure 12Aa), while HCT-15 cells were more compact, preferring to be close to neighboring cells (Figure 12Ab).

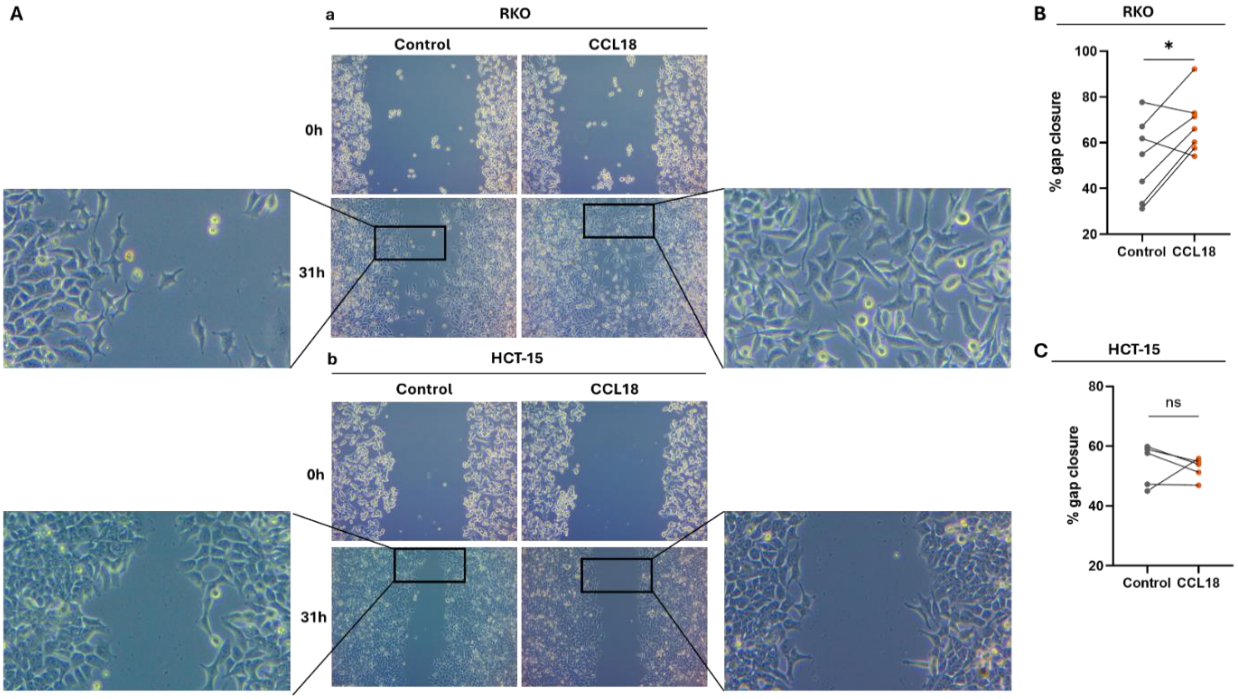

Figure 12. rhCCL18 (10ng/mL) stimulates RKO colon cancer cell collective migration. (A) Wound-healing assay where (a) RKO and (b) HCT-15 cells were stimulated with 10ng/mL rhCCL18, and the gap was monitored every 3h until 31h. **(B, C)** The % of gap closure was evaluated in comparison to the initial gap. Images and graphic data are representative of 5-7 independent experiments. *p<0.05; ns: not significant.

4.3. rhCCL18 (10ng/mL) does not affect colon cancer cell proliferation

To understand how CCL18 affects colon cancer cell proliferation, a cell cycle assay was performed. For that, RKO and HCT-15 cells were stimulated with 10ng/mL of rhCCL18 and, after 48h or 72h of stimulation, cells were fixed, incubated with viable dyes, and analyzed by flow cytometry. The results suggested that rhCCL18 does not influence the proliferation of RKO nor of HCT-15 cells, as there were no statistically significant differences observed at any of the time points studied (Figure 13).

Interestingly, 48h after stimulation, approximately, 60% of the RKO population was arrested in the G1 phase, 20% in the S phase, and 20% in the G2/M phase, with no significant differences between control and treated cells. At 72h, we observed an increase of RKO cells arrested in the S phase to approximately 40%, with G2/M maintaining 20%, and G1 decreasing to 40%, with again no significant differences between control and treated cells (Figure 13B).

Regarding the HCT-15 population, 35% of the cells were arrested at the G1 phase, 40% at the S phase, and 25% at the G2/M phase, after 48h of stimulation. In addition, there appeared to occur a slight increase in rhCCL18-stimulated cells arrested in the S phase, compared to the control, and a minor decrease in the G2/M phase. However, these results were not statistically significant. At 72h, we observed an increase to 50% of HCT-15 cells arrested in the G1 phase, and a decrease to 30% in the S phase and to 20% in the G2/M phase. Similar to the time point of 48h, there appeared to exist a small increase in the percentage of cells stimulated with CCL18 (10ng/mL) arrested in the S phase, compared with control, although this result was not statistically significant either (Figure 13C).

Considering that the differences between time points were present in both conditions, control and experimental, we can assume that they are inherent to the cell type and not to the treatment. Nevertheless, further experiments should be performed to enhance the number of experimental replicates and empower the statistical analysis.

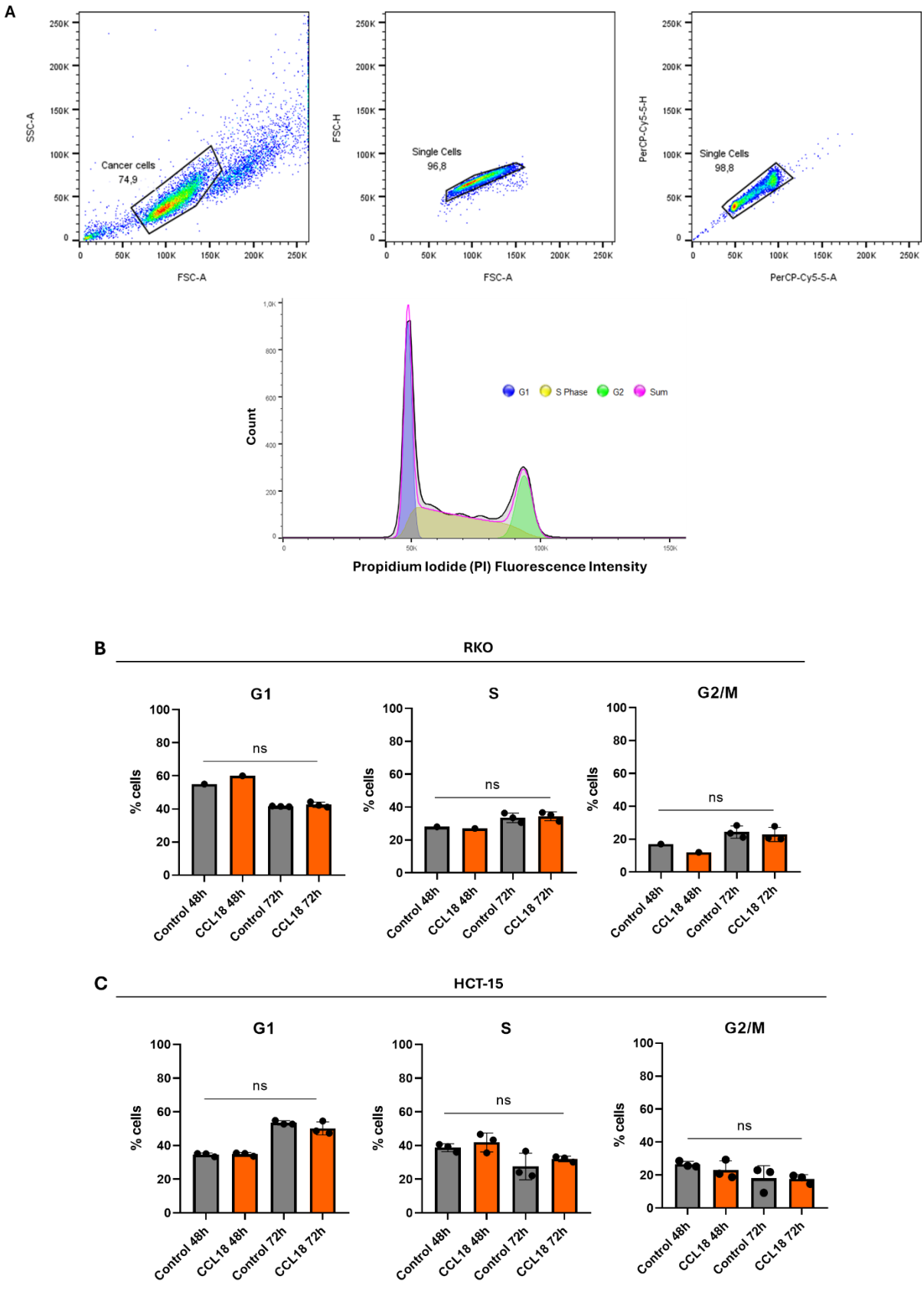

Figure 13. rhCCL18 (10ng/mL) does not affect colon cancer cell proliferation. (A) Representative images of the gating strategy applied in these experiments, and of cell cycle histogram. **(B, C)** Cell cycle assay where (a) RKO and (b) HCT-15 cells were stimulated with 10ng/mL rhCCL18. After 48h and 72h of stimulation, cells were fixed and analyzed by flow cytometry. The % of cells arrested in each cell cycle phase was evaluated. Graphic data are representative of 1-3 independent experiments. ns: not significant.

4.4. rhCCL18 (10ng/mL) does not induce matrix metalloproteinases (MMP) activity

To unveil the possible mechanism underlying CCL18-mediated invasion, conditioned media derived from Matrigel invasion assays of colon cancer cells exposed to this chemokine were analyzed, by gelatin zymography. Through this technique, the presence and the proteolytic profiles of, pro-active and active, matrix metalloproteases MMP-2 and MMP-9 were assessed and further quantified (Figure 14). Since in our previous experiments, rhCCL18 only stimulated RKO cancer cell invasion, we decided to use only this cell line conditioned medium along these analyses.

Our results evidenced the presence of pro-active and of active MMP-9 forms in both conditions, but only the pro-form of MMP2 was visible (Figure 14A). Furthermore, no significant differences between the proteolytic activity of these pro- and active MMPs were observed in the presence or absence of rhCCL18 (10ng/mL) (Figure 14B). These findings suggest that CCL18 does not promote invasion through the degradation of the ECM. However, further experiments with higher concentrations of rhCCL18 should be used in parallel with invasion and migration assays.

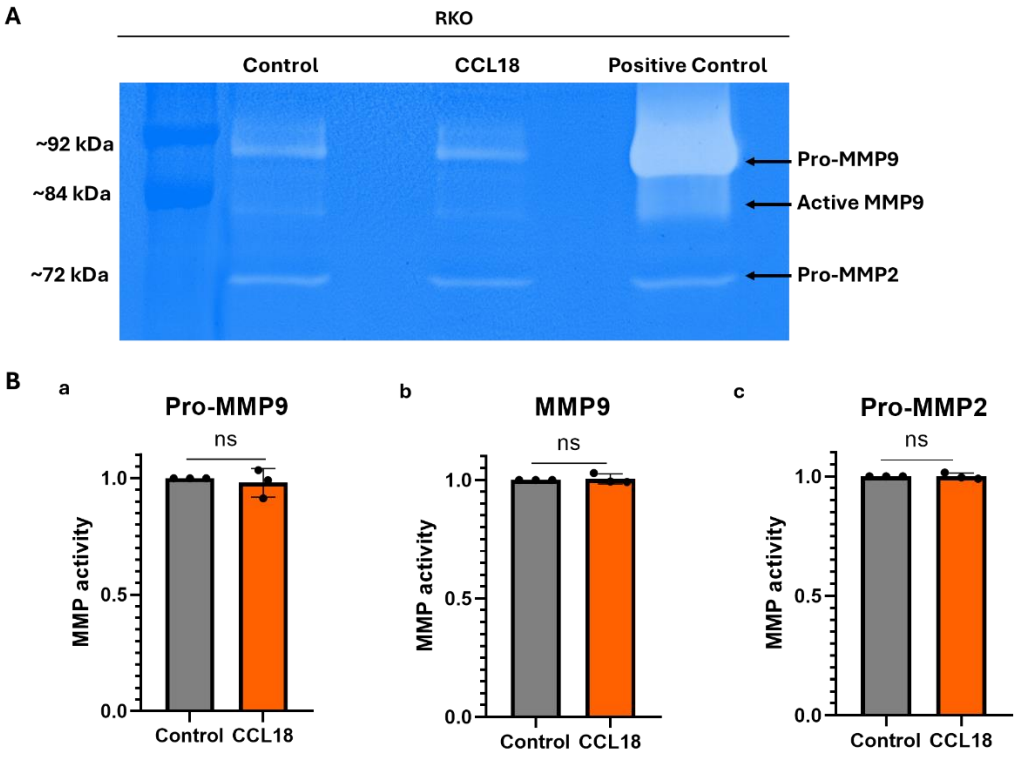

Figure 14. rhCCL18 (10ng/mL) does not induce MMP proteolytic activity. Conditioned media from invasion assays with 10ng/mL of rhCCL18 were evaluated on gelatin zymograms. **(A)** Representative image of a gelatin zymogram. **(B)** (a) Pro-MMP9, (b) Active MMP9, and (c) Pro-MMP2 gelatin proteolytic activity was quantified. Images and graphic data are representative of 3 independent experiments. ns: not significant.

4.5. rhCCL18 does not induce tumor growth and neoangiogenesis in the chicken ChorioAllantoic Membrane (CAM) assay

Our next aim was to ascertain the potential impact of CCL18 *in vivo*, having established its influence on cell invasion *in vitro*. Considering that CCL18 is a primate-specific chemokine, with no described murine ortholog, the use of a mouse model brings no particular advantage. Thus, we decided to proceed with the implantation of the human colon cancer cells on the chicken CAM to unravel the *in vivo* impact of rhCCL18, particularly on tumor growth and neoangiogenesis.

A preliminary test was conducted to understand the growth pattern of RKO and of HCT-15 cells in the CAM, and to infer the necessity of using or not Matrigel, when implanting the human cancer cells. For that, fertilized chicken eggs were maintained for 3 days in the incubator, prior to the overture of a small window on the eggshell to remove albumin and detach the CAM for further implantation. After this step, a piece of transparent scotch tape was placed on top of the egg, to impair any contamination, and eggs were returned to the incubator. At day 10, a sterile silicone ring was introduced on top of the CAM, and $1x10^6$ RKO or HCT-15 cells, resuspended in 10µL of complete RPMI 1640 medium or of 5µL Matrigel (diluted 1:1 in RMPI 1640 medium), were placed inside. After cancer cell implantation, eggs were further incubated for 3 additional days at 37ºC (Figure 15A). Our results demonstrated that although tumors were formed by both cell lines, in the absence of rhCCL18, RKO tumors were smaller than those formed by HCT-15 cells (Figure 15B). Matrigel was also considered as necessary since no tumor formation occurred when both cells were implanted in its absence (Figure 15B).

Since we have previously reported that CCL18 stimulates cancer cell invasion, and that the HCT-15 tumors were already very large, further experiments were carried out only with RKO cells, to better visualize the stimulation effect. Also, larger tumors often caused a loss of neoangiogenesis readout, solidifying our decision to proceed with this cell line and to exclude the use of HCT-15 cells. Considering this, fertilized chicken eggs were then implanted, as previously described, in the presence of 5µL Matrigel (diluted 1:1 in RMPI 1640 medium), and of 20ng/mL of rhCCL18. After 3 days of additional incubation at 37ºC, the CAMs were fixed, further analyzed under a stereomicroscope, or embedded in paraffin for further histological analysis (Hematoxylin/Eosin and Cytokeratin stainings). These experiments were performed in triplicate, and in each experiment, 10 to 15 eggs were considered per condition.

Although in the initial experiments, some apparent differences were found, our final results evidenced that rhCCL18 (20ng/mL) did not promote, in comparison to the untreated control, tumor growth or tumor neoangiogenesis (Figure 15C). In fact, no statistically

significant differences were observed, regarding tumor area or of new blood vessels formation, when RKO-induced tumors were exposed or not to rhCCL18 (Figure 15D). It is, however, possible that the concentration used was not sufficient for *in vivo* assays or that the model is limited for the application of a chemokine that has no known mouse or avian ortholog. Further experiments should be performed to further exploit the *in vivo* impact of CCL18.

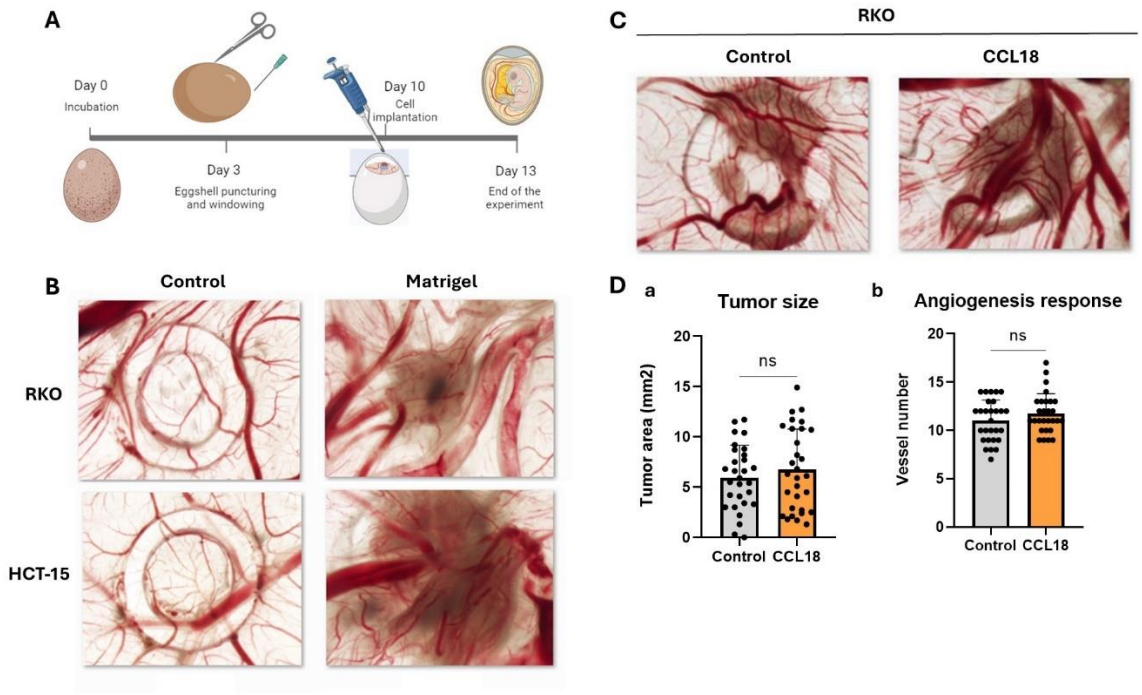

Figure 15. rhCCL18 (20ng/mL) does not promote RKO tumor growth nor RKO tumor neoangiogenesis. (A) Representative scheme of the experimental setup. **(B)** Pilot CAM study to observe the growth pattern of RKO and of HCT-15 cells implanted with and without Matrigel (1:1). **(C)** CAM assay with RKO cells, in the presence of 5µL of Matrigel, stimulated with 20ng/mL of CCL18. **(D)** (a) Tumor size (mm2) and (b) angiogenesis response (vessel number) were evaluated using a stereomicroscope. Images are representative of 4 independent experiments with 10 to 15 eggs per experiment. ns: not significant.

Although rhCCL18 did not promote tumor growth, the impact of this chemokine on the invasive ability of RKO cells through the CAM was further evaluated through a detailed histological analysis. 6 cases from each condition, non-stimulated and stimulated with rhCCL18, were selected and stained for hematoxylin/eosin and for cytokeratin (Figure 16). Our results show that no major differences have been found regarding the dimension of the tumors formed in the presence or the absence of rhCCL18, nor their invasive capacity (Figure 16).

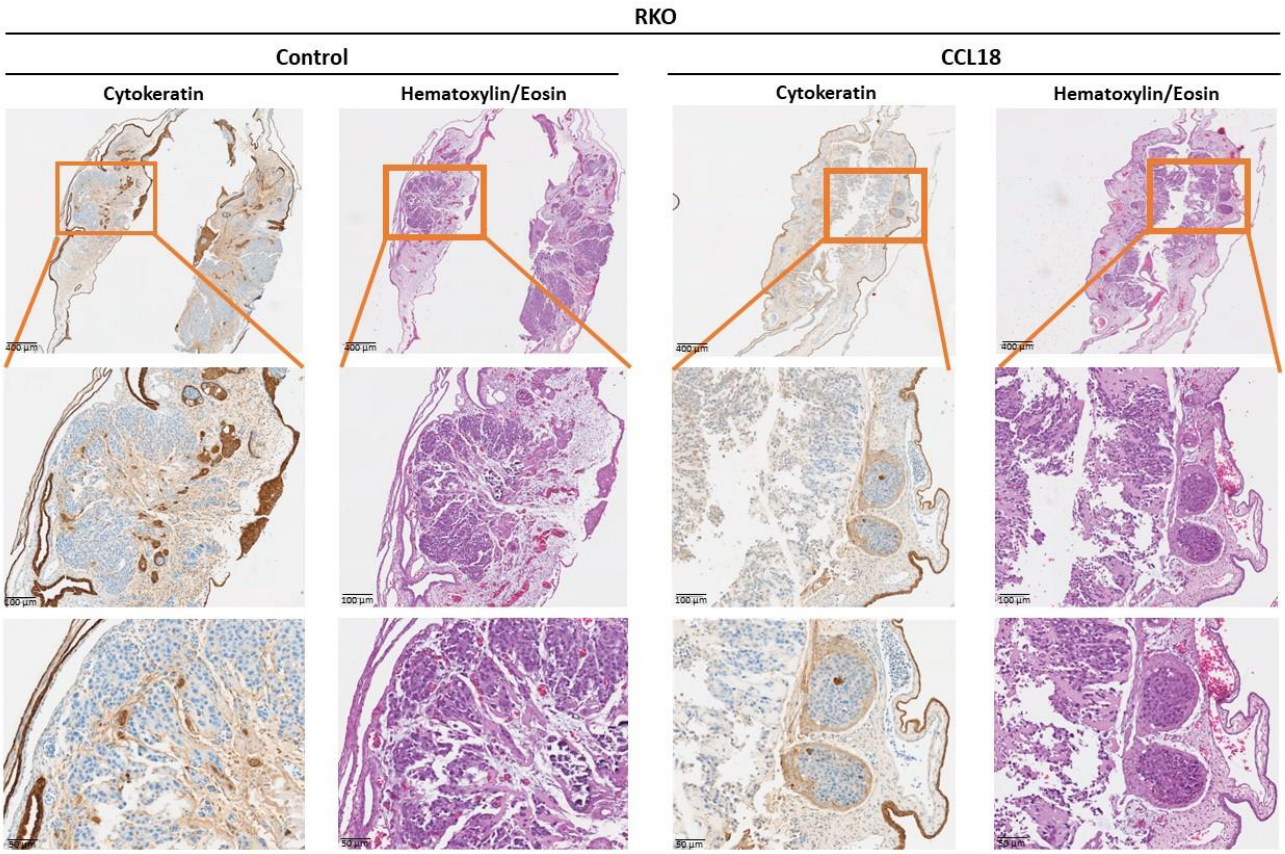

Figure 16. rhCCL18 does not influence the size of the tumors nor their invasive capacity. Tumors formed in the chorioallantoic membrane, in the presence and the absence of rhCCL18 (20ng/mL), were excised from the CAM, fixed, and embedded in paraffin, followed by staining for hematoxylin/eosin and for cytokeratin. Tumor size and invasive capacity were evaluated blindly by two independent observers. Images are representative of 6 cases from 4 independent experiments, with 10 to 15 eggs per experiment.

4.6. Study of the CCL18 receptor(s)

4.6.1. Establishment of RKO and of HCT-15 KO clones for the expression of PITPNM3 and of CCR8 receptors

Our group has previously described that the immunosuppressive CCL18 chemokine stimulates, on RKO and on HCT-15 cells, the phosphorylation of the EGFR and of its associated downstream partners: 1) the FAK, 2) the tyrosine kinase Src, 3) the serine-threonine kinase Akt and 4) the Extracellular signal-regulated kinase ERK (unpublished, data not shown). Nevertheless, EGFR has never been described as a putative CCL18 receptor. Instead, this chemokine was associated, in other tumor types, with three well-described receptors: PITPNM3, CCR8, and GPR30. However, in CRC there is no available information. To uncover the putative CCL18 receptor in this cancer, that may possibly, upon binding to the chemokine, interact with EGFR and activate the downstream signaling pathway, we decided to employ the CRISPR-Cas9 technology. To this end, appropriate single-guides RNA

(sgRNAs) for the deletion of CCR8 and of PITPNM3 were designed and cloned into the pSpCas9(BB)-2A-GFP vector. Vector production was achieved by the transformation of the chemically competent *E. coli* strain *Stbl3* (Figure 17A). RKO or HCT-15 colon cancer cells were then transfected with the plasmid DNA, and incorporation by the cells was verified by the GFP tag present in the plasmid (as green cells) (Figure 17B). DNA was extracted and a PCR reaction was carried out to confirm the plasmid internalization by the cancer cells. The sgRNAs were designed to target regions of each gene that codify important aspects for the function an expression of the proteins. In the case of PITPNM3, the region of the DDHD domain encompassing 3 exons (exons 9-11) was selected owing to its important role in the function of the protein, namely in the membrane turnover, intracellular trafficking, and lipid transport and metabolism (135). For CCR8 gene, the deletion region included the coding sequence of the disulfide bridges (on exon 2) crucial for the structural stability and conformational dynamics of the proteins (136). Sequence of sgRNAs and primers are specified on Table 1. It is worth noting that a guanine (G) nucleotide was added in the beginning of the guides sequence (5' region) because the U6 RNA polymerase III promoter used to express the sgRNAs prefers a G as the first base (137).

The length of the PCR reaction products was previously estimated based on the nucleotide coding sequence of each gene (Figure 17C). Importantly, both WT and PN primers chosen for each gene were also validated by a PCR reaction, to confirm their ability to hybridize with the region of interest (Figure 17D). A KO population was found in both cell lines (RKO and HCT-15, as annotated) for PITPNM3 (Figure 17Ea) and CCR8 (Figure 17Eb), shown by the ~900bp and <200bp bands for the WT primers, respectively, the expected size for a KO population in each gene (Figure 17 Cb).

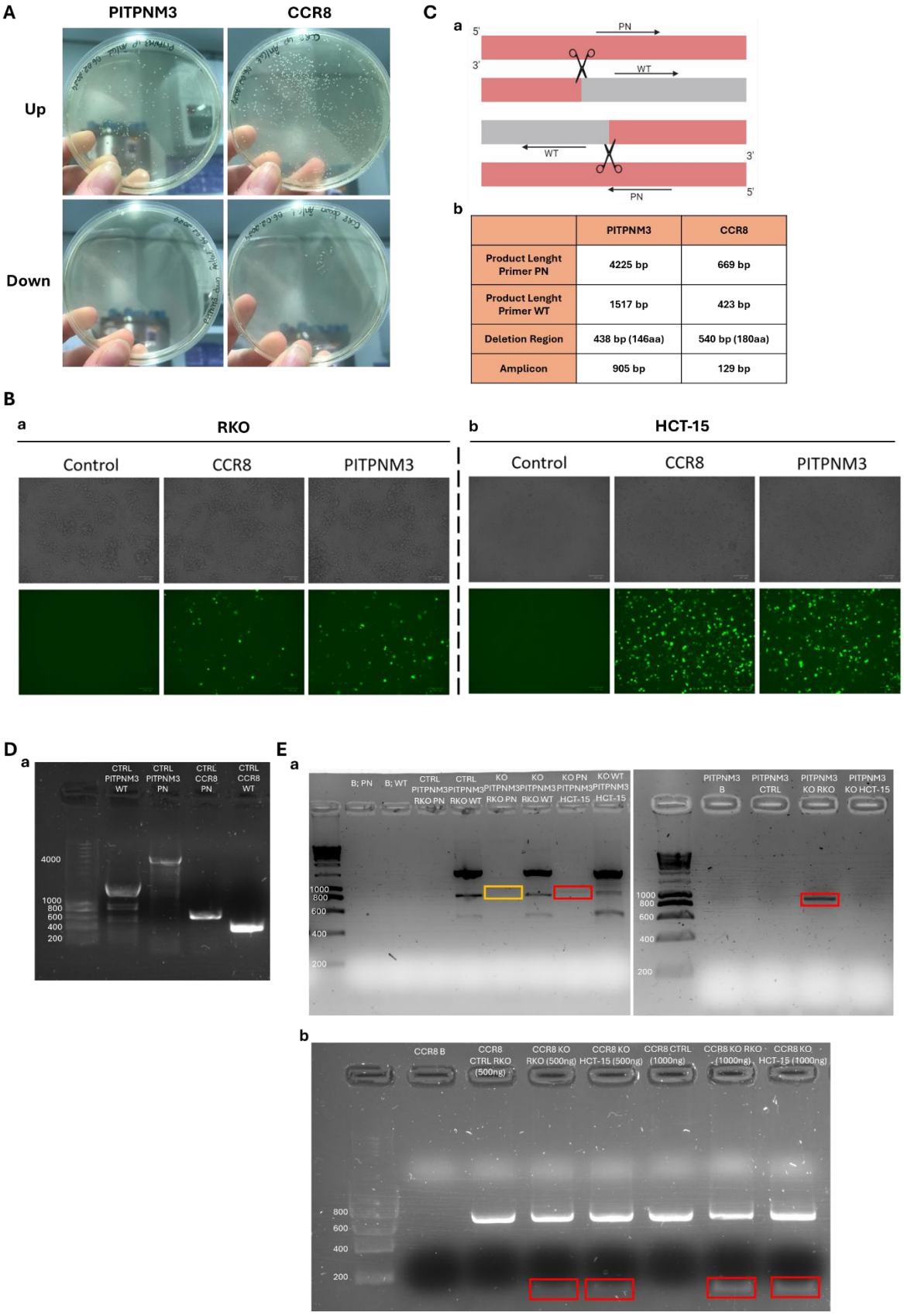

Figure 17. Preparative steps for the silencing of both putative CCL18 receptors (CCR8 and PITPNM3) in CRC cells. CRISPR-Cas9 was used to knockout PITPNM3 and CCR8 genes in RKO and in HCT-15 cells. **(A)** Bacteria transfected with the plasmid for PITPNM3 or CCR8 are being selected. **(B)** GFP+ cells (in green) incorporated the pSpCas9(BB)-2A-GFP (PX458) plasmid in both (a) RKO and (b) HCT-15 cells. **(C)**

(a) Representative scheme of the deletion performed. (b) Length of WT and PN primers, the deletion region, and the resulting amplicon involved in the deletion. WT: wild-type primer and PN: pioneer primer **(D)** Validation of the chosen primers for each gene by PCR reaction. **(E)** PCR analysis of (a) PITPNM3 and (b) CCR8 genes evidences a lack of amplification, suggesting the successful establishment of both a PITPNM3-knockout and a CCR8-knockout population in HCT-15 and in RKO cells (yellow and red rectangles).

After validating all necessary components, we sorted the GFP^+ transfected cells to obtain isolated clones to be expanded and further validated. In total, we obtained 29 CCR8 clones and 15 PITPNM3 clones. Following their expansion, isolated clones underwent testing for KO via PCR analysis, and then 6 WT and 13 putative KO clones were obtained for CCR8, and 7 WT and 4 putative KO clones were obtained for PITPNM3. After this preliminary confirmation, a second PCR was carried out using both wild-type (WT) and pioneer (PN) primers to ensure the existence of a KO population for each receptor. While most of the CCR8 clones (Figure 18A) appear to be KOs, the PITPNM3 clones (Figure 18B) failed this confirmation, with every clone displaying a heterozygous (or polyclonal) phenotype, which we can conclude from the presence of two bands with distinct molecular weights in the PN lane. However, we could observe a change in the PN band pattern of the clones, in comparison to that of the controls (wild-type clones). In fact, there seems to be two high-molecular weight bands migrating closely together in the wild-type control clone, while there is only one band observed in the putative KO clones. The lower band might represent non-specific amplification. If this is the case, the WT PCR indicates that only one of the tested clones (1/3 G2) might be a KO. Sequencing analysis is required to further understand the status of the deletion site in PITPNM3.

Further experiments will be needed to confirm the protein expression levels of CCR8 and PITPNM3 receptors in each of the clones, which will allow another confirmation of KO. Currently, all the expanded clones were frozen, and prepared for DNA extraction and for cell lysates. In the near future, the lysates will be used for western blot analysis aiming to confirm the loss of expression of PITPNM3 and of CCR8 in each RKO and HCT-15 clones, allowing the identification of the real KO ones. Unfortunately, the distinct technical problems encountered, during the expansion of these clones and during the PCR KO confirmation, did not allow us to advance with the western blot analysis and to confirm if the generated clones were indeed KO for the candidate receptors.

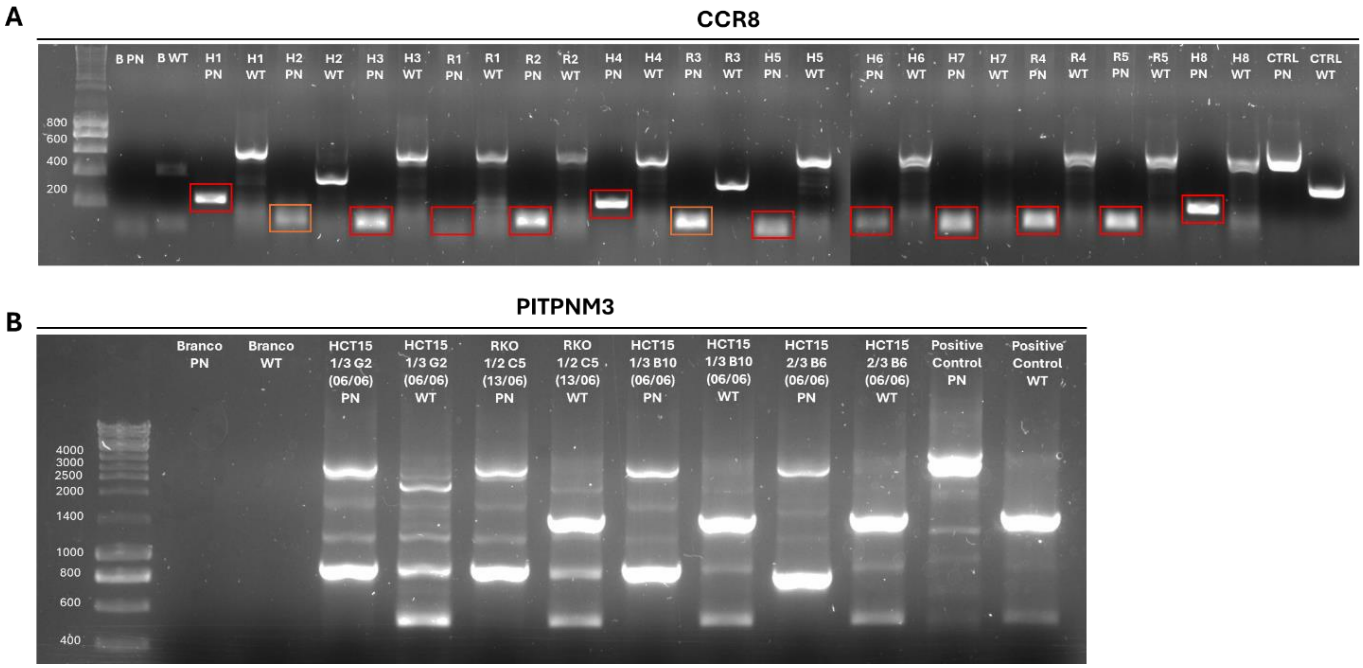

Figure 18. Establishment of CCR8 KO clones. Confirmation of the presence of **(A)** CCR8 knockout clones (indicated by red rectangles) and the absence **(B)** PITPNM3 knockout clones, conducted using PCR analysis, with both WT and PN primers. WT: wild-type primer and PN: pioneer primer

4.6.2. Proteomic crosslinking assay for identifying CCL18 receptors in CRC cell lines

In parallel with the CRISPR-Cas9 technology, performed for the establishment of KO models of CCL18 canonical receptors, we conducted a crosslinking mass spectrometry assay using CCL18-coated magnetic beads as a decoy, to uncover the putative receptor of CCL18 chemokine in our colon cancer cell lines, under native conditions. Since we had previously demonstrated that RKO cells respond and invade in the presence of CCL18, this cell line was selected for this crosslinking assay, in an attempt to pulldown and to identify the CCL18 receptor. In contrast, SW480 cells that do not respond and do not invade in the presence of CCL18, were used as a negative control.

Aiming to pulldown the receptor using the chemokine ligand as a decoy, we performed the coating of the magnetic beads with rhCCL18 protein, the same used for the functional assays in the previous sections. The coating efficacy and epitope recognition were verified by flow cytometry using a specific anti-CCL18 antibody. Our results evidence a clear increase in the mean fluorescence intensity (MFI) for the CCL18-coated beads in comparison to the control non-coated beads, both stained with anti-human CCL18 antibody, which confirmed the binding of CCL18 to the beads (Figure 19A). Additionally, we performed the interaction of the control and CCL18-coated beads with RKO and SW480 colon cancer cells to form conjugates, subsequently isolated for proteomic analysis (Figure 19B). It is possible

to conclude the occurrence of successful binding, considering the presence of the beads (black dots) in the colon cancer cells surroundings (Figure 19B).

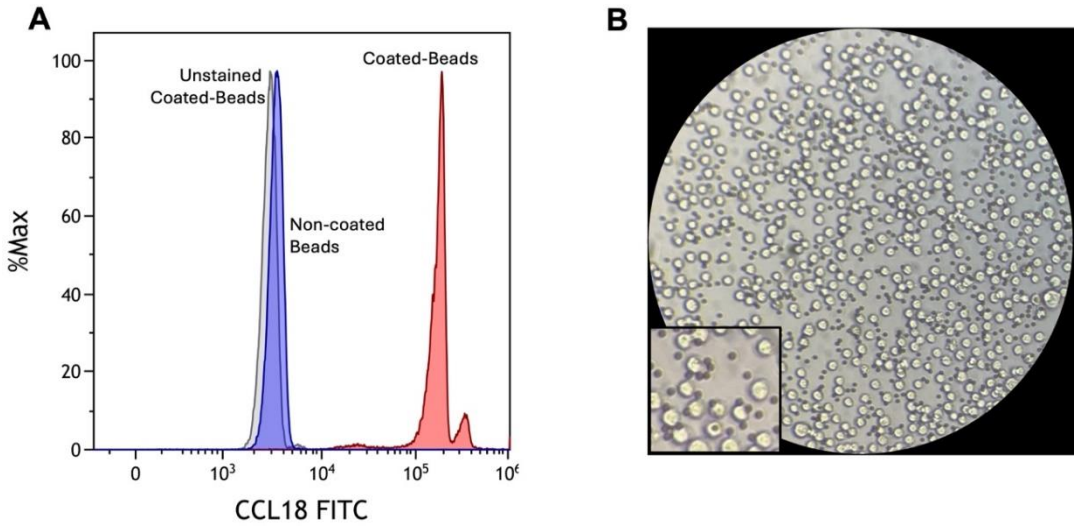

Figure 19. Magnetic beads were successfully coated with CCL18 and conjugated with CRC cells. (A) Representative image of a flow cytometry histogram regarding the coating of the magnetic beads with CCL18 (red histogram), at a ratio of 10µg of CCL18 per 20 million beads. **(B)** Representative image demonstrating the conjugation of the magnetic beads (black dots) with the cancer cells (white dots), after 1h of interaction in a native environment. FITC: fluorescein-5-isothiocyanate.

After conjugation formation and isolation of protein-protein interactions, the samples were digested and analyzed by mass spectrometry. For all conditions, we cross-referenced this information with the human proteome. After filtering out known contaminants and low-confidence hits, we identified high-confidence proteins using the Proteome Discoverer software. It should also be noted that contaminating proteins, meaning proteins that came attached to the beads but did not specifically interact with CCL18, were manually excluded from further analysis.

After filtering, we compared the list of proteins obtained upon the interaction of CCL18-coated beads with RKO samples and with SW480 samples, and excluded those that were enriched or exclusively present in the SW480 samples. This decision was based, as previously stated, on the fact that SW480 cells are not responsive to CCL18-mediated invasion. Then, to restrict the number of candidates, we selected, in the Panther database, the proteins that had the GO term “membrane” and specifically “plasma membrane”, obtaining 29 proteins (Figure 20A). To refine our list of proteins and confirm their plasma membrane association, we searched for the GO terms “plasma membrane” and “cell membrane” in the Uniprot database, in the Subcellular Location section, obtaining a list of 20 proteins (Figure 20B). Finally, we searched for protein-protein interactions in the STRING database and enriched pathways in Cytoscape, using the ClueGo network (Figure 20A).

A

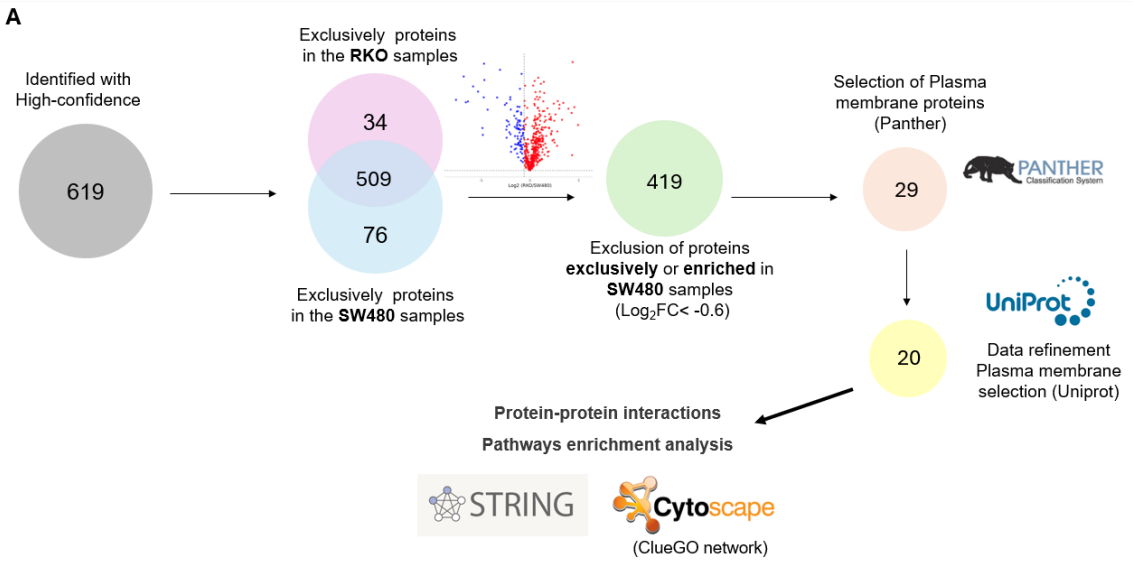

B

Acession	Gene	Protein Name
P51148	RAB5C	Ras-related protein Rab-5C
P07900	HSP90AA1	Heat shock protein HSP 90-alpha
Q9Y4C2	TCAF1	TRPM8 channel-associated factor 1
P14923	JUP	Junction plakoglobin
P07355	ANXA2	Annexin A2
Q9Y490	TLN1	Talin-1
P62873	GNB1	Guanine nucleotide-binding protein G(I)_G(S)_G(T) subunit beta-1
P49006	MARCKSL1	MARCKS-related protein
P51153	RAB13	Ras-related protein Rab-13
P15924	DSP	Desmoplakin
P08195	SLC3A2	4F2 cell-surface antigen heavy chain
P11142	HSPA8	Heat shock cognate 71 kDa protein
O95793	STAU1	Double-stranded RNA-binding protein Staufen homolog 1
P08238	HSP90AB1	Heat shock protein HSP 90-beta
Q99959	PKP2	Plakophilin-2
P08758	ANXA5	Annexin A5
Q13835	PKP1	Plakophilin-1
P01833	PIGR	Polymeric immunoglobulin receptor
P61224	RAP1B	Ras-related protein Rap-1b
P02788	LTF	Lactotransferrin

Figure 20. Proteomic workflow for identifying CCL18-interacting proteins. (A) Schematic overview of the proteomic workflow for selecting the proteins interacting with CCL18-beads. Briefly, the proteins interacting with CCL18-beads were identified using Proteome Discoverer software. Contaminants were excluded, as well as proteins that were either enriched or exclusively found in SW480 conjugates. From the remaining set, only proteins annotated with the GO terms “plasma membrane” and/or “cell membrane” were selected. Further analyses included assessing protein-protein interactions (PPIs) and identifying enriched biological pathways linked to these proteins. **(B)** List of plasma membrane proteins identified using the described roadmap.

Through this strategy, we found a network with 4 major pathways present and enriched in our proteins of interest, with 6 secondary and associated pathways also present (Figure 21A). The major pathways and functions displayed are: positive regulation of intracellular transport (grey), cadherin binding (light blue), cell adhesion and molecule binding (light and dark blue), and neutrophil degranulation (green). Associated with this are: the regulation of intracellular transport (grey), cell-cell junction assembly (dark blue), cell junction assembly (dark blue), cell-cell junction organization (light and dark blue), cell junction organization (dark blue), and innate immune system (green). These pathways can be grouped into three major groups: cell-cell junction organization, positive regulation of intracellular transport, and cadherin binding, with the majority of the proteins (~71%) associated with the first one (Figure 21B).

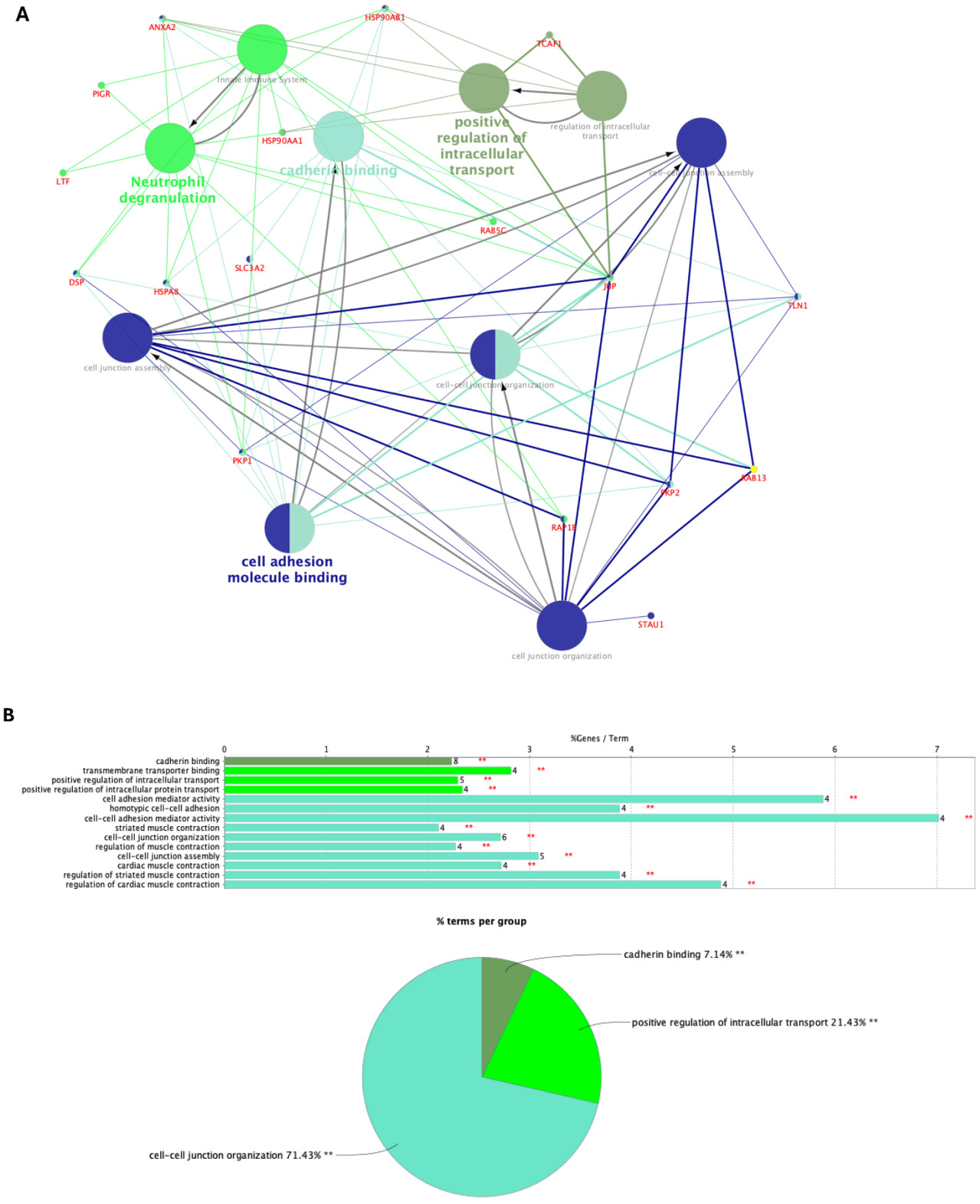

Figure 21. Pathways Enrichment Analysis. (A) Cytoscape was used to visualize and analyze the enriched pathways associated with the selected proteins. This analysis revealed key biological pathways that are significantly overrepresented in the dataset, providing insights into the potential functional roles of the proteins interacting with CCL18. **(B)** The identified proteins were categorized based on their associated biological functions. The percentage of genes per functional group was calculated, illustrating the distribution of protein functions across various cellular processes, including signaling, adhesion, and membrane transport.

Then, considering that we described that EGFR interacts with CCL18 and that this chemokine leads to EGFR and its downstream targets phosphorylation (unpublished results, data not shown), we searched the STRING database for protein-protein interactions between CCL18, EGFR, and our list of targeted proteins. As shown in Figure 22, none of the proteins were previously identified as directly interacting with CCL18. However, the analysis revealed a well-established interaction network centered around EGFR, with 8 proteins interacting directly with this receptor. In addition, other proteins interconnect with these 8 main proteins, suggesting one or more plausible pathways of action within this network.

Conversely, although the STRING network did not identify any proteins interacting with CCL18, there is evidence from the literature of an interaction between CCL18 and annexin 2 (ANXA2) (138), a calcium-dependent phospholipid-binding protein known to organize exocytosis of intracellular proteins to the extracellular milieu but an interactor of the Wnt signaling pathway, suggesting that the database may not yet be fully up to date. To further investigate, we performed an advanced search on PubMed, querying each protein individually using the search terms "*gene name*"[Title/Abstract] AND "*ccl18*"[Title/Abstract], and, to be certain, "*protein name*"[Title/Abstract] AND "*ccl18*"[Title/Abstract], to see if there was indeed a link between other proteins and this chemokine. This search revealed a second study confirming the link between ANXA2 and CCL18 in lung adenocarcinoma (139), in addition to the breast cancer study we were already aware of (138). In addition to ANXA2, the search also yielded results for lactotransferrin (LTF). However, the studies presented, in addition to not being on cancer, do not demonstrate an interaction between these proteins, but only show that both are highly expressed in severe aplastic anemia (140) and in IgG4-related disease (141). Having this in consideration, ANXA2 remains the most likely target for CCL18 interaction but all other appointed molecules remain currently under detailed investigation.

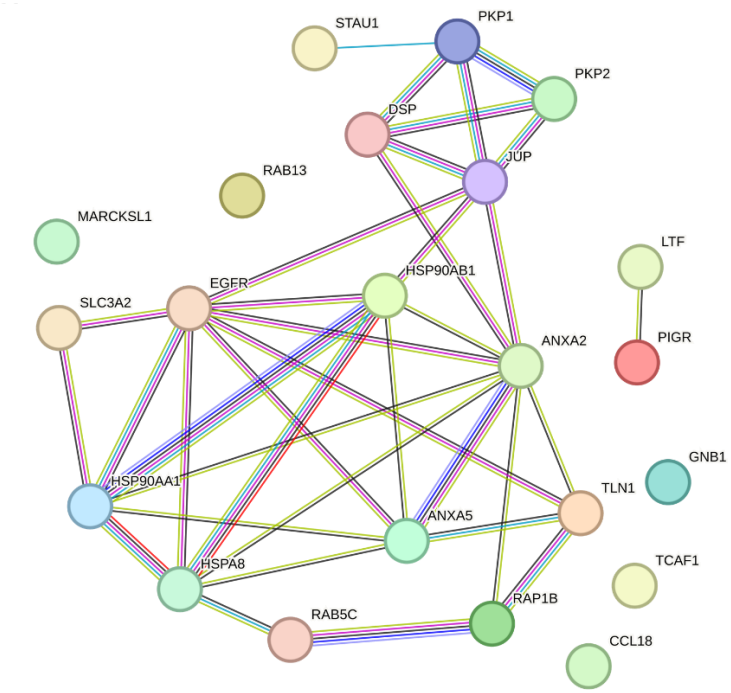

Figure 22. Protein-protein interactions. To investigate potential interactions, we queried the STRING database for CCL18, EGFR, and the proteins on our target list. This analysis aimed to identify known or predicted protein-protein interactions between these molecules.

Chapter 5: Discussion

TAMs have been implicated in the development of tumors considering their pro-migratory, pro-invasive, pro-metastatic, and proteolytic functions. Their primary mechanism of action is the release of various growth factors, including chemokines and cytokines, which influence the behavior of tumor cells or other surrounding immune cells. One of these molecules that captured our attention was CCL18, primarily produced by anti-inflammatory macrophages at the TME, and known to exhibit pro-fibrotic and immunosuppressive functions (53), but also to promote cancer cell invasion and metastasis, in breast, ovary, and lung cancer (49). Nevertheless, in CRC the role of this primate-specific chemokine is still under characterization.

Our group demonstrated that CCL18 produced by anti-inflammatory macrophages, differentiated over decellularized tumor matrices from CRC patients' surgical resections, promoted the invasion of colon cancer cells (46). Importantly, this effect was inhibited upon the usage of a specific anti-CCL18 neutralizing antibody, and involved the phosphorylation of EGFR and of its downstream signaling partners, FAK, Src, Akt, and ERK (46). With the present work, we aimed to understand the underlying mechanisms that sustain CCL18-mediated invasion and to investigate if this chemokine also impacts cancer cell migration, proteolytic activity, proliferation, and induces cell cycle alterations.

Cell migration is a highly dynamic phenomenon that together with gained proteolysis may promote basement membrane invasion, and later cancer metastasis. Our results show that although CCL18 induces RKO and HCT-15 individual cell migration alterations with an overall decrease of the migrated distance, with faster and directional migratory speediness, it promotes RKO collective cancer cell migration. These results support literature data showing that CCL18 causes the migration of breast (85), bladder (104), hepatocellular (84), non-small cell lung (83), prostate (142), glioma (100), glioblastoma (102), ovarian (91,110), pancreatic (93), multiple myeloma (101), osteosarcoma (90), and gastric cancer cells (108). However, it should be noted that different concentrations of CCL18 were tested in all studies. We tested 1ng/mL and 10ng/mL, with stimulation occurring in the higher concentration, which correlates with the results obtained in the breast (85) and pancreatic cancer cells, with the latter also testing 5ng/mL and 25ng/mL, but obtaining better results with the 10ng/mL of CCL18 (93). The studies regarding glioma (100), glioblastoma (102), osteosarcoma (90), ovarian (110), gastric (108,143), and non-small lung cancer cells (83) showed a progressive increase in the migratory capacity of the cancer cells, in parallel with an increase in the concentration of CCL18. In fact, the concentration range started at 10ng/mL, continued through 20ng/mL (90,102,110), and generally ended at 50ng/mL (102,108,110) or 100ng/mL (100,108,143), depending on the study and time of exposure, being the latter concentrations

those generally associated with the greatest migratory capacity. One study, with non-small cell lung cancer, has even tested 1000ng/mL (83). There have also been studies that have only tested one concentration, this being 20ng/mL (84), 50ng/mL (104), or 100ng/mL (101), always showing stimulation of cell migration. Furthermore, the studies that tested collective cell migration, through wound-healing assay, also applied serum reduction, similarly to our experiments (83,85,90,100,102). Although these studies also evidenced the promotion of cancer cell migration, there were many variations in the approaches adopted, starting with the method used to assess migration and ending with the different concentrations tested. Altogether this suggests that standardization is required and caution should be applied when analyzing distinct studies data. Considering all this, further experiments with our cell lines are necessary to analyze whether higher concentrations of CCL18 are required to promote a more significant migratory capacity.

Reports on the effect of CCL18 on proliferation and cell cycle dynamics are more heterogeneous. Our results show that CCL18 does not affect cancer cell cycle, which is in line with what was seen regarding the impact on the proliferation of gastric, pancreatic ductal adenocarcinoma, multiple myeloma, and glioblastoma multiforme cancer cells (92,93,101,102,143). Contrarily, there was an induction of proliferation in breast cancer, diffuse large B cell lymphoma, ovarian cancer, osteosarcoma, urothelial carcinoma, and glioma (90,91,97–100); and a reduction in non-small cell lung cancer cells and pre-B acute lymphocytic leukemia cells (56,96), upon stimulation with this chemokine. Similarly to the migration tests, proliferation experiments also varied in terms of concentrations of CCL18 used. Several concentrations were tested, 1ng/mL, 5ng/mL, 10ng/mL, 20ng/mL, 25ng/mL, 50ng/mL, and 100ng/mL. Effects were seen at 100ng/mL in glioma, but not with 1ng/mL and 10ng/mL (100). In osteosarcoma cells, effects were seen in both concentrations tested (10ng/mL and 20ng/mL), with a better effect at the highest concentration and longer exposure (48h instead of 24h) (90). However, even with a range of concentrations, from 1ng/mL to 100ng/mL, at different time points (24h, 48h, and 72h) no effects were seen in several cancers, including glioblastoma, pancreatic, multiple myeloma, gastric, and non-small lung cancer (92,93,101,102,143). Further studies are necessary to test other concentrations of CCL18 in our colon cancer cell lines, to be certain of the obtained result. Nevertheless, our results suggest that CCL18 at the concentration of 10ng/mL, despite promoting the invasion of colon cancer cells, does not seem to affect cancer cell cycle dynamics, at least *in vitro*.

Another activity associated with the invasion of cancer cells is the degradation of ECM components. Matrix metalloproteases, termed MMPs, are enzymes involved in ECM proteolysis, cell surface receptors cleavage, adhesion molecules degradation, and soluble factors activation, stimulating tumor growth, invasion, and metastasis. These proteases are synthesized in a latent, inactive form called zymogen and contain a zinc atom in their active

site. The contact between the zinc molecule and the cysteine switch in the pro-domain is disrupted during MMP activation, resulting in the pro-form cleavage and production of the active enzyme (144). Active form production typically occurs simultaneously with a decrease in molecular mass and active site exposure. Two members of the MMP family have been highly researched, regarding their role in tumor invasion and metastasis, the gelatinases MMP-2 and MMP-9 (145). Since these gelatinases are typically highly expressed in human malignant tumors, their expression and activity are linked to tumor progression. The term gelatinases derives from their ability to hydrolyze denatured collagen I (gelatin) (144,145). Actually, our group has previous work showing that anti-inflammatory macrophages are efficient in inducing MMP-2 and MMP-9 activity, which was essential for macrophage-mediated cancer cell invasion (146). Moreover, as previously mentioned, we also demonstrated that macrophages differentiated within tumor derived matrices stimulated cancer cell invasion through a mechanism involving CCL18 (46), which led us to hypothesize that CCL18 stimulates MMP activity and promotes cancer cell invasion through this action. Considering the importance of these MMPs for tumor cell invasion, we evaluated their expression in our colon cancer cell lines, in the presence and absence of stimulation with CCL18. Our results show similar gelatinolytic activities of pro-form and active MMP-9 form, and of the pro-form of MMP-2, in the presence and absence of rhCCL18. As such, the activation of these MMPs does not seem to result from the action of the chemokine, suggesting that CCL18 does not promote invasion through ECM degradation. Unfortunately, as there is no research into the association of CCL18 and these MMPs in other cancer types, it is not possible to do a direct comparison with other findings to see whether our results were the norm or the exception. However, it is reported that CCL18, together with MMP-2 and MMP-9, influences pulmonary inflammation and fibrosis, with overexpression of the chemokine increasing the levels of the gelatinases (147). Moreover, although there are no cancer reports on these specific MMPs, there are with other proteases from the MMP family. For example, MMP-3 expression in gastric cancer is increased upon stimulation with CCL18, resulting in cell invasion and migration increase. This stimulation occurs in a dose-dependent manner, with 10ng/mL, 50ng/mL, and 100ng/mL of CLL18 tested, with the latter concentration presenting the better result (143). This suggests that further experiments with higher concentrations of rhCCL18 should be used in parallel with invasion assays. Additionally, it would also be necessary to perform this assay on another colon cell line, to confirm and reinforce our conclusions.

An important aspect to consider in our *in vitro* experiments (migration, proliferation, proteolytic activity) is that they don't reflect necessarily the concentrations of CCL18 present in the serum. CCL18 is described as present in serum at concentrations of 30ng/mL (119), and we are employing 10ng/mL in our tests, since our preliminary results indicated that this concentration was sufficient to induce cancer cell invasion (46). Although this is sufficient to

promote invasion, it may not be sufficient for other types of assays. Considering that other studies have tested various concentrations of CCL18, obtaining results that are dose-dependent, perhaps we should test increasing concentrations of this chemokine in future experiments.

Altogether, our *in vitro* results suggest that the concentration of 10ng/mL of CCL18 seems to promote colon cancer cell invasion by stimulating cells to migrate without the promotion of proteolysis. Tumor cells can migrate as collective groups or as individual cells using mesenchymal or amoeboid modes of dissemination (148). Mesenchymal cells exhibit an elongated morphology and can move forward by producing traction force through integrin-mediated extracellular matrix adhesion and cytoskeletal contractility (148). In our results, we observed a change in cell morphology in our collective cell migration studies, which is in line with this mechanism of action. Usually, the production of migration paths by mesenchymal tumor cells is also dependent on proteolysis-dependent ECM degradation. Conversely, in the lack of proteolysis-dependent ECM remodeling, amoeboid cells with a rounded and deformable morphology can fit through small pores and tight spaces in the ECM. This kind of movement is characterized by the cells' exhibiting protrusions, which maintain dynamic and weak cell adhesion to the ECM, resulting in rapid movement (148). Considering our lack of results regarding the proteolytic activity of MMPs, this could be the preferred mechanism of action, at least for the RKO cell line, which showed the mentioned changes in cell morphology. The HCT-15 cell line did not show the same morphological change, preferring to remain close to neighboring cells. Similarly, it did not show the same capacity for cell migration as the RKO cells.

Additionally, a sign of tumor growth, invasion, and metastasis is the formation of new blood vessels surrounding the tumor (neoangiogenesis). Due to the fact that CCL18 is a primate-specific chemokine, with no known mouse or avian ortholog (53), research on the role of this chemokine in cancer progression has proven challenging, since there is a lack of adequate *in vivo* experimental models. Nevertheless, having ascertained the impact of CCL18 *in vitro* we decided to investigate the impact of this chemokine in tumor growth and neoangiogenesis *in vivo*, using CAM assays. In fact, another study, in breast cancer, also used this model to investigate the relation of this chemokine with their cancer type (149), and was successful. However, our results did not show stimulation regarding tumor area or tumors' new blood vessels formation, upon exposure to rhCCL18. These results contrast with those obtained in the previously mentioned study, in which they verified an increase in the number of vessels when stimulated with CCL18, which acted synergistically with VEGF (111). This study was carried out with the same concentration of CCL18 used in ours (20ng/mL), but its experimental design seems to be different from the one we employed. While we implanted colon cancer cells into the CAM, stimulated them with CCL18, and then assessed

the appearance of new vessels around the tumor; they stimulated the CAM directly with CCL18 in the absence of cancer cells. Considering these circumstances, the rhCCL18 concentration that we used may not be sufficient. Further experiments should be performed to exploit the *in vivo* impact of CCL18.

CCL18 receptors remained unknown for several years upon its discovery. Recently, three receptors were described as CCL18 receptors: CCR8, PITPNM3, and GPR30, in distinct tissue types. However, nothing was described in CRC. As such, we employed the CRISPR-Cas9 technology to uncover the CCL18 receptor in our CRC cell lines. Since the activation of GPR30 by CCL18 does not result in direct signal transduction, only disturbs the signal transmission from the receptor for the CXCL12, resulting in reduced chemotaxis and proliferation of tumor cells exhibiting high expression of this chemokine (56), we decided to proceed only with CCR8 and PITPNM3, which are well-described to be CCL18 receptors. Unfortunately, due to the distinct technical problems encountered, during the expansion of these clones and the PCR KO confirmation, we did not completely confirm if the candidate receptors were indeed KO at the protein level. We performed PCR to ensure the existence of a KO population, being successful for the CCR8 clones, while the PITPNM3 clones failed this confirmation, with every clone displaying a heterozygous (or polyclonal) phenotype. However, we could observe a change in the PN band pattern of the clones, in comparison to that of the controls (wild-type clones). In fact, there seems to be two high-molecular weight bands migrating closely together in the wild-type control clone, while there is only one band observed in the putative KO clones. The lower band might represent non-specific amplification. If this is the case, the WT PCR indicates that only one of the tested PITPNM3 clones (1/3 G2) might be a KO. Sequencing analysis is required to understand the status of the deletion site in PITPNM3. Further experiments will be needed to confirm the protein expression levels of the clones, which will allow another KO confirmation and reach a conclusion regarding the putative receptor for our colon cancer cell lines. In the near future, western blot analysis will confirm the expression levels of PITPNM3 and of CCR8 in each RKO and HCT-15 clones, allowing the identification of the real KO ones.

In parallel, considering that the colon cancer cells' CCL18 receptor may be not yet described, we employed a crosslinking mass spectrometry assay using CCL18-coated magnetic beads as a decoy, to uncover this chemokine putative receptor. Interestingly, none of the receptors previously described by others to bind to CCL18, such as CCR8, PITPNM3, or GPR30, emerged through this strategy as putative CCL18 receptors. After a curated analysis, where we confidently selected plasma membrane proteins, we performed a search for protein-protein interactions involving our list of proteins with CCL18 and EGFR, as we have previously described that this chemokine induces EGFR and its downstream targets tyrosine phosphorylation. Subsequent confirmation of our results using PubMed revealed

that ANXA2 emerges as the most likely target, as it is the only protein identified with documented connections to both EGFR and to CCL18 in cancer contexts. Notably, ANXA2 has been reported to interact with CCL18 in breast and lung cancer, and has been described to promote cancer cell invasion, migration, proliferation, and metastasis. Interestingly, these effects were attributed to the activation of signaling pathways associated with EGFR (138,139).

ANXA2 is a member of the annexin family, which comprises calcium-dependent phospholipid-binding proteins known for their diverse intra- and extracellular functions. These proteins play critical roles in signal transduction pathways and in the regulation of cellular growth. ANXA2 exists in four distinct forms: cytoplasmatic, membrane-bound, nuclear, and secreted. It is overexpressed in several malignant tumors and described to contribute to invasion, metastasis, angiogenesis, proliferation, F-actin polymerization, EMT, and drug resistance, playing an important role in the progression of cancer (138,150). Its multifaceted roles underscore its importance in cancer biology and highlights its potential as a therapeutic target.

ANXA2 was described to interact with CCL18, promoting CCL18-induced breast cancer progression and metastasis. Moreover, through the stabilization of Snail, which is a transcriptional factor crucial to the PI3K/Akt/GSK3β/Snail signaling pathway, ANXA2 was also described to promote CCL18-induced EMT, in breast cancer cells. This effect seems to be mediated through the PI3K/Akt/GSK3β/Snail pathway, since depletion of ANXA2 impaired CCL18-induced phosphorylation of Akt and GSK3β (138). While this study did not explicitly describe an association between ANXA2 and EGFR, it is noteworthy that Akt, a key component of the EGFR pathway, could be a common partner of both molecules (151). Nevertheless, in other studies, ANXA2 has been reported as directly interacting with EGFR and, indirectly, with its downstream signaling targets.

EGFR is a member of the receptor tyrosine kinase (RTK) family, which regulates activities associated with cancer progression, such as cell proliferation, differentiation, and motility. Upon binding to its ligands, which include EGF, TGFα, and heparin-binding EGF (HbEGF), the EGFR tyrosine kinase (TK) domain dimerizes and activates downstream effector partners. Alternatively, other TK receptors and GPCR are also described to transactivate EGFR (151). Following TK activation, trans-phosphorylation of tyrosine residues within the intracellular domain of the receptor occurs, acting as docking sites for the interaction with downstream effector pathways. This cascade activates several critical signaling pathways, including the PKC pathway, the PI3K-Akt pathway, the phospholipase D1 and D2 and STAT signaling, and the MAPK pathway (151–153).

Interestingly, ANXA2 is described as being involved in the internalization and sorting of EGFR, upon ligand activation, in early endosomes. Furthermore, it is also involved in the translocation of Src to the plasma membrane, which is one of the major regulators of the EGFR signaling pathway (154). EGF and insulin are growth factors also known to induce PI3K and Src-mediated phosphorylation and activation of ANXA2. ANXA2 is also described to bind to FAK, another important member of the EGFR signaling pathway (152,153) and to be, indirectly, implicated in the regulation of the Akt pathway (155). In CRC, ANXA2 is described to promote cell invasion via Src/ANXA2/STAT3 pathway (156). In this study, the inhibition and silencing of Scr, STAT3, and ANXA2 prevented cancer cell invasion induced by TGF-β. Moreover, Scr and STAT3 inhibition also interfered with EMT, and delayed cell proliferation (156). In breast cancer, a study has reported a direct interaction between EGFR and ANXA2, independently of EGF stimulation, suggesting that ANXA2 is inherently part of the EGFR protein complex rather than being transiently recruited upon stimulation, although the precise sequence of events was not described (153). In this study, it has been suggested that ANXA2 binds to EGFR at the cell membrane and modulates EGFR phosphorylation and functions. The use of an anti-ANXA2 blocking antibody, suppressed EGF-mediated EGFR tyrosine phosphorylation, homodimerization, and signaling, impairing PI3K-Akt and Raf-MEK-ERK phosphorylation, cell migration, and proliferation (153).

Our previous results suggest that EGFR and CCL18 also interact. Our group has demonstrated that CCL18 stimulates the phosphorylation of the EGFR and of its downstream associated members, FAK, Src, Akt, and ERK, on CRC cells (unpublished, data not shown). Also, CCL18 was identified as the most effective component in the co-incubation medium promoting esophageal adenocarcinoma cell proliferation and tumor growth, with this effect being dependent on the level of EGFR (157).

Considering all the information described above, ANXA2 seems to be a suitable target for further studies regarding its interaction with EGFR and with CCL18 in colon cancer cell lines. One could speculate that CCL18 may bind to ANXA2 and through it induce EGFR dimerization, phosphorylation, and activation of downstream interacting partners that culminate in the induction of cancer cell invasion and migration. However, additional studies are needed to elucidate the impact of ANXA2 on the activation of EGFR and of its downstream targets' phosphorylation, but also of the canonical CCL18 receptors, as GPR30, PITPNM3, and CCR8. Further invasion assays with cells lacking these receptors expression and exposed to CCL18 will be crucial to validate their relevance for CCL18-mediated cancer cell invasion.

Chapter 6: Conclusions and Future Perspectives

In conclusion, we report that the apparent underlying mechanism of action by which CCL18 promotes colon cancer cell invasion is through promoting cell migration, particularly collective cell migration, considering that it did not enhance MMP proteolytic activities. Furthermore, after stimulating invasion, CCL18 did not induce cell cycle dynamics alterations *in vitro*, nor tumor growth and neoangiogenesis *in vivo*. Considering that CCL18 may have an effect on the stimulation of metastasis, as suggested in other tumor types, there appear to be other underlying mechanisms to ensure the survival of the circulating tumor cells and subsequent formation of a secondary tumor. However, in the future, further studies with higher CCL18 concentrations are first needed to ensure that our results and conclusions are valid. Only then could other mechanisms be considered.

In the future, it would be necessary to complete the search for the putative CCL18 receptor in our colon cell lines. Considering the promising results obtained through our two distinct approaches, through CRISPR-Cas9 technology and the crosslinking mass spectrometry assay, it is possible that we will reach concrete conclusions soon. At first, we plan to improve our PCR analysis to confirm PITPNM3, followed by western blot confirmation that the selected RKO and HCT-15 KO clones are indeed lacking the expression of CCR8 and of PITPNM3 receptors. The successful KO clones will be subsequently selected for additional functional assays to confirm if CCL18 is still, in the lack of these receptors' expression, inducing the stimulation of cancer cell invasion and of EGFR and its interacting partners' tyrosine phosphorylation. The candidate molecules encountered through our crosslinking mass spectrometry search approach will be also know subject of more research. Namely, ANXA2 and EGFR blocking antibodies will be used to exploit the impact on cancer cell invasion and on the downstream pathways' activation.

As future perspectives, it could also be interesting to move on to humans and, through patients' cohorts, evaluate and monitor serum levels of CCL18 during the evolution of the disease, the various phases of treatment, and post-treatment recovery. In this way, we could uncover the possible role of CCL18 as a biomarker of this disease. Having this into consideration we have already designed, in collaboration with the IPO-Porto oncologists and gastroenterologists, a prospective study to longitudinally monitor CCL18 serum levels that we plan to initiate soon.

Thesis Associated Outputs

During the past year, this thesis work was showcased in first-author poster presentations at the VII iBiMED Symposium, the 17th Young Researchers Meeting of the University of Porto (IJUP), and the Symposium on Immunomodulation in Cancer and Regeneration (SICR). The latter was also selected as a speed talk presentation.

Additionally, the results from this thesis will be incorporated in a scientific article, soon to be prepared. A review article, focused on CCL18 receptors is also being prepared for submission.

References

1. World Health Organization. Health topics: cancer. Available from: https://www.who.int/health-topics/cancer#tab=tab_1.

2. Nature Education. Cell division and Cancer. Available from: https://www.nature.com/scitable/topicpage/cell-division-and-cancer-14046590/.

3. Bray F, Laversanne M, Sung H, Ferlay J, Siegel RL, Soerjomataram I, et al. Global cancer statistics 2022: GLOBOCAN estimates of incidence and mortality worldwide for 36 cancers in 185 countries. CA Cancer J Clin. 2024 May 4;74(3):229–63.

4. Dekker E, Tanis PJ, Vleugels JLA, Kasi PM, Wallace MB. Colorectal cancer. The Lancet. 2019 Oct;394(10207):1467–80.

5. Lee S, Meyerhardt JA. Impact of Diet and Exercise on Colorectal Cancer. Hematol Oncol Clin North Am. 2022 Jun;36(3):471–89.

6. Ferlay J, Ervik M, Lam F, Laversanne M, Colombet M, Mery L, et al. Global Cancer Observatory: Cancer Today. Lyon, France: International Agency for Research on Cancer. Available from: https://gco.iarc.who.int/today, accessed 03/09/2024.]. 2024.

7. Ahmed S, Johnson K, Ahmed O, Iqbal N. Advances in the management of colorectal cancer: from biology to treatment. Int J Colorectal Dis. 2014 Sep 24;29(9):1031–42.

8. Mármol I, Sánchez-de-Diego C, Pradilla Dieste A, Cerrada E, Rodriguez Yoldi M. Colorectal Carcinoma: A General Overview and Future Perspectives in Colorectal Cancer. Int J Mol Sci. 2017 Jan 19;18(1):197.

9. Yamagishi H, Kuroda H, Imai Y, Hiraishi H. Molecular pathogenesis of sporadic colorectal cancers. Chin J Cancer. 2016 Dec 6;35(1):4.

10. Ionescu VA, Gheorghe G, Bacalbasa N, Chiotoroiu AL, Diaconu C. Colorectal Cancer: From Risk Factors to Oncogenesis. Medicina (B Aires). 2023 Sep 12;59(9):1646.

11. Adebayo AS, Agbaje K, Adesina SK, Olajubutu O. Colorectal Cancer: Disease Process, Current Treatment Options, and Future Perspectives. Pharmaceutics. 2023 Nov 12;15(11):2620.

12. Balchen V, Simon K. Colorectal cancer development and advances in screening. Clin Interv Aging. 2016 Jul;Volume 11:967–76.

13. Duan B, Zhao Y, Bai J, Wang J, Duan X, Luo X, et al. Colorectal Cancer: An Overview. Gastrointestinal Cancers Brisbane (AU): Exon Publications. 2022;

14. Kumar A, Gautam V, Sandhu A, Rawat K, Sharma A, Saha L. Current and emerging therapeutic approaches for colorectal cancer: A comprehensive review. World J Gastrointest Surg. 2023 Apr 27;15(4):495–519.

15. Gupta S. Screening for Colorectal Cancer. Hematol Oncol Clin North Am. 2022 Jun;36(3):393–414.

16. Jayasinghe M, Prathiraja O, Caldera D, Jena R, Coffie-Pierre JA, Silva MS, et al. Colon Cancer Screening Methods: 2023 Update. Cureus. 2023 Apr 12;

17. FDA-NIH Biomarker Working Group. BEST (Biomarkers, EndpointS, and other Tools) Resource [Internet]. Silver Spring (MD): Food and Drug Administration (US); 2016 [cited 2023 Dec 11]. Available from: https://www.ncbi.nlm.nih.gov/books/NBK326791/ Co-published by National Institutes of Health (US), Bethesda (MD).

18. Lech G. Colorectal cancer tumour markers and biomarkers: Recent therapeutic advances. World J Gastroenterol. 2016;22(5):1745.

19. Hauptman N, Glavač D. Colorectal Cancer Blood-Based Biomarkers. Gastroenterol Res Pract. 2017 Sep 25;2017:1–11.

20. Arneth B. Tumor Microenvironment. Medicina (B Aires). 2019 Dec 30;56(1):15.

21. He X, Lee B, Jiang Y. Cell-ECM Interactions in Tumor Invasion. In: Systems Biology of Tumor Microenvironment. 2016. p. 73–91.

22. Dzobo K, Dandara C. The Extracellular Matrix: Its Composition, Function, Remodeling, and Role in Tumorigenesis. Biomimetics. 2023 Apr 5;8(2):146.

23. Watnick RS. The Role of the Tumor Microenvironment in Regulating Angiogenesis. Cold Spring Harb Perspect Med. 2012 Dec 1;2(12):a006676–a006676.

24. Norton SE, Ward-Hartstonge KA, Taylor ES, Kemp RA. Immune cell interplay in colorectal cancer prognosis. World J Gastrointest Oncol. 2015;7(10):221.

25. Shapouri-Moghaddam A, Mohammadian S, Vazini H, Taghadosi M, Esmaeili S, Mardani F, et al. Macrophage plasticity, polarization, and function in health and disease. J Cell Physiol. 2018 Sep;233(9):6425–40.

26. Gouveia-Fernandes S. Monocytes and Macrophages in Cancer: Unsuspected Roles. In: Serpa J, editor. Tumor Microenvironment. Cham: Springer International Publishing; 2020. p. 161–85.

27. Yao Y, Xu XH, Jin L. Macrophage Polarization in Physiological and Pathological Pregnancy. Front Immunol. 2019 Apr 15;10.

28. Zhang W, Wang M, Ji C, Liu X, Gu B, Dong T. Macrophage polarization in the tumor microenvironment: Emerging roles and therapeutic potentials. Biomedicine & Pharmacotherapy. 2024 Aug;177:116930.

29. Mantovani A, Sozzani S, Locati M, Allavena P, Sica A. Macrophage polarization: tumor-associated macrophages as a paradigm for polarized M2 mononuclear phagocytes. Trends Immunol. 2002 Nov 1;23(11):549–55.

30. Sica A, Larghi P, Mancino A, Rubino L, Porta C, Totaro MG, et al. Macrophage polarization in tumour progression. Semin Cancer Biol. 2008 Oct;18(5):349–55.

31. Poh AR, Ernst M. Targeting Macrophages in Cancer: From Bench to Bedside. Front Oncol. 2018 Mar 12;8.

32. Bingle L, Brown NJ, Lewis CE. The role of tumour-associated macrophages in tumour progression: implications for new anticancer therapies. J Pathol. 2002 Mar 22;196(3):254–65.

33. Zhang Q wen, Liu L, Gong C yang, Shi H shan, Zeng Y hui, Wang X ze, et al. Prognostic Significance of Tumor-Associated Macrophages in Solid Tumor: A Meta-Analysis of the Literature. PLoS One. 2012 Dec 28;7(12):e50946.

34. Zhang Q, Sioud M. Tumor-Associated Macrophage Subsets: Shaping Polarization and Targeting. Int J Mol Sci. 2023 Apr 19;24(8):7493.

35. Yang Z, Zhang M, Peng R, Liu J, Wang F, Li Y, et al. The prognostic and clinicopathological value of tumor-associated macrophages in patients with colorectal cancer: a systematic review and meta-analysis. Int J Colorectal Dis. 2020 Sep 14;35(9):1651–61.

36. Li J, Li L, Li Y, Long Y, Zhao Q, Ouyang Y, et al. Tumor-associated macrophage infiltration and prognosis in colorectal cancer: systematic review and meta-analysis. Int J Colorectal Dis. 2020 Jul 17;35(7):1203–10.

37. Curren Smith EW. Macrophage Polarization and Its Role in Cancer. J Clin Cell Immunol. 2015;06(04).

38. Erreni M, Mantovani A, Allavena P. Tumor-associated Macrophages (TAM) and Inflammation in Colorectal Cancer. Cancer Microenvironment. 2011 Aug 17;4(2):141–54.

39. Roelands J, van der Ploeg M, Ijsselsteijn ME, Dang H, Boonstra JJ, Hardwick JCH, et al. Transcriptomic and immunophenotypic profiling reveals molecular and immunological hallmarks of colorectal cancer tumourigenesis. Gut. 2023 Jul;72(7):1326–39.

40. Bao X, Li Q, Chen D, Dai X, Liu C, Tian W, et al. A multiomics analysis-assisted deep learning model identifies a macrophage-oriented module as a potential therapeutic target in colorectal cancer. Cell Rep Med. 2024 Feb;5(2):101399.

41. Walker C, Mojares E, Del Río Hernández A. Role of Extracellular Matrix in Development and Cancer Progression. Int J Mol Sci. 2018 Oct 4;19(10):3028.

42. Yue B. Biology of the Extracellular Matrix. J Glaucoma. 2014;23:S20–3.

43. Lu P, Weaver VM, Werb Z. The extracellular matrix: A dynamic niche in cancer progression. Journal of Cell Biology. 2012 Feb 20;196(4):395–406.

44. Brassart-Pasco S, Brézillon S, Brassart B, Ramont L, Oudart JB, Monboisse JC. Tumor Microenvironment: Extracellular Matrix Alterations Influence Tumor Progression. Front Oncol. 2020 Apr 15;10.

45. Marques-Magalhães Â, Cruz T, Costa ÂM, Estêvão D, Rios E, Canão PA, et al. Decellularized Colorectal Cancer Matrices as Bioactive Scaffolds for Studying Tumor-Stroma Interactions. Cancers (Basel). 2022 Jan 12;14(2):359.

46. Pinto ML, Rios E, Silva AC, Neves SC, Caires HR, Pinto AT, et al. Decellularized human colorectal cancer matrices polarize macrophages towards an anti-inflammatory phenotype promoting cancer cell invasion via CCL18. Biomaterials. 2017 Apr 1;124:211–24.

47. Do HTT, Lee CH, Cho J. Chemokines and their Receptors: Multifaceted Roles in Cancer Progression and Potential Value as Cancer Prognostic Markers. Cancers (Basel). 2020 Jan 24;12(2):287.

48. Chenivesse C, Tsicopoulos A. CCL18 – Beyond chemotaxis. Cytokine. 2018 Sep;109:52–6.

49. Korbecki J, Olbromski M, Dzięgiel P. CCL18 in the Progression of Cancer. Int J Mol Sci. 2020 Oct 26;21(21):7955.

50. Legendre B, Tokarski C, Chang Y, De Freitas Caires N, Lortat-Jacob H, Nadaï P De, et al. The disulfide bond between cysteine 10 and cysteine 34 is required for CCL18 activity. Cytokine. 2013 Oct;64(1):463–70.

51. Kodelja V, Müller C, Politz O, Hakij N, Orfanos CE, Goerdt S. Alternative Macrophage Activation-Associated CC-Chemokine-1, a Novel Structural Homologue of Macrophage Inflammatory Protein-1α with a Th2-Associated Expression Pattern. The Journal of Immunology. 1998 Feb 1;160(3):1411–8.

52. Pinto AT, Pinto ML, Velho S, Pinto MT, Cardoso AP, Figueira R, et al. Intricate Macrophage-Colorectal Cancer Cell Communication in Response to Radiation. PLoS One. 2016 Aug 11;11(8):e0160891.

53. Cardoso AP, Pinto ML, Castro F, Costa ÂM, Marques-Magalhães Â, Canha-Borges A, et al. The immunosuppressive and pro-tumor functions of CCL18 at the tumor microenvironment. Cytokine Growth Factor Rev. 2021 Aug;60:107–19.

54. Islam SA, Ling MF, Leung J, Shreffler WG, Luster AD. Identification of human CCR8 as a CCL18 receptor. Journal of Experimental Medicine. 2013 Sep 23;210(10):1889–98.

55. Hong R, Shen MH, Xie XH, Ruan SM. Inhibition of Breast Cancer Metastasis Via PITPNM3 by Pachymic Acid. Asian Pacific Journal of Cancer Prevention. 2012 May 30;13(5):1877–80.

56. Catusse J, Wollner S, Leick M, Schröttner P, Schraufstätter I, Burger M. Attenuation of CXCR4 responses by CCL18 in acute lymphocytic leukemia B cells. J Cell Physiol. 2010 Dec 15;225(3):792–800.

57. Peng Q, Jiang H, Cheng X, Wang N, Zhou S, Zhang Y, et al. Cryo-EM Structure and Biochemical Analysis of the Human Chemokine Receptor CCR8. Biochemistry. 2024 Aug 6;63(15):1892–900.

58. Horuk R. Chemokine receptors. Cytokine Growth Factor Rev. 2001 Dec;12(4):313–35.

59. Sun D, Sun Y, Janezic E, Zhou T, Johnson M, Azumaya C, et al. Structural basis of antibody inhibition and chemokine activation of the human CC chemokine receptor 8. Nat Commun. 2023 Dec 1;14(1):7940.

60. Sokol CL, Camire RB, Jones MC, Luster AD. The Chemokine Receptor CCR8 Promotes the Migration of Dendritic Cells into the Lymph Node Parenchyma to Initiate the Allergic Immune Response. Immunity. 2018 Sep;49(3):449-463.e6.

61. Gombert M, Dieu-Nosjean MC, Winterberg F, Bünemann E, Kubitza RC, Da Cunha L, et al. CCL1-CCR8 Interactions: An Axis Mediating the Recruitment of T Cells and Langerhans-Type Dendritic Cells to Sites of Atopic Skin Inflammation. The Journal of Immunology. 2005 Apr 15;174(8):5082–91.

62. Bishop B, Lloyd CM. CC Chemokine Ligand 1 Promotes Recruitment of Eosinophils But Not Th2 Cells During the Development of Allergic Airways Disease. The Journal of Immunology. 2003 May 1;170(9):4810–7.

63. Wang L, Jenkins TJ, Dai M, Yin W, Pulido JC, LaMantia-Martin E, et al. Antagonism of chemokine receptor CCR8 is ineffective in a primate model of asthma. Thorax. 2013 Jun;68(6):506–12.

64. Goya I, Villares R, Zaballos A, Gutiérrez J, Kremer L, Gonzalo JA, et al. Absence of CCR8 Does Not Impair the Response to Ovalbumin-Induced Allergic Airway Disease. The Journal of Immunology. 2003 Feb 15;170(4):2138–46.

65. Chung CD, Kuo F, Kumer J, Motani AS, Lawrence CE, Henderson WR, et al. CCR8 Is Not Essential for the Development of Inflammation in a Mouse Model of Allergic Airway Disease. The Journal of Immunology. 2003 Jan 1;170(1):581–7.

66. Rucker J, Edinger AL, Sharron M, Samson M, Lee B, Berson JF, et al. Utilization of chemokine receptors, orphan receptors, and herpesvirus-encoded receptors by diverse human and simian immunodeficiency viruses. J Virol. 1997 Dec;71(12):8999–9007.

67. Jinno A, Shimizu N, Soda Y, Haraguchi Y, Kitamura T, Hoshino H. Identification of the Chemokine Receptor TER1/CCR8 Expressed in Brain-Derived Cells and T Cells as a New Coreceptor for HIV-1 Infection. Biochem Biophys Res Commun. 1998 Feb;243(2):497–502.

68. Puttur F, Denney L, Gregory LG, Vuononvirta J, Oliver R, Entwistle LJ, et al. Pulmonary environmental cues drive group 2 innate lymphoid cell dynamics in mice and humans. Sci Immunol. 2019 Jun 7;4(36).

69. Knipfer L, Schulz-Kuhnt A, Kindermann M, Greif V, Symowski C, Voehringer D, et al. A CCL1/CCR8-dependent feed-forward mechanism drives ILC2 functions in type 2–mediated inflammation. Journal of Experimental Medicine. 2019 Dec 2;216(12):2763–77.

70. Kang L, Schmalzl A, Leupold T, Gonzalez-Acera M, Atreya R, Neurath MF, et al. CCR8 Signaling via CCL1 Regulates Responses of Intestinal IFN-γ Producing Innate Lymphoid Cells and Protects From Experimental Colitis. Front Immunol. 2021 Feb 5;11.

71. Korbecki J, Grochans S, Gutowska I, Barczak K, Baranowska-Bosiacka I. CC Chemokines in a Tumor: A Review of Pro-Cancer and Anti-Cancer Properties of Receptors CCR5, CCR6, CCR7, CCR8, CCR9, and CCR10 Ligands. Int J Mol Sci. 2020 Oct 15;21(20):7619.

72. De Simone M, Arrigoni A, Rossetti G, Gruarin P, Ranzani V, Politano C, et al. Transcriptional Landscape of Human Tissue Lymphocytes Unveils Uniqueness of Tumor-Infiltrating T Regulatory Cells. Immunity. 2016 Nov;45(5):1135–47.

73. Plitas G, Konopacki C, Wu K, Bos PD, Morrow M, Putintseva EV, et al. Regulatory T Cells Exhibit Distinct Features in Human Breast Cancer. Immunity. 2016 Nov;45(5):1122–34.

74. Wang L, Simons DL, Lu X, Tu TY, Solomon S, Wang R, et al. Connecting blood and intratumoral Treg cell activity in predicting future relapse in breast cancer. Nat Immunol. 2019 Sep 8;20(9):1220–30.

75. Barsheshet Y, Wildbaum G, Levy E, Vitenshtein A, Akinseye C, Griggs J, et al. CCR8+FOXp3+ Treg cells as master drivers of immune regulation. Proceedings of the National Academy of Sciences. 2017 Jun 6;114(23):6086–91.

76. Villarreal DO, L'Huillier A, Armington S, Mottershead C, Filippova E V., Coder BD, et al. Targeting CCR8 Induces Protective Antitumor Immunity and Enhances Vaccine-Induced Responses in Colon Cancer. Cancer Res. 2018 Sep 15;78(18):5340–8.

77. Hoelzinger DB, Smith SE, Mirza N, Dominguez AL, Manrique SZ, Lustgarten J. Blockade of CCL1 Inhibits T Regulatory Cell Suppressive Function Enhancing Tumor Immunity without Affecting T Effector Responses. The Journal of Immunology. 2010 Jun 15;184(12):6833–42.

78. Van Damme H, Dombrecht B, Kiss M, Roose H, Allen E, Van Overmeire E, et al. Therapeutic depletion of CCR8+ tumor-infiltrating regulatory T cells elicits antitumor immunity and synergizes with anti-PD-1 therapy. J Immunother Cancer. 2021 Feb 15;9(2):e001749.

79. Liu L, Doijen J, D'huys T, Verhaegen Y, Dehaen W, De Jonghe S, et al. Biological characterization of ligands targeting the human CC chemokine receptor 8 (CCR8) reveals the biased signaling properties of small molecule agonists. Biochem Pharmacol. 2021 Jun;188:114565.

80. Köhn L, Kadzhaev K, Burstedt MSI, Haraldsson S, Hallberg B, Sandgren O, et al. Mutation in the PYK2-binding domain of PITPNM3 causes autosomal dominant cone dystrophy (CORD5) in two Swedish families. European Journal of Human Genetics. 2007 Jun 21;15(6):664–71.

81. Liu Z, Shi Y, Lv L, Chen J, Jiang WenG, Li J, et al. Small Molecular Inhibitors Reverse Cancer Metastasis by Blockading Oncogenic PITPNM3. Advanced Science. 2022 Dec 26;9(35).

82. Reinis A, Golovleva I, Köhn L, Sandgren O. Ocular phenotype of CORD5, an autosomal dominant retinal dystrophy associated with PITPNM3 p.Q626H mutation. Acta Ophthalmol. 2013 May 9;91(3):259–66.

83. Shi L, Zhang B, Sun X, Zhang X, Lv S, Li H, et al. CC chemokine ligand 18(CCL18) promotes migration and invasion of lung cancer cells by binding to Nir1 through Nir1-ELMO1/DOC180 signaling pathway. Mol Carcinog. 2016 Dec 12;55(12):2051–62.

84. Lin Z, Li W, Zhang H, Wu W, Peng Y, Zeng Y, et al. CCL18/PITPNM3 enhances migration, invasion, and EMT through the NF-κB signaling pathway in hepatocellular carcinoma. Tumor Biology. 2016 Mar 8;37(3):3461–8.

85. Zhang B, Yin C, Li H, Shi L, Liu N, Sun Y, et al. Nir1 promotes invasion of breast cancer cells by binding to chemokine (C–C motif) ligand 18 through the PI3K/Akt/GSK3β/Snail signalling pathway. Eur J Cancer. 2013 Dec;49(18):3900–13.

86. Tirado-Garibay AC, Falcón-Ruiz EA, Ochoa-Zarzosa A, López-Meza JE. GPER: An Estrogen Receptor Key in Metastasis and Tumoral Microenvironments. Int J Mol Sci. 2023 Oct 8;24(19):14993.

87. Hernández-Silva CD, Villegas-Pineda JC, Pereira-Suárez AL. Expression and Role of the G Protein-Coupled Estrogen Receptor (GPR30/GPER) in the Development and Immune Response in Female Reproductive Cancers. Front Endocrinol (Lausanne). 2020 Aug 20;11.

88. Martin TA, Ye L, Sanders AJ, et al. Cancer Invasion and Metastasis: Molecular and Cellular Perspective. In: Madame Curie Bioscience Database [Internet]. Austin (TX): Landes Bioscience; 2000-2013.

89. Chen J, Yao Y, Gong C, Yu F, Su S, Chen J, et al. CCL18 from Tumor-Associated Macrophages Promotes Breast Cancer Metastasis via PITPNM3. Cancer Cell. 2011 Apr;19(4):541–55.

90. Su Y, Zhou Y, Sun Y jue, Wang YL, Yin J yi, Huang Y jing, et al. Macrophage-derived CCL18 promotes osteosarcoma proliferation and migration by upregulating the expression of UCA1. J Mol Med. 2019 Jan 13;97(1):49–61.

91. Wang Q, Tang Y, Yu H, Yin Q, Li M, Shi L, et al. CCL18 from tumor-cells promotes epithelial ovarian cancer metastasis via mTOR signaling pathway. Mol Carcinog. 2016 Nov 12;55(11):1688–99.

92. Hou X, Zhang Y, Qiao H. CCL18 promotes the invasion and migration of gastric cancer cells via ERK1/2/NF-κB signaling pathway. Tumor Biology. 2016 Jan 5;37(1):641–51.

93. Meng F, Li W, Li C, Gao Z, Guo K, Song S. CCL18 promotes epithelial-mesenchymal transition, invasion and migration of pancreatic cancer cells in pancreatic ductal adenocarcinoma. Int J Oncol. 2015 Mar;46(3):1109–20.

94. Peng Q, Zhao L, Hou Y, Sun Y, Wang L, Luo H, et al. Biological Characteristics and Genetic Heterogeneity between Carcinoma-Associated Fibroblasts and Their Paired Normal Fibroblasts in Human Breast Cancer. PLoS One. 2013 Apr 5;8(4):e60321.

95. Solinas G, Germano G, Mantovani A, Allavena P. Tumor-associated macrophages (TAM) as major players of the cancer-related inflammation. J Leukoc Biol. 2009 Sep 9;86(5):1065–73.

96. Ploenes T, Scholtes B, Krohn A, Burger M, Passlick B, Müller-Quernheim J, et al. CC-Chemokine Ligand 18 Induces Epithelial to Mesenchymal Transition in Lung Cancer A549 Cells and Elevates the Invasive Potential. PLoS One. 2013 Jan 18;8(1):e53068.

97. Zhou Q, Huang L, Gu Y, Lu H, Feng Z. The expression of CCL18 in diffuse large B cell lymphoma and its mechanism research. Cancer Biomarkers. 2018 Mar 14;21(4):925–34.

98. Wang L, Wang Y xia, Zhang D zhong, Fang X jie, Sun P sheng, Xue H chao. Let-7a mimic attenuates CCL18 induced breast cancer cell metastasis through Lin 28 pathway. Biomedicine & Pharmacotherapy. 2016 Mar;78:301–7.

99. Bo S, Donghao S, Guangqi K, Ye T. CC Chemokine Ligand 18 Promotes Cell Proliferation and Metastasis of Urothelial Carcinoma via Activating PI3K/mTOR Signaling in Patient with Renal Transplantation. Urol Int. 2018;101(4):450–8.

100. Huang Y, Motta E, Nanvuma C, Kuhrt LD, Yuan Y, Xia P, et al. Microglia/macrophage-derived human CCL18 promotes glioma progression via CCR8-ACP5 axis analyzed in humanized slice model. Cell Rep. 2022 Apr;39(2):110670.

101. Qiao B, Chen L, Cheng Q, Wang G, Li Q, Zhang B, et al. CCL18 promotes migration and invasion of multiple myeloma cells and is associated with poor prognosis. Carcinogenesis. 2023 May 15;44(1):38–45.

102. Grochans S, Korbecki J, Simińska D, Żwierełło W, Rzeszotek S, Kolasa A, et al. CCL18 Expression Is Higher in a Glioblastoma Multiforme Tumor than in the Peritumoral Area and Causes the Migration of Tumor Cells Sensitized by Hypoxia. Int J Mol Sci. 2022 Aug 1;23(15):8536.

103. Zhang Y, Weinberg RA. Epithelial-to-mesenchymal transition in cancer: complexity and opportunities. Front Med. 2018 Aug 24;12(4):361–73.

104. Liu X, Xu X, Deng W, Huang M, Wu Y, Zhou Z, et al. CCL18 enhances migration, invasion and EMT by binding CCR8 in bladder cancer cells. Mol Med Rep. 2018 Dec 24;

105. Lin X, Chen L, Yao Y, Zhao R, Cui X, Chen J, et al. CCL18-mediated down-regulation of miR98 and miR27b promotes breast cancer metastasis. Oncotarget. 2015 Aug 21;6(24):20485–99.

106. Ploenes T, Scholtes B, Krohn A, Burger M, Passlick B, Müller-Quernheim J, et al. CC-Chemokine Ligand 18 Induces Epithelial to Mesenchymal Transition in Lung Cancer A549 Cells and Elevates the Invasive Potential. PLoS One. 2013 Jan 18;8(1):e53068.

107. Wang H, Liang X, Li M, Tao X, Tai S, Fan Z, et al. Chemokine (CC motif) ligand 18 upregulates Slug expression to promote stem-cell like features by activating the mammalian target of rapamycin pathway in oral squamous cell carcinoma. Cancer Sci. 2017 Aug 18;108(8):1584–93.

108. Hou X, Zhang Y, Qiao H. CCL18 promotes the invasion and migration of gastric cancer cells via ERK1/2/NF-κB signaling pathway. Tumor Biology. 2016 Jan 5;37(1):641–51.

109. Li H, Cui X, Wu W, Yu F, Yao H, Liu Q, et al. Pyk2 and Src Mediate Signaling to CCL18-Induced Breast Cancer Metastasis. J Cell Biochem. 2014 Mar 19;115(3):596–603.

110. Lane D, Matte I, Laplante C, Garde-Granger P, Carignan A, Bessette P, et al. CCL18 from ascites promotes ovarian cancer cell migration through proline-rich tyrosine kinase 2 signaling. Mol Cancer. 2016 Dec 9;15(1):58.

111. Lin L, Chen YS, Yao YD, Chen JQ, Chen JN, Huang SY, et al. CCL18 from tumor-associated macrophages promotes angiogenesis in breast cancer. Oncotarget. 2015 Oct 27;6(33):34758–73.

112. Ma L, Wang H, Li Z, Geng X, Li M. Chemokine (C-C motif) ligand 18 is highly expressed in glioma tissues and promotes invasion of glioblastoma cells. J Cancer Res Ther. 2019;15(2):358.

113. Omland SH, Wettergren EE, Mollerup S, Asplund M, Mourier T, Hansen AJ, et al. Cancer associated fibroblasts (CAFs) are activated in cutaneous basal cell carcinoma and in the peritumoural skin. BMC Cancer. 2017 Dec 7;17(1):675.

114. Nariţa D, Seclaman E, Ursoniu S, Ilina R, Cireap N, Anghel A. Expression of CCL18 and interleukin-6 in the plasma of breast cancer patients as compared with benign tumor patients and healthy controls. Rom J Morphol Embryol. 2011;52(4):1261–7.

115. Struyf S, Schutyser E, Gouwy M, Gijsbers K, Proost P, Benoit Y, et al. PARC/CCL18 Is a Plasma CC Chemokine with Increased Levels in Childhood Acute Lymphoblastic Leukemia. Am J Pathol. 2003 Nov;163(5):2065–75.

116. Gao J, Li Z h., Tang W, Wu Q n., Liu G h., Zheng W b. Chemokine C-C motif ligand 18 expression correlates with tumor malignancy in breast cancer. Pathologie Biologie. 2015 Sep;63(4–5):199–203.

117. Wang J, Qin Y, Zhu G, Huang D, Wei M, Li G, et al. High serum CCL18 predicts a poor prognosis in patients with laryngeal squamous cell carcinoma. J Cancer. 2019;10(27):6910–4.

118. Huang H, Li J, Hu W jia, Chen C, Luo H qing, Tang X dong, et al. The serum level of CC chemokine ligand 18 correlates with the prognosis of non-small cell lung cancer. Int J Biol Markers. 2019 Jun 3;34(2):156–62.

119. Plönes T, Krohn A, Burger M, Veelken H, Passlick B, Müller-Quernheim J, et al. Serum Level of CC-Chemokine Ligand 18 Is Increased in Patients with Non-Small-Cell Lung Cancer and Correlates with Survival Time in Adenocarcinomas. PLoS One. 2012 Jul 25;7(7):e41746.

120. Yuan L, Wan J, Huang C, Liang J, Liu M, Yue C, et al. Evaluation of serum CCL18 as a potential biomarker for ovarian cancer. Cancer Biomarkers. 2017 Dec 12;21(1):97–104.

121. Xu Y, Zhang L, Sun S kun, Zhang X. CC Chemokine Ligand 18 and IGF-Binding Protein 6 as Potential Serum Biomarkers for Prostate Cancer. Tohoku J Exp Med. 2014;233(1):25–31.

122. Miyagaki T, Sugaya M, Suga H, Ohmatsu H, Fujita H, Asano Y, et al. Increased CCL18 expression in patients with cutaneous T-cell lymphoma: association with disease severity and prognosis. Journal of the European Academy of Dermatology and Venereology. 2013 Jan 9;27(1).

123. Miyake M, Ross S, Lawton A, Chang M, Dai Y, Mengual L, et al. Investigation of CCL18 and A1AT as potential urinary biomarkers for bladder cancer detection. BMC Urol. 2013 Dec 5;13(1):42.

124. Huang H, Li J, Hu W jia, Chen MH, Chen SS, Chen C, et al. Positive expression of chemokine (CC Motif) ligand 18 and prognosis in cancer: A meta-analysis. Journal of BU ON: Official Journal of the Balkan Union of Oncology. 2018;23(4):1185–94.

125. Schmid S, Le UT, Haager B, Mayer O, Dietrich I, Elze M, et al. Local Concentrations of CC-Chemokine-Ligand 18 Correlate with Tumor Size in Non-small Cell Lung Cancer and Are Elevated in Lymph Node-positive Disease. Anticancer Res. 2016 Sep 9;36(9):4667–72.

126. Wang W, Wu D, He X, Hu X, Hu C, Shen Z, et al. CCL18-induced HOTAIR upregulation promotes malignant progression in esophageal squamous cell carcinoma through the miR-130a-5p-ZEB1 axis. Cancer Lett. 2019 Sep;460:18–28.

127. Su S, Liu Q, Chen J, Chen J, Chen F, He C, et al. A Positive Feedback Loop between Mesenchymal-like Cancer Cells and Macrophages Is Essential to Breast Cancer Metastasis. Cancer Cell. 2014 May;25(5):605–20.

128. Sun JH, Fan N, Zhang Y. Correlation between serum level of chemokine (C-C motif) ligand 18 and poor prognosis in breast cancer. Genetics and Molecular Research. 2016;15(3).

129. Yang B, Fan Y, Chen M, Tang L, Tang X, Li H, et al. Identification and validation of a CCL18-related signature for prediction of overall survival in patients with uveal melanoma. Exp Eye Res. 2023 May;230:109448.

130. Leung SY, Yuen ST, Chu KM, Mathy JA, Li R, Chan ASY, et al. Expression profiling identifies chemokine (C-C motif) ligand 18 as an independent prognostic indicator in gastric cancer. Gastroenterology. 2004 Aug;127(2):457–69.

131. Schmid S, Csanadi A, Kozhuharov N, Tchudjin M, Kayser C, Rawluk J, et al. CC-Chemokine Ligand 18 Is an Independent Prognostic Marker in Lymph Node-positive Non-small Cell Lung Cancer. Anticancer Res. 2018 Jul 3;38(7):3913–8.

132. Yuan R, Chen Y, He X, Wu X, Ke J, Zou Y, et al. CCL18 as an independent favorable prognostic biomarker in patients with colorectal cancer. Journal of Surgical Research. 2013 Jul;183(1):163–9.

133. Ran FA, Hsu PD, Wright J, Agarwala V, Scott DA, Zhang F. Genome engineering using the CRISPR-Cas9 system. Nat Protoc. 2013 Nov 24;8(11):2281–308.

134. Grada A, Otero-Vinas M, Prieto-Castrillo F, Obagi Z, Falanga V. Research Techniques Made Simple: Analysis of Collective Cell Migration Using the Wound Healing Assay. Journal of Investigative Dermatology. 2017 Feb;137(2):e11–6.

135. Lev S. The role of the Nir/rdgB protein family in membrane trafficking and cytoskeleton remodeling. Exp Cell Res. 2004 Jul;297(1):1–10.

136. Manteca A, Alonso-Caballero Á, Fertin M, Poly S, De Sancho D, Perez-Jimenez R. The influence of disulfide bonds on the mechanical stability of proteins is context dependent. Journal of Biological Chemistry. 2017 Aug;292(32):13374–80.

137. Guschin DY, Waite AJ, Katibah GE, Miller JC, Holmes MC, Rebar EJ. A Rapid and General Assay for Monitoring Endogenous Gene Modification. In 2010. p. 247–56.

138. Zhao C, Zheng S, Yan Z, Deng Z, Wang R, Zhang B. CCL18 promotes the invasion and metastasis of breast cancer through Annexin A2. Oncol Rep. 2019 Dec 11;

139. Deng Z, Xiao Q, Zheng Y, Feng R, Sheng Z, Zhang B. CCL18 Promotes the Invasion of Lung Adenocarcinoma through ANXA2. Zhongguo Fei Ai Za Zhi. 2021 Jul 20;24(7):461-467.

140. Qi W, Zhang Y, Yang W, Liu C, Wang H, Fu R, et al. Abnormal Proteomics Profile of Plasma Reveals the Immunological Pathogenesis of Severe Aplastic Anemia. Dis Markers. 2022 May 6;2022:1–10.

141. Tsuboi H, Honda F, Takahashi H, Ono Y, Abe S, Kondo Y, et al. Pathogenesis of IgG4-related disease. Comparison with Sjögren's syndrome. Mod Rheumatol. 2020 Jan 2;30(1):7–16.

142. Chen G, Liang Y xiang, Zhu J guo, Fu X, Chen Y fei, Mo R jun, et al. CC Chemokine Ligand 18 Correlates with Malignant Progression of Prostate Cancer. Biomed Res Int. 2014;2014:1–10.

143. Hou X, Zhang Y, Qiao H. CCL18 promotes the invasion and migration of gastric cancer cells via ERK1/2/NF-κB signaling pathway. Tumor Biology. 2016 Jan 5;37(1):641–51.

144. Niland S, Riscanevo AX, Eble JA. Matrix Metalloproteinases Shape the Tumor Microenvironment in Cancer Progression. Int J Mol Sci. 2021 Dec 23;23(1):146.

145. Toth M, Fridman R. Assessment of Gelatinases (MMP-2 and MMP-9) by Gelatin Zymography. In: Metastasis Research Protocols. New Jersey: Humana Press; p. 163–74.

146. Cardoso AP, Pinto ML, Pinto AT, Pinto MT, Monteiro C, Oliveira MI, et al. Matrix metalloproteases as maestros for the dual role of LPS- and IL-10-stimulated macrophages in cancer cell behaviour. BMC Cancer. 2015 Dec 5;15(1):456.

147. Pochetuhen K, Luzina IG, Lockatell V, Choi J, Todd NW, Atamas SP. Complex Regulation of Pulmonary Inflammation and Fibrosis by CCL18. Am J Pathol. 2007 Aug;171(2):428–37.

148. Wu J shun, Jiang J, Chen B jun, Wang K, Tang Y ling, Liang X hua. Plasticity of cancer cell invasion: Patterns and mechanisms. Transl Oncol. 2021 Jan;14(1):100899.

149. Lin L, Chen YS, Yao YD, Chen JQ, Chen JN, Huang SY, et al. CCL18 from tumor-associated macrophages promotes angiogenesis in breast cancer. Oncotarget. 2015 Oct 27;6(33):34758–73.

150. Ibrahim FMk, Helal DS, Ali DA, Abd-Ellatif RN, Elkady AM, Sharshar R, et al. Prognostic role of annexin A2 and cancer-associated fibroblasts in advanced non-small cell lung cancer: Implication in epithelial-mesenchymal transition and gefitinib resistance. Pathol Res Pract. 2023 Jan;241:154293.

151. Gao J, Huo Z, Song X, Shao Q, Ren W, Huang X, et al. EGFR mediates epithelial-mesenchymal transition through the Akt/GSK-3β/Snail signaling pathway to promote liver cancer proliferation and migration. Oncol Lett. 2023 Dec 18;27(2):59.

152. Reynolds AR, Tischer C, Verveer PJ, Rocks O, Bastiaens PIH. EGFR activation coupled to inhibition of tyrosine phosphatases causes lateral signal propagation. Nat Cell Biol. 2003 May 22;5(5):447–53.

153. Shetty PK, Thamake SI, Biswas S, Johansson SL, Vishwanatha JK. Reciprocal Regulation of Annexin A2 and EGFR with Her-2 in Her-2 Negative and Herceptin-Resistant Breast Cancer. PLoS One. 2012 Sep 5;7(9):e44299.

154. Hayes MJ, Moss SE. Annexin 2 Has a Dual Role as Regulator and Effector of v-Src in Cell Transformation. Journal of Biological Chemistry. 2009 Apr;284(15):10202–10.

155. Kanagasabai R, Karthikeyan K, Vedam K, Qien W, Zhu Q, Ilangovan G. Hsp27 Protects Adenocarcinoma Cells from UV-Induced Apoptosis by Akt and p21-Dependent Pathways of Survival. Molecular Cancer Research. 2010 Oct 1;8(10):1399–412.

156. Rocha MR, Barcellos-de-Souza P, Sousa-Squiavinato ACM, Fernandes P V., de Oliveira IM, Boroni M, et al. Annexin A2 overexpression associates with colorectal cancer invasiveness and TGF-ß induced epithelial mesenchymal transition via Src/ANXA2/STAT3. Sci Rep. 2018 Jul 26;8(1):11285.

157. Chen C, Ding J, Ma Z, Xie Y, Zhang L, Zhu D. Exosome-Delivered EGFR Induced by Acidic Bile Salts Regulates Macrophage M2 Polarization to Promote Esophageal Adenocarcinoma Cell Proliferation. Onco Targets Ther. 2024 Feb;Volume 17:113–28.